

University of Granada

PhD programme in Biomedicine



3D Additive Fabrication for Regenerative Therapies

An innovative Modular Multicomponent Work
Station for 3D Bioprinting in Regenerative Medicine
(REGEMAT 3D)

Author:

D. José Manuel Baena Martínez

Supervisors:

**D. Juan Antonio Marchal Corrales
D. Guillermo Rus Carlborg**

Granada, October 2018

Editor: Universidad de Granada. Tesis Doctorales
Autor: José Manuel Baena Martínez
ISBN: 978-84-1306-183-2
URI: <http://hdl.handle.net/10481/55744>

Table of contents

Table of contents	5
Abstract.....	9
Acknowledgements	13
List of Figures.....	15
List of tables	19
List of symbols and abbreviations	21
Introduction	25
1 Stem cells-based therapies and regenerative medicine.....	36
1.1 Differentiation, dedifferentiation and transdifferentiation of SC.....	39
1.2 Stem cells derived from adipose tissue (ASCs)	41
1.3 Problems related to stem cell therapies	42
2 Biomaterials for Regenerative therapies.....	45
2.1 Scaffolds.....	49
2.2 Hydrogels	52
3 Growth factors	56
4 Additive manufacturing technologies for RM	59
4.1 Types of AM technologies	60
4.2 Application of AM technologies to RM approaches.....	68
5 Bioreactors and ultrasounds in RM	71

6 Cartilage injuries.....	77
7 Use of bioprinting in the development of new drugs.....	80
Hypothesis	83
Objectives	87
Materials and methods.....	89
1 Bioprinting system development	91
1.1 Concept design of the system.....	91
1.2 Development of the bioprinting unit	93
1.3 ECU, Sensors and actuators of the work station	94
1.4 Software and graphical user interface	96
2 Validation of the work station	98
2.1 Bioprinter and software configuration	100
2.2 Chondrocytes isolation and characterization.....	102
2.3 Volume-by-volume printing of 3D hybrid scaffolds.....	103
2.4 Confocal microscopy.....	104
2.5 Apoptosis evaluation.....	104
2.6 Cell proliferation assay.....	105
2.7 Statistical analysis	105
3 New meshes structures, scaffolds and bioink formulations.....	106
Results	109
1 Bioprinting system.....	110
1.1 Bioprinting unit	111

1.2 ECU, Sensors and actuators	115
1.3 Software and GUI.....	124
1.4 Improvements and technical contributions in the printing process.....	131
1.5 Improvements and technical contributions in the ECU	144
2 Validation of the work station	153
2.1 Volume-by-volume printing of 3D hybrid scaffolds.....	153
2.2 Evaluation of the VbV printing process on cell viability and distribution.....	156
3 New meshes structures, scaffolds and bioink formulations.....	160
Discussion.....	163
Conclusions	171
References	175

Abstract

The lack of tissue regeneration after trauma, degenerative diseases and other pathologies is a highly challenging problem to be solved by biomedicine scientists in this century. New advances in stem cell research for the regeneration of tissue injuries have opened a new promising research field. However, research carried out nowadays with 2D cell cultures do not provide the expected results, as 2D cultures do not mimic the 3D structure of a living tissue.

Additive Manufacturing techniques, also known as 3D printing, are based on the principle of adding material layer by layer allowing manufacturing complex external and internal shapes with a mesh structure (scaffold). Bioprinting technologies aim at joining together tissue engineering, regenerative medicine and 3D printing disciplines and have emerged as a powerful tool for researchers due to the ability to mimic the 3D structure of any tissue. Bioprinting can help to overcome the problems that researchers have found working with cell cultures in 2D.

This thesis is aimed at generating new knowledge and evidence on the use of bioprinting for clinical therapies. In order to do that we have developed an innovative Modular Multicomponent Work Station for 3D Bioprinting in Regenerative Medicine (project called REGEMAT 3D) with its software and manufacturing algorithms, that can manufacture layer by layer 3D constructs with customized external shapes and an internal meshed structure. Besides the system can be configured and adapted to print with a wide range of biomaterials as scaffolds and bioinks.

In order to proof the efficacy of the developed system and biofabrication algorithms, chondrocytes have been printed using a novel procedure known as Volume-by-Volume 3D-biofabrication process followed by volume injection filling of the cell loaded bioink.

The process divides the printed part in different volumes and injects the cells after each volume has been printed, once the temperature of the printed thermoplastic fibers has decreased. In our study chondrocytes were isolated from osteoarthritic patient's samples and after characterization were used to test the feasibility of the process. Human chondrocytes were bioprinted together with polylactic acid (PLA) and apoptosis, proliferation and metabolic activity were analyzed. In our trial, chondrocytes survived to the manufacturing process with 90% of viability 2 hours after printing, and after 7 days in culture, chondrocytes proliferated and totally colonized the scaffold, concluding that the use of the developed bioprinting system shows a valuable potential in the short-term development of bioprinted-based clinical therapies for tissue regeneration.

Resumen

La falta de regeneración tisular tras un traumatismo, enfermedades degenerativas u otras patologías, es uno de los retos más importantes que afrontan los científicos biomédicos en este siglo. Los avances en la investigación con células troncales para la regeneración de lesiones en los tejidos han abierto un prometedor campo de trabajo. Sin embargo, las investigaciones llevadas a cabo con cultivos celulares en 2D no están generando los resultados esperados debido a que un cultivo bidimensional no recrea las condiciones tridimensionales de un tejido vivo.

Las técnicas de fabricación aditiva, también conocidas como impresión 3D, se basan en el principio de adición de material capa a capa, permitiendo la fabricación de geometrías externas complejas y geometrías internas con una estructura mallada (scaffold). Las tecnologías de bioimpresión tienen como objetivo unir las disciplinas de la ingeniería tisular, la medicina regenerativa y la impresión 3D, y han surgido como una potente herramienta para los investigadores debido a la posibilidad de recrear la estructura tridimensional de un tejido vivo. La bioimpresión de tejidos puede ayudar a solucionar los problemas que estos investigadores han encontrado trabajando con cultivos celulares bidimensionales.

El objetivo del presente trabajo es generar conocimiento y evidencia en el uso de la bioimpresión con futuras aplicaciones clínicas. Para ello hemos desarrollado una estación de trabajo modular y multicomponente para la bioimpresión 3D de tejidos en medicina regenerativa (proyecto cuyo nombre es REGEMAT 3D), que incluye un software y algoritmos de fabricación, que posibilitan la fabricación capa a capa de piezas tridimensionales con geometría personalizada y una estructura interna mallada cargadas con células. Además, el sistema puede ser configurado y adaptado para

imprimir con un amplio rango de biomateriales tanto para la matriz como para las biotintas.

Con el objetivo de probar la eficacia del sistema y los algoritmos de biofabricación desarrollados, células de cartílago humano (condrocitos) han sido impresos usando un novedoso proceso llamado biofabricación Volumen a Volumen seguido de un proceso de inyección volumétrica de una biotinta cargada con las células.

El proceso divide la parte a fabricar en diferentes volúmenes e inyecta las células tras la fabricación de cada volumen, una vez que la temperatura de las fibras impresas del termoplástico ha bajado. En nuestro estudio los condrocitos fueron obtenidos de muestras pacientes con osteoartritis y tras su caracterización se utilizaron para probar la viabilidad del proceso. Dichos condrocitos humanos fueron impresos con una matriz de ácido poliláctico (PLA), analizando la apoptosis, proliferación y actividad metabólica. En nuestro estudio, los condrocitos sobrevivieron al proceso de fabricación con una viabilidad del 90% 2 horas después de la bioimpresión y, tras 7 días en cultivo, los condrocitos proliferaron hasta colonizar totalmente el scaffold, concluyendo que el uso del sistema de bioimpresión implementado presenta un gran potencial en el desarrollo a corto plazo de terapias clínicas basadas en la bioimpresión para regeneración tisular.

Acknowledgements

Many years ago, maybe in the last years of university I decided to develop my career in health care. Don't ask me why but, when I saw the amazing world of technology applied to living organism I understood that this was going to be the future and the basis of my motivation, to develop new ideas that can help improve people's quality of life.

Some years later when I was in the UK finishing my Master of Science in Motor Sport Engineering at Oxford Brookes University after a degree in Industrial Engineering and a specialization in mechanical engineering, it might seem I haven't follow my dreams and I was on the track of a promising career in motorsport industry. Nothing further from the truth as what I have been doing during the last years, from my stay at the Laser Zentrum Hannover, at the University of Buenos Aires and the Institute of Biomechanics of Valencia to the founding of BRECA Health Care in 2011 and REGEMAT 3D in 2015 and my incorporation to the research group of the University of Granada and the Tissue Engineering and 3D Printing Platform in one of the biggest Spanish hospital is to join dots. This thesis closes the loop, finish a path that have led me to a starting point of my future way to develop new solutions for health care, joining living sciences and technology. And there is still a lot of work to do, with BRECA Health Care we have today over 100 patients treated with our solutions and REGEMAT 3D is an award-winning company, leading the development of bioprinting solutions in 20 countries, but the good thing is that we are still at the beginning of this revolution. A big thank to all the people I found during this path.

A special thanks to my supervisors, Juan Antonio Marchal and Guillermo RusCarlborg that could vision the potential of the technology, trust me and assist me during the development of this project.

Another special thanks to the team of BRECA Health Care, REGEMAT 3D and the IBIMER. This project is a multidisciplinary one, professionals from different areas as biology, medical science, electronics, design and computer science are needed in such a project. Without this team this work did not come true.

To conclude a big thanks to my parents, family, friends and all the researchers, business professionals and clinicians I met around the world during the last years that have enriched the vision I have to change the world. The only limit is your imagination.

José Manuel Baena Martínez

josbaema@gmail.com

es.linkedin.com/in/jмбаena

www.twitter.com/josbaema

List of Figures

Figure 1 Ambystoma mexicanum. Photograph by Stephen Dalton/Animals Animals—Earth Scenes	27
Figure 2 Neurosurgery PEEK implant manufactured with Computer numerical control machining implanted by BRECA Health Care (Image used with permission of the company).....	28
Figure 3 Neurosurgery Ti implant manufactured with 3D printing technology Electron Beam Melting implanted by BRECA Health Care (Image used with permission of the company).....	29
Figure 4 Neurosurgery polyamide surgical guides and biomodels by 3D printing Selective Laser Sintering manufactured by BRECA Health Care for a frontal skull reconstruction using autologous bone of the patient with craniosynostosis (Image used with permission of the company).....	29
Figure 5 Thermoplastic Bioprinted scaffold of a nose shape using the bioprinter system described in the present work and commercialized by the company REGEMAT 3D (Image used with permission of the company).....	29
Figure 6 Bioprinting technologies aim at joining together tissue engineering, regenerative medicine and 3D printing disciplines	31
Figure 7 Three main components of a bioprinted 3D construct	32
Figure 8 Two blocks of processes to be defined to design a successful strategy to create a functional living tissue	36
Figure 9 Potential uses of stem cells (source Wikimedia Commons).....	38
Figure 10 FDM working principle (source Wikimedia Commons).....	61
Figure 11 FDM model of a nose (courtesy of REGEMAT3D)	62
Figure 12 An SLA model of a medical an ultrasound device (courtesy of END Lab University of Granada).....	62
Figure 13 SLS working principle (source Wikimedia Commons)	63
Figure 14 SLS skull patient specific biomodel (courtesy of BRECA Health Care)	63
Figure 15 EBM hip prosthesis stem(Ferrís-Oñate, Morales-Martín et al. 2010).....	64
Figure 16 LC working principle (Comesaña, Lusquiños et al. 2011).....	65
Figure 17 A typical setup for DOD IPT. From Xu et al. (2007).....	67
Figure 18 In-bioreactor ultrasonic monitoring of 3D culture human engineered cartilage. J. Melchor, E. López-Ruiz J. Soto, G. Jiménez, C. Antich, M. Perán, J.M. Baena, J.A. Marchal, G. Rus. Sensors and Actuators B:Chemical 266 (2018) 841-852.....	75
Figure 19 Sub projects in the development of the work station.	91
Figure 20 Sub parts of the 3D bioprinter.....	92

Figure 21 Bioprinter characteristics, hardware and software of the bioprinting system. Process flow of bioprinting system (A). System and bioprinter images (B) (Extracted from the publication of the author)	101
Figure 22 Build-up and assembly of the system.....	110
Figure 23 REGEMAT 3D V1.....	111
Figure 24 Head extrusion tools.....	112
Figure 25 Head options, compact or individual Z-axis for each tool	113
Figure 26 Some options of the printing head.....	113
Figure 27 3 Main manufacturing modes that can be used in the system	115
Figure 28 Arduino Mega microcontroller	116
Figure 29 Power indicator sketch	116
Figure 30 Voltage reference supply sketch	117
Figure 31 Heater control sketch	117
Figure 32 Temperature monitoring sketch	118
Figure 33 Fan control sketch	118
Figure 34 I ² C communication sketch	119
Figure 35 Stepper motors drivers sketch	119
Figure 36 End stops sketch.....	120
Figure 37 Emergency stop sketch.....	120
Figure 38 ECU Sketch render.....	121
Figure 39 Diagram of the main functions of the firmware.	122
Figure 40 Loading a predefined ST.....	125
Figure 41 Scaffold settings	126
Figure 42 Syringes settings	127
Figure 43 Generation of G code	128
Figure 44 Distal femur section printing trajectories	129
Figure 45 Printing parameters configuration.....	129
Figure 46 STL file code with the normal vectors and the vertex.....	132
Figure 47 Operations applied to obtain the perimeter mesh	132
Figure 48 Printing settings of the mesh infill.	133
Figure 49 Operations applied to obtain the layer infill.	135

Figure 50 G code segment generated by REGEMAT 3D	138
Figure 51 Operations applied to obtain the file	140
Figure 52 "Movements" tab.....	141
Figure 53 Command-line.....	142
Figure 54 Communication messages.....	142
Figure 55 Initiation of the communication	143
Figure 56 Start printing	144
Figure 57 Operations that are carried out by the receptor for identifying the command, checking and returning a message notifying about it.	146
Figure 58 Operations applied to received G command management	148
Figure 59 Bioprinter configuration. Layout of the Designer GUI (A) and scaffold parameters configuration (B). Example of VbVconfiguration process selecting the layer in which VbV will take place, the volume to be injected and the infill model (C) (Extracted from the publication of the author)	154
Figure 60 Bioprinter system. Configuration of the printing head, with the FDM unit (right), a syringe with a pink needle (T0) and 2 syringes with a blue tip (T1,T2) (left) (A). Injection volume filling after a few layers in a cylindrical shape (B). Representative examples of shapes with different mesh structures that can be printed (C) (Extracted from the publication of the author).....	155
Figure 61 Comparison between conventional FDM deposition and VbV printing procedure.Schematic representation of the printing procedures found in the literature with restricted geometries to avoid the contact of the cell laden material (pink) with the high temperature parts of the printed thermoplastics (grey). FDM deposition of the first layer and filling the spaces with the cell laden materials. Zoom of the spaces filling, FDM of next layer, and restricted multimaterial scaffold (A).Working process diagram represented by schematic representation of the VbVprinting procedure (B). FDM deposition of the x layers without restrictions in the mesh geometry. Zoom of the volume to be filled with the cell loaded bioink, and injection in the N points selected by the software (C) (Extracted from the publication of the author)	156
Figure 62 IVF printing process. Schematic images of the bioprinter with the FDM extruder (right) and the 3 syringes (T0,T1 and T2) (A) and the bioprinting process with the FDM deposition of 4 layers of PLA by the nozzle, and the injection of alginate with chondrocytes (T0) and calcium chloride (T1) in the selected points (B). Images of representative 3D printed scaffolds with cells embedded in alginate and cultured during 7 days (C) (Extracted from the publication of the author)	157
Figure 63 Effect of the VbV bioprinting process on cell viability. Characterization of freshly isolated chondrocytes that displayed a typical polygonal shape, high expression of collagen 2 (Col2) and proteoglycans. Original magnification: 10X (A). Cell viability values of chondrocytes manually printed with alginate (ALG) and bioprinted using the VbV method with alginate and alginate in combination with PLA. *p<0.05 compared with control cells before printing process (B). Cell proliferation using Alamar blue assay at different time points (C). Confocal laser scanning microscopy images of bioprinted human chondrocytes stained with CTG (green) and DAPI (blue) after 24 hours and 7 days. Scale bars indicate 100 µm (D) (Extracted from the publication of the author)	159
Figure 64 Printing of different thermoplastic materials for the scaffolds.....	160
Figure 65 Poster presented by one of the user of REGEMAT3D. Printed meniscus from PCL	161
Figure 66 printing of nanocellulose using REGEMAT3D bioprinter.....	162
Figure 67 Printing of methacrylate modified pectin bioink.....	162

List of tables

Table 1 Types of thermoplastics and printing parameters	108
Table 2 Types of G instructions and function	123
Table 3 Types of M instructions and function	123
Table 4 Types of T instructions and function	123

List of symbols and abbreviations

3D Printing (3DP)

Additive manufacturing (AM)

Adhesive Inkjet printing (AIP)

Adipose tissue (AT)

Adipose-derived stem cells (ASCs)

Adipose-derived stromal cells (ADSC)

Alzheimer's Disease (AD)

American Heart Association (AHA)

Autologous chondrocyte transplantation (ACT)

Bone marrow stromal cells (BMSCs)

Bone morphogenetic proteins (BMPs)

brown Adipose tissue (bAT)

Cardiovascular disease (CVD)

Cellular differentiation (CD)

Commercially-pure titanium (cp-Ti)

Computational fluid dynamics (CFD)

Computer aided design (CAD)

Computer aided manufacturing (CAM)

Continuous ejection (CE)

Direct current (DC)

Direct metal laser sintering (DMLS)

Droplets on demand (DOD)

Dulbecco's modified eagle's medium (DMEM)

Electron beam melting (EBM)

Embryonic stem cells (ESC)
Epidermal growth factor (EGF)
Extracellular matrix (ECM)
Fetal bovine serum (FBS)
Fibroblast growth factor (FGF)
Finite element (FE)
Fused deposition modelling (FDM)
Growth factors (GFs)
Hyaluronic acid (HA)
Impaction bone grafting (IBG)
Individually pore filling (IPF)
Induced pluripotent stem cells (IPS)
Infrapatellar fat pad (IFP)
Injection Volume Filling (IVF)
Inkjet printing technology (IPT)
Insulin-like growth factor (IGF)
Keratinocyte growth factor (KGF)
Laser cladding (LC)
Laser-Induced-Forward-Transfer (LIFT)
Mesenchymal stem cells (MSCs)
Musculoskeletal disorders (MSDs)
Negative Temperature Coefficient (NTC)
Nerve growth factor (NGF)
Osteoarthritis (OA)
Osteochondritis dissecans (OCD)

Osteogenic protein (OP)

Parkinson's Disease (PD)

Peripheral vascular disease (PVD)

Platelet-derived growth factor (PDGF)

Poly(caprolactone fumarate) (PCLF)

Poly(glycolic acids) (PGAs)

Poly(lactic-co-glycolic acids) (PLGAs)

Poly(ortho esters) (POEs)

Polycaprolactones (PCLs)

Polydioxanones (PDO)

Polyhydroxyalkanoates (PHAs)

Poly-lactic acid (PLA)

Poly-L-lactic acid (PLLA)

Proportional-integral-derivative (PID)

Pulse-Width Modulation (PWM)

Regenerative medicine (RM)

Regenerative therapies (RT)

Scanning electron microscopy (SEM)

Selective laser melting (SLM)

Selective laser sintering (SLS)

Standard Tessellation Language (STL)

Stem cell (SC)

Stereolithography (SLA)

Tetracalcium phosphate (TTCP)

Three-dimensional (3D)

Tissue engineering (TE)

Tissue regeneration (TR)

Titanium-aluminum-vanadium alloy (Ti6Al4V)

Total hip reconstruction (THR)

Transforming growth factor (TGF)

Tricalcium phosphate (TCP)

Two-dimensional (2D)

Two-photon polymerization (2PP)

Vascular endothelial growth factor (VEGF)

Volume-by-Volume (VbV)

White Adipose tissue (wAT)

Introduction

The lack of tissue regeneration (TR) after trauma, degenerative diseases and other pathologies is probably the most challenging problem to be solved by biomedicine scientists in this century. Tissue engineering (TE) is a multidisciplinary science that aims at solving the problems of TR developing new approaches and technologies to promote the regeneration of damaged tissues and organs and the creation *in vitro* of functional tissues that can restore or even improve the functionality of the tissues and organs. TE strategies include the use of cell therapies, biomaterials and a wide range of different manufacturing process aiming at promoting the regeneration *in vivo*.

TE shows a huge potential in solving pathologies, this could improve the quality of life of people around the world suffering from tissue damages. The main pathologies following the RM annual report, March 2012 – March 2013 of the alliance for regenerative medicine (www.alliancerm.org) are: i) cardiovascular disease (CVD), ii) peripheral vascular disease (PVD), iii) non-healing wounds, iv) spinal cord injury, v) Alzheimer's Disease (AD), vi) Parkinson's Disease (PD), vii) musculoskeletal disorders (MSDs), viii) autoimmune disorders, ix) stroke, x) diabetes and xi) ocular disease. In some tissue damages the solution is still unavailable as for example in some cancers or orphan diseases, and in others, tissues and organ transplantation have shown very good results but the demand is higher than the availability (Phillips 2012). There is an emergence of TE as a research field, where new solutions and approaches have to be investigated.

We have some examples in the nature as the *Ambystoma mexicanum* that can regenerate some parts of the body (Figure 1). This amphibian can regenerate lost appendages in

months, and even more vital structures. In some cases the less vital parts of their brains (Roy and Gatien 2008).



Figure 1 *Ambystoma mexicanum*. Photograph by Stephen Dalton/Animals Animals—Earth Scenes

New advances in stem cell (SC) research during the last decades have opened a new promising research field with a lot of potential in finding solutions that can help patients around the world. However, there are still a lot of things to do. Research carried out nowadays with two-dimensional (2D) cell cultures do not mimic the 3D structure of a living tissue and do not provide the expected results.

Traditional manufacturing techniques used in many manufacturing procedures, are based on the subtraction of material (Figure 2) or on shaping it using a mold. On the other hand, Additive Manufacturing (AM) techniques are based on the principle of layer by layer material addition allowing manufacturing internal shapes with a mesh structure (scaffold) and complex external geometries. New AM technologies enable the manufacturing of complex multimaterial parts in 3D and are commonly known as 3D printing. Recent mass use of 3D printing technologies has allowed developing cost

competitive systems with very good performance and very innovative solutions to overcome the difficulties faced in the early years of development.

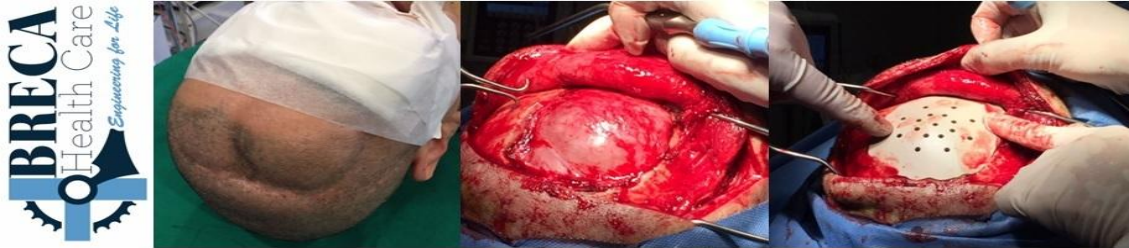


Figure 2 Neurosurgery PEEK implant manufactured with Computer numerical control machining implanted by BRECA Health Care (Image used with permission of the company)

The main advantages of 3D printing for the manufacturing of medical devices and its application in TE are:

- As a layer by layer AM procedure we can add things and components during the procedure (this is very useful for TE as we can add biomolecules and cells during the procedure, creating a 3D structure seeded with living cells and biomolecules).
- We can create very complex shapes, mimicking the anatomical structure of living tissues and organs.
- We can manufacture mesh structures that can create complex internal structures that improve the attachment of surrounded tissues and tune the mechanical behaviour of the scaffold, that will affect the behaviour of the cells.

The use of 3D printing in health care can cover from the manufacturing of patient specific biomodels, to the surgical guides, the implants and prosthesis, the biodegradable biomaterials and scaffolds and the tissue engineered constructs seeded with cells and bio molecules (Figure 3, Figure 4, Figure 5).

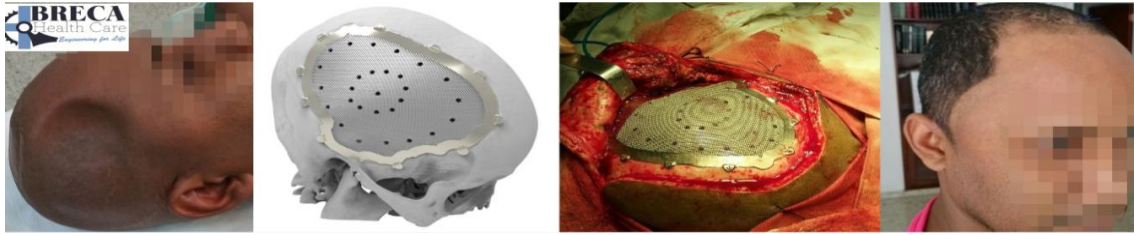


Figure 3 Neurosurgery Ti implant manufactured with 3D printing technology Electron Beam Melting implanted by BRECA Health Care (Image used with permission of the company)

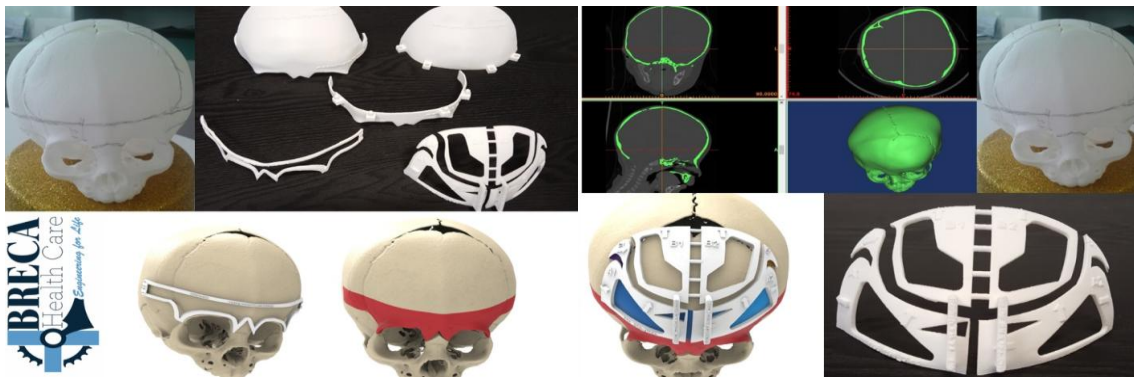


Figure 4 Neurosurgery polyamide surgical guides and biomodels by 3D printing Selective Laser Sintering manufactured by BRECA Health Care for a frontal skull reconstruction using autologous bone of the patient with craniosynostosis (Image used with permission of the company)

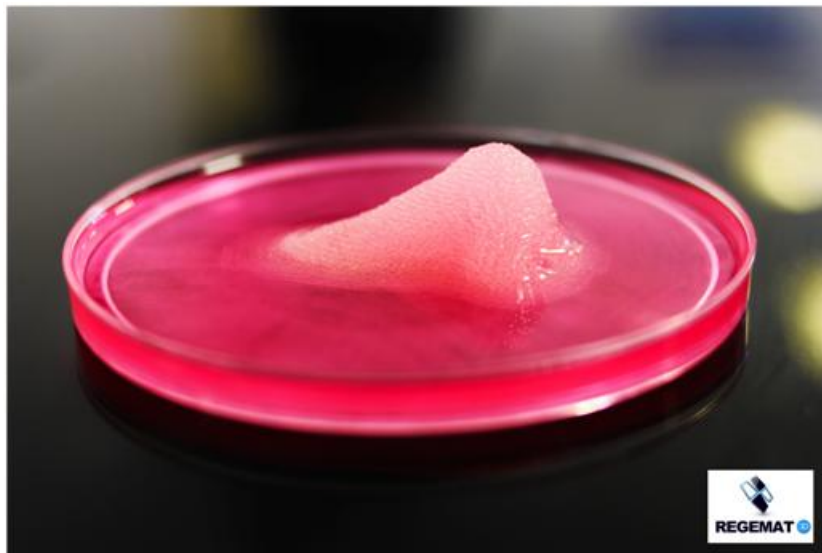


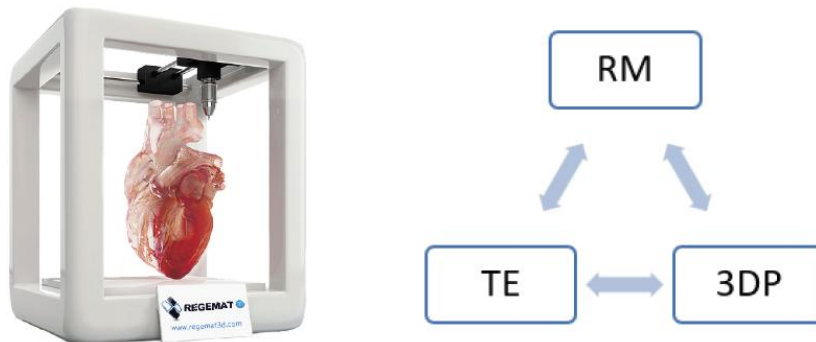
Figure 5 Thermoplastic Bioprinted scaffold of a nose shape using the bioprinter system described in the present work and commercialized by the company REGEMAT 3D (Image used with permission of the company)

Furthermore, this freedom of fabrication of synthetic medical devices using 3D printing opens the door to offering a personalized solution to each patient and to include also tissue engineered biomaterials and living tissues creating a solution that can not only restore the function of the damaged anatomy but promote the tissue formation and regeneration. A new era in the medical devices industry and its combination with TE is born.

SC therapies and 3D printing technologies can be used together to overcome the problems that researchers have found working with 2D cell cultures. 3D AM has shown a huge field of application in TE, but there are still many questions to answer and to be solved in order to develop a new manufacturing industrial procedure in SC based therapies for TR.

During the first decade of the 21st century the advances of AM in RM, also known as bioprinting, have been increasing in frequency (Mironov, Prestwich et al. 2007). In spite of being a very promising technology, it still requires research and development to achieve the clinical application. Bioprinters create 3D scaffolds with cells and another biomolecules as GFs and cytokines, amongst others, but this is still far away from being a functional tissue. The maturation procedure and the stimuli applied to this constructs also play a very important role in the formation of a functional tissue.

Bioprinting technologies have emerged as a powerful tool for TE due to the ability to mimic the 3D structure of any tissue. The use of biomaterials, cells and biomolecules combined with this manufacturing technique is gaining an increasing interest within the scientific community (Boland et al., 2006; Tsang and Bhatia, 2007; Billiet et al., 2012). There is a wide range of different bioprinting technologies, therefore, the election of an appropriate technology must be based on the characteristics of the tissue to regenerate (Cui et al., 2017).



Regenerative medicine (RM) is the branch of the medicine that aims at finding solutions to regenerate damaged tissues.

Tissue engineering (TE) is the use of a combination of cells, engineering and materials methods, and suitable signaling factors to improve or replace biological functions.

Figure 6 Bioprinting technologies aim at joining together tissue engineering, regenerative medicine and 3D printing disciplines

The high cost, in some cases, and poor adaptability of bioprinters is one of the main limitations of the technology. Systems currently on the market do not allow researchers to configure the tools according to their needs and innovate in their investigation. Just few parameters can be tuned, and these companies seem to forget that the technology is still far from the clinical application. A reliable and easy adaptable 3D bioprinting workstation is necessary in order to help researchers to convert 2D cultures into 3D cultures. Another advantage of bioprinting is the possibility to automatize the manufacturing process, keeping all the variables under control towards and industrial application (scale-up) and regulatory clearance (Placzek, Chung et al. 2009).

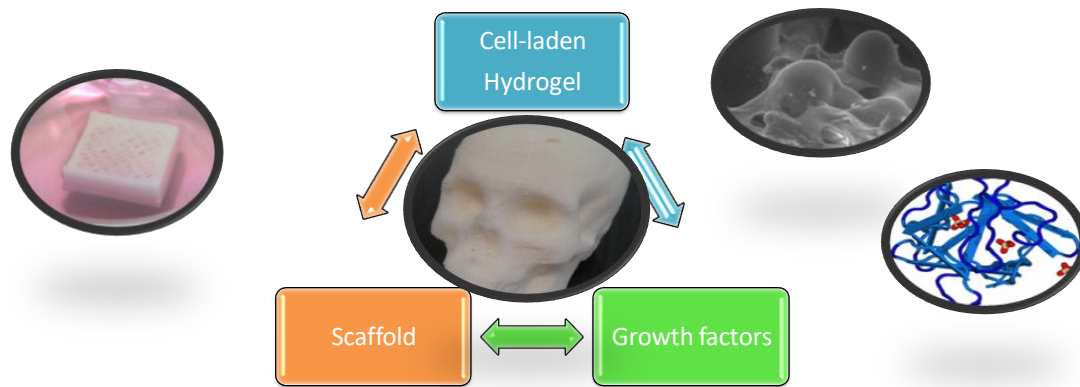


Figure 7 Three main components of a bioprinted 3D construct

Furthermore, 3D printed parts containing cells and formed tissues could help to accelerate the testing and developing of new drugs, eliminating pre-clinical trials, reducing the required number of participants in clinical trials and shortening the time to market of new drugs. Being able to maintain the environmental parameters under control and the uniformity of the samples will help to accelerate the development of new drugs towards a personalized medicine (Ma, Barker et al. 2012).

The aim of this project is to develop a modular workstation with 3D printing technologies with enhanced printing processes that can manufacture 3D biodegradable constructs loaded with cells and another biomolecules that can be used in the creation of living tissues and organs and in the regeneration of damaged tissues. This system will allow researchers to print 3D multicomponent parts; with a scaffolds structure, hydrogels with cells and fibres, to produce parts *in vitro* to regenerate living tissues. Besides we aim at demonstrating the viability of the system to print new 3D parts with enhanced properties for TR. With this development we aim at fostering the research and validation of the technology for new applications in RM accelerating the uptake of the technology in clinical applications. This project will help to bring the technology to the patients sooner.

3D printing or 3D AM has shown a huge field of application in TE. Nevertheless, there are still many problems to solve and barriers to overcome related to biomaterials, cell types extraction and treatment, growth and differentiation factors, and technical challenges related to the sensitivities of living cells and the construction of tissues and the complexity of non uniform vascular structures that cannot be easily manufactured layer by layer. These problems have to be addressed towards the clinical application. Following the review published in Nature biotechnology by Sean Murphy & Anthony Atala with the title of "3D bioprinting of tissues and organs" these problems can be classified as (Murphy and Atala 2014):

- Related to bioprinter technology: It is necessary the further development of bioprinting technologies compatible with physiologically relevant materials and cells, improving the resolution and the speed of the printing and combining different bioprinting technologies in order to achieve results that, after maturation, mimics the structure of living tissues.
- Related to biomaterials: It is necessary to develop new biomaterials that after the printing and maturation can mimic the biological materials with similar mechanical and chemical properties. These materials have to be printable and its parameters have to be controllable either during the printing process or afterwards.
- Related to cell sources: It is necessary to work more in the characterization and proliferation of cells, having access to a higher quantities of cells and developing procedures that increase the viability of them. It is also needed to overcome the problems currently found when working with cells in the lab.

- **Vascularization and innervation:** If we want to be able to manufacture complex tissues and in the future organs, we need to develop a reliable technology that can manufacture veins, arteries and nerves. These tubes may be manufacturing in the printing process, incorporated afterwards or inducible using pharmacologic or GF signalling. But the high 3D non uniformity of vasculature makes difficult to generate these geometries layer by layer in an additive manufacturing procedure. These structures are necessary to generate functional tissues.
- **Related to maturation:** After the printing process, time is required for assembly and maturation before the cells can interact and create tissues. It is necessary to develop new maturation strategies and also non invasive procedures to assess the quality of the formed tissue. Specific bioreactors have to be developed to maintain tissues *in vitro*, contribute to the nutrient exchange, and reproduce the physiological conditions necessary to create tissues.

In the present project we want to be part of this new scientific revolution and develop the tools that help researchers to find solutions to solve these issues. In 2011 we identified the need of a reliable and adaptable machine to be used with different configurations and in different applications that can help to overcome these barriers. Nowadays different commercial bioprinters have been developed, but so far ours is the only customizable platform that can be configured and adapted to the specific aims. We have been the world pioneers in creating bioprinting based procedures adapting the software and the hardware to the specifications and the final objective of the research. Using engineering state of the art technologies it is possible to generate a system, with its software and manufacturing algorithms, that can manufacture layer by layer 3D

constructs with customized external shapes and an internal meshed structure. Each layer and mesh filament can be seeded with cells in order to *in vitro* produce a 3D structure that, after maturation, mimic a human living tissue. The cells in this 3D construct will behave in a similar way as they do *in vivo*, producing the right ECM and regenerating the damaged tissues.

For the creation of a living tissue it is crucial the bioprinting process and the ingredients selected to achieve the objective to create a functional specific tissue. The selection of the right ingredients and the bioprinting procedure will be very important in the success of the creation of functional living tissues, but these are not the only important things to consider. If we think about bioprinting as a technology to recreate all the structure in the same form as shown in a living tissue, we are going to fail. We have to think on bioprinting as a way of creating cell laden 3D constructs as a precursor of a functional tissue. The maturation and tissue formation process will be as important or even more than the bioprinting one. Considering the strategies of both blocks in the diagram below will be crucial to obtain the desired functional tissue (Figure 8).

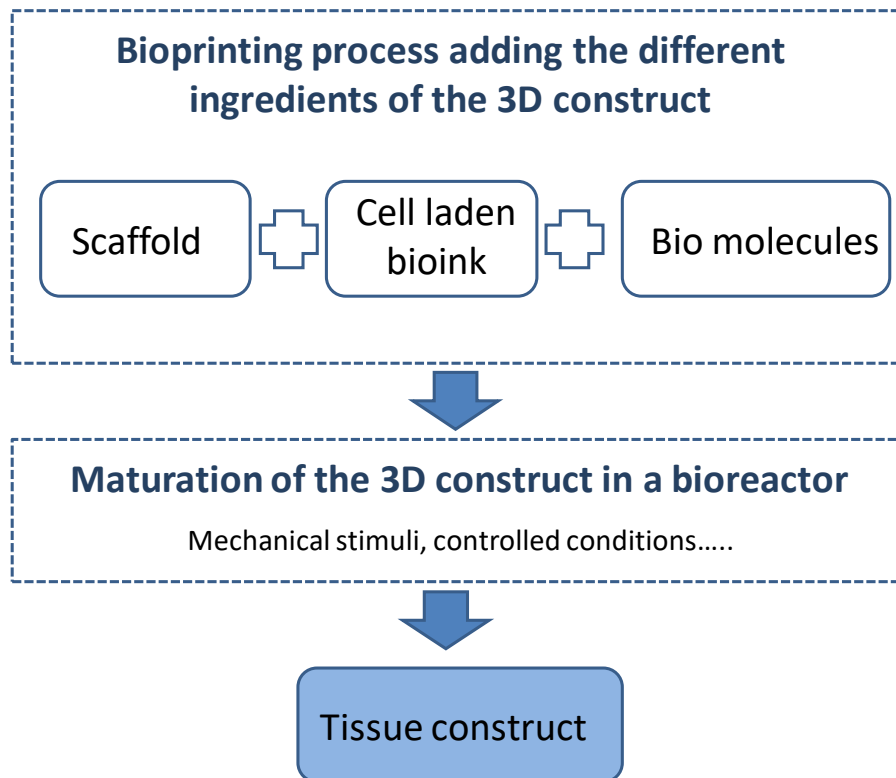


Figure 8 Two blocks of processes to be defined to design a successful strategy to create a functional living tissue

1 Stem cells-based therapies and regenerative medicine

The US National Institutes of Health defined regenerative medicine as "the process of creating living, functional tissues to repair or replace tissue or organ function lost due to age, disease, damage, or congenital defects". Many of these processes involve the use of SC, biomaterials and another signalling biomolecules as GFs.

The main properties of SC are the self-renewal and the regeneration potency. Self-renewal relates to cell division ability while maintaining the undifferentiated state. Potency relates to the capacity to differentiate into tissue specific and specialized cell types (Obokata and Vacanti 2014).

SC can be classified according to their differentiation potency as totipotent, pluripotent, multipotent, oligopotent and unipotent. Totipotent SC can differentiate into embryonic

and extra embryonic cell types. These cells are produced from the fusion of an egg and sperm cell and can construct a complete, viable organism. (Mitalipov and Wolf 2009). Pluripotent SC are the descendants of totipotent cells and can differentiate into nearly all cells derived from any of the three germ layers, endoderm, mesoderm and ectoderm (Ulloa-Montoya, Verfaillie et al. 2005). Multipotent SC can differentiate into a number of cell types. Oligopotential SCs can differentiate into only a few cell types. Unipotent cells can produce only its own type of cell having the property of self-renewal. Non-SCs are called progenitor cells (Obokata and Vacanti 2014). The most important difference between SCs and progenitor cells is that SCs can replicate indefinitely, whereas progenitor cells can divide only a limited number of times (Weissman, Anderson et al. 2001).

SC cells can also be classified according to the accessible source as embryonic stem cell (ESC) and adult SC. Adult SC, also known as somatic SC, are SCs which maintain and repair the tissue in which they are found. They can be found in children and adults (Obokata and Vacanti 2014).

Since the discovery of the potential of SC in the 20th century many clinical applications have been reported. In recent years, SC technology has made a major contribution to the field of RM. Another results from this 21st century as Nobel prize awarded induced pluripotent stem cells (iPSCs), have opened also a lot of possibilities for researchers. iPSCs are a type of pluripotent SC artificially derived from a non-pluripotent cell as somatic cells, by means of inducing the expression of specific genes (Takahashi and Yamanaka 2006). Also, some recent studies show the potential of iPSCs in cartilage applications (Castro-Vinuelas, Sanjurjo-Rodriguez et al. 2018).

An interesting type of adult and non-hematopoietic SCs are mesenchymal stem cells (MSCs). MSCs can differentiate into tissues that have both mesenchymal and non-

mesenchymal origin. MSC have been differentiated into osteoblastic, chondrogenic, and adipogenic cells amongst others (Shiota, Heike et al. 2007). MSCs have been harvested from many tissues, being easily isolated and expanded in the labs. The therapeutic potential of SC include the areas of immune associated diseases, heart diseases, tumours, ischemic injury and orthopaedics as critical size bone defects, metabolic bone diseases and cartilage regeneration amongst others (Rastegar, Shenaq et al. 2010) (see Figure 9).

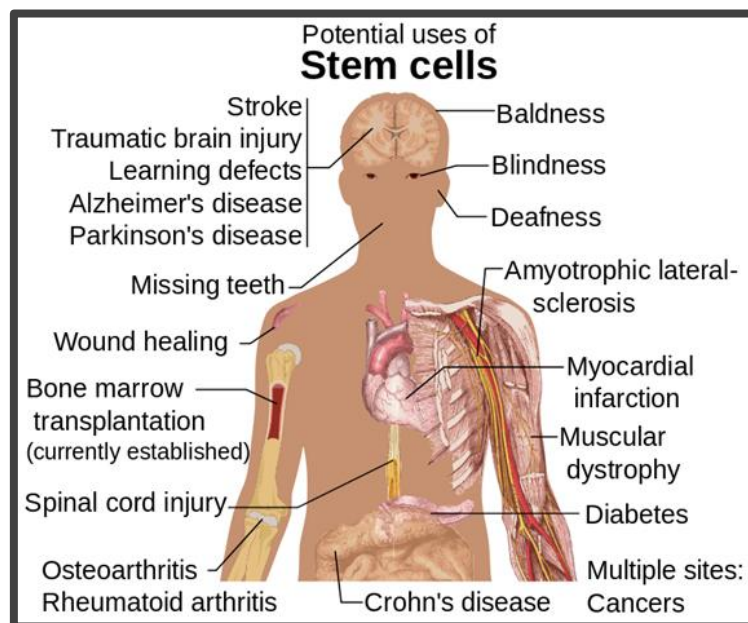


Figure 9 Potential uses of stem cells (source Wikimedia Commons)

Cartilage found in the joints is a connective tissue without innervations and vascularization composed of an specific ECM (Bhosale and Richardson, 2008). This lack of vascularization makes the healing process slow (Fuller and Ghadially 1972) and results in a fibrous scar-like tissue which functional properties are different from the hyaline cartilage leading to irreversible tissue degeneration (Shelbourne, Jari et al. 2003) (Fosang and Beier, 2011). Current surgical treatments as bone marrow stimulation, mosaicplasty and autologous chondrocyte transplantation (ACT) are not very effective, motivating the development of new approaches. In this sense, TE and, in

particular, bioprinting have emerged as an alternative (Koga, Engebretsen et al. 2009) (Rai et al., 2017).

SC based therapies for cartilage regeneration have been successful in animals *in vivo* however TE techniques in humans are still in a starting point of development. Higher level of evidence studies are needed, and any stated benefit have to be supported with scientific results (Pastides, Chimutengwende-Gordon et al. 2013).

The synergies of AM and SC therapies are very interesting. Joining together both areas of expertise will bring promising therapeutic solutions in the next years. Evidence studies to probe the effectiveness of these therapies are needed. New tools to facilitate researchers to undergo this evidence studies using 3D printing have to be developed.

1.1 Differentiation, dedifferentiation and transdifferentiation of SC

In 1998 a group led by Dr. James Thomson at the University of Wisconsin developed a technique to isolate and grow human ESC (Thomson et al., 1998). In the last decades different niches of SCs have been identified and characterized in adult organs (Rezza, Sennett et al. 2014) as the blood (Zvaifler, Marinova-Mutafchieva et al. 2000), the umbilical cordon (Troyer and Weiss 2008), the bone marrow (Jones, Crawford et al. 2008), and the AT (Pittenger, Mackay et al. 1999; Zuk, Zhu et al. 2002), amongst others (Smith, Neaves et al. 2007).

Isolation of SCs can be a delicate and multistep process. Protocols need to be adjusted based on the SC source or species. The isolation of SCs is crucial to get the correct type of cell without damaging them and can be done with techniques as gradient separation,

as with Percoll or Histopaque, or enzymatic digest, as with trypsin and collagenase (Fernandes, Diogo et al. 2013).

Cellular differentiation (CD) is the process by which a cell becomes more specialized. Differentiation is a normal process that occurs many times during the development of an human being and in tissue repair processes and turnover (Juliandi, Abematsu et al. 2011). **Dedifferentiation** is a cellular process in which a differentiated cell reverts to an earlier developmental stage (Schnabel, Marlovits et al. 2002). **Transdifferentiation** is the process where one mature cell transforms into another mature cell directly without undergoing an intermediate pluripotent state or progenitor cell type (Graf and Enver 2009). Differentiation related problems have to be solved in order to clinically use stem cells-based therapies. Researchers have still to deeply investigate the mechanisms that induce CD and use it in order to develop regeneration strategies without the drawbacks that cause CD.

Currently large-scale expansion of highly functional adult human MSCs is an unaddressed challenge. Adult human MSCs undergo drastic phenotypic changes during prolonged culture on tissue culture materials. Specifically, the proliferation capacity of the cells decreases, the self-renewal capacity of the cells decreases, and the cells often begin to express behaviour of cells with a committed lineage or reach senescence. Furthermore, MSC quantity/quality declines with donor age and disease, thus it is indeed challenging to expand sufficient numbers for treatments in older donors who are typically the patients in need of such therapy. These limitations clearly illustrate the need to develop cell culture conditions which enable prolonged expansion of the SCs without loss of their SC characteristics. One type of cell culture substrate which has recently shown promise in maintaining adult human MSCs phenotype during *ex vivo* expansion is adult human MSCs decellularized ECM (Ng, Sharif et al. 2014).

Cell culture quality is a key factor in RM and it is necessary to develop systems that allows the scale up of the procedures maintaining the quality of the resulted products (Placzek, Chung et al. 2009).

1.2 Stem cells derived from adipose tissue (ASCs)

AT is a specialized connective tissue derived from preadipocytes that plays a very important role in homeostasis. There are two types of AT in the body whose function appears to be clearly differentiated, white AT (wAT) (Vazquez-Vela, Torres et al. 2008) and brown AT (bAT) (Cannon and Nedergaard 2004). wAT stores energy reserves as fat, whereas brown AT has a metabolic function of lipid oxidation to produce heat.

Although the characteristic cell of AT is the adipocyte, this is not the only cell type present in AT, neither the most abundant. Other cell types in AT described include preadipocytes, macrophages, neutrophils, lymphocytes, endothelial cells and SC (Esteve Ràfols 2014). A type of multipotent MSCs were identified by several studies to exist in fat tissue, and designated as adipose-derived stem cell (ASC) (Zuk, Zhu et al. 2001).

Bone marrow stromal cells (BMSCs) are the commonly used seed cells in some applications of TE. However, due to the limitation of the obtainable amount of autologous bone marrow, extensive *in vitro* culture is routinely required to achieve a therapeutic cell dose, whereas long-term *in vitro* expansion is not favourable for cells to maintain their genomic stability as stated before. Therefore, it is of great interest to use an alternative cell source which is abundant, easy to access, easy to expand in culture and with high differentiation potential such as ASCs. Compared with BMSCs, ASCs obviously exhibit advantages including ease of isolation, relative abundance, rapidity of expansion, and multipotency that is independent upon serum source and quality (De

Ugarte, Morizono et al. 2003). AT is easy to access in all individuals and contains a large proportion of MSC, which account for about 5% of all stromal cells, yielding a density about 100 times that found in bone marrow (Jurgens, Oedayrajsingh-Varma et al. 2008). So far, ASCs have been effectively differentiated into different cell lineages to regenerate tissues using 2D and 3D models, as bone (Xu, Malladi et al. 2005; Hattori, Masuoka et al. 2006; Weinzierl, Hemprich et al. 2006), cartilage (Awad, Wickham et al. 2004; Wei, Sun et al. 2007), AT (Yoshimura, Sato et al. 2008) and neurones (Lin, Xin et al. 2008).

Despite the explained in this section the reality is that either ASC and BMSC have supporters and detractors. Future research is needed in order to define which are the best ingredients and procedures to create a functional tissue. Probably none of them ASC and BMSC are better than the other by itself, and the key to success has to be found in a combination with the other factors and maturation procedure.

Infrapatellar fat pad (IFP) of patients with osteoarthritis (OA) contains multipotent and highly clonogenic ASCs that can be isolated by low invasive methods. It has been demonstrated that extracts obtained from chondrocytes of osteoarthritic knees promote chondrogenic differentiation of autologous IFPSCs. Moreover, combination of transdifferentiated IFPSCs with biodegradable Poly(lactic-co-glycolic acids) (PLGAs) 3D scaffolds can serve as an efficient system for the maintenance and maturation of cartilage tissue (Lopez-Ruiz, Peran et al. 2013).

1.3 Problems related to stem cell therapies

SC show a huge potential in RM as they are able to form new tissue and regenerate injuries, but there are still many problems related to their use that have to be solved in

order to offer a reliable and safe treatment for patients. It is still not understood the process of TR and tumour formation. Differentiation, dedifferentiation and transdifferentiation processes have to be deeply investigated and understood. The related problems of dedifferentiation and transdifferentiation and its mechanisms have to be investigated.

In order to utilize MSCs it is important to expand these cells *in vitro* in order to obtain sufficient quantities for therapeutic uses. Unfortunately MSC demonstrate limited and highly variable proliferation and differentiation capacity *in vitro* (Digirolamo, Stokes et al. 1999).

Tumour and more rarely teratoma¹ formation is one of the most important drawbacks of using SC for RT. Understanding the process beyond the formation of new tissues and tumors are a key factor for the success of SC related therapies (Hentze, Soong et al. 2009).

Regarding the use of genetics, TE can generally be divided into three main methodological areas of interest: i) direct gene delivery; ii) cell therapy that does not involve genetic modification; and iii) genetically modified cell-mediated therapy (Sheyn, Mizrahi et al. 2010). Genetically engineered cell therapy employs tissue-specific or therapeutic genes and primary cells that over express these genes, to produce therapeutic proteins at sites of regeneration or to differentiate new cells in the desired cellular lineage, and thus promote TR (Kimelman, Pelled et al. 2007). Nevertheless, overproduction of proteins can be problematic.

¹ A teratoma is an encapsulated tumor with tissue or organ components resembling normal derivatives of more than one germ layer. Although the teratoma may be monodermal or polydermal (originating from one or more germ layers), its cells may differentiate in ways suggesting other germ layers. The tissues of a teratoma, although normal in themselves, may be quite different from surrounding tissues and may be highly disparate. Teratomas have been reported to contain hair, teeth, bone and, very rarely, more complex organs or processes such as eyes.

In cartilage regeneration, the chondrogenic factors have very short half-lives. Insufficient expression of chondrogenic genes and their products will result in dedifferentiation of the cells (Xia, Jin et al. 2009). Researchers are trying to combine a few chondrogenic factors together in order to further promote chondrogenic differentiation and maintain high levels of the chondrogenic growth and transcription factors needed for proper tissue development (Steinert, Palmer et al. 2009). An enhanced understanding of the optimal levels of chondrogenic genes and their cross-signalling and interrelationships is needed to advance this field.

Increasing cell survival and reproduction is a key factor for the industrial application of SC based RT. MSCs have been expanded in different kinds of mediums as fetal bovine serum (FBS) and autologous human serum (Horwitz, Gordon et al. 2002). However, supplementation with FBS has several risks, such as disease transmission and immune reaction (Selvaggi, Walker et al. 1997). Increasing the safety of MSC transplantation requires the use of safe and effective medium.

2D cultures do not mimic real tissue structures, novel systems and processes to manufacture tissue like construct as AM have to be further developed. The efficiency and cell culture quality have to be improved towards a reliable clinical use. Sufficient evaluation of scaffolds and the control of foreign body reactions are essential, even for the autologous transplantation, because immunoglobulins or complements secreted in association with the foreign body response against scaffold materials interfere with the survival of the transplanted cells, if they are not close to blood cells under normal immune conditions (Kanazawa, Fujihara et al. 2013).

Ethical problems related to the use of totipotent ESC seems to be overcome due to last year's advances (Petersen and Niklason 2007) and the discovery of new cell sources and

iPSCs. However there are still some problems related to iPSCs use in clinical therapies that have to be solved (Zhao, Li et al. 2009; Zhou, Wu et al. 2009).

Large-scale expansion of functional adult human mesenchymal SC (aMSCs) is another problem that has to be addressed as drastic phenotypic changes occur during prolonged culture on tissue materials and low quantity of cells and tissue formation required long culture periods (Ng, Sharif et al. 2014).

In the area of cartilage regeneration, the chondrocyte appears as the best candidate for repairing cartilage defects. Chondrocytes can be harvested from joint or nasal cartilage (Vinatier, Magne et al. 2007). However, cartilage harvesting is an invasive procedure that supplies a limited number of cells. In addition, when chondrocytes are grown into single layers, they tend to dedifferentiate, acquiring a fibroblastic phenotype and ceasing to express the main chondrocyte markers (aggrecan and type II collagen) (Bonaventure, Kadhom et al. 1994).

To conclude, SC therapies show promising results in TR but It is necessary to develop a modular system that can produce 3D multi components parts made from different biomaterials, controlling the manufacturing parameters, allowing for the automation, scale-up and safety. This system will help researchers of the different areas to overcome the problems related to the use of SC therapies in RM.

2 Biomaterials for Regenerative therapies

There are different kinds of biomaterials with several characteristics such as strength, stiffness, biocompatibility, biodegradation ratio, thermal and electrical conductivity, density, porosity, temperature of fusion and roughness amongst others. Biomaterials can

be polymers, metals, ceramics and composites. Some applications of biomaterials are to replace or restore functions of: i) the cardiovascular system as cardiac pacemakers, artificial heart valves and totally artificial hearts; ii) the lung as oxy-generator machines; iii) the eyes as contact lens and intraocular lens; iv) the ear as cochlea implants; v) the bones as bone plates, intra-medullary rods and joint prostheses; vi) the kidney as kidney dialysis machines; and the bladder as catheters and stents (Ivanova, Bazaka et al. 2014).

Biomaterials are also widely used in RT. Most of them are manufactured from polymers mainly due to the biocompatibility and biodegradation ratio that can also be used to deliver biochemicals and signalling molecules to promote TR. In order to be used in 3D AM based regenerative therapies (RT) these materials have to meet some requirements to be printed using one of the available printing technologies (Chua, Leong et al. 2014). Polymeric biomaterials with excellent biocompatibility are being used as bioactive and biomimetic materials to promote the regeneration of damaged parts (He and Benson 2014).

TE has evolved as a new field, promising *in vitro* construction of whole transplantable tissues. Basically, three main components are required for successful TE (Figure 7): Firstly, a scaffold providing an adequate 3D surrounding. Secondly, a bioink containing a hydrogel with the appropriate cells which are able to differentiate and maintain the specific cell phenotype. Thirdly, the addition of the right bioactive substances such as GFs, cytokines, hormones or exosomes as a suitable stimulus for specific lineage differentiation of the cells (Kuo, Li et al. 2006).

Recent advances in 3D AM have open a wide range of new possibilities for the customization of regenerative devices, due to the possibility of computer aided reconstruction of the anatomical parts to be regenerated, giving custom made shape and internal multicomponent scaffolding structures, that facilitate the grown of cells, the

transportation of nutrients and the formation of new tissue (Leong, Cheah et al. 2003). In order to be able to recreate in 3D a living tissue it is necessary to print the scaffold structure, the compound containing autologous cells, the nutrients and other biomolecules as proteins, and fibers that can be also found in living tissues. Reproducing *in vitro* all these parts, or the promoters of these parts, is a key factor for the success of bioprinting technologies in RT (Schmeichel and Bissell 2003).

Now it is necessary to develop new technologies to be able to print the biomaterials needed for the regeneration of tissue injuries. One of the key parameters to be controlled is the velocity of biodegradation in order to meet the requirement of stiffness-regeneration velocity as too high biodegradable velocity may compromise the mechanical behaviour and too slow speed may not allow for the regeneration of the damaged part. The correct use of a material and an internal structure is a key factor and have to be deeply investigated (Sanz-Herrera, Garcia-Aznar et al. 2009; Sanz-Herrera, Garcia-Aznar et al. 2009).

There are two differentiated approaches in the science of biomaterials in RT. One aiming at producing human body like parts adding cells *in vitro*, using the biopolymer as a scaffold that give the 3D shape, the mechanical properties and being used as signalling molecules carriers to allow the cells regenerate the injury. A second one that aim at developing biomaterials that promote self TR without adding cells *in vitro*.

There have been made a lot of effort using ceramic materials for RT, mainly to replace bones, due to the ceramic like structure of bone matrix (Lopes, Martins-Cruz et al. 2018). Calcium phosphates have been widely investigated as a biomaterial for bone regeneration (Maeda, Hojo et al. 2013; Stiller, Kluk et al. 2014). Another technology using laser to produce calcium phosphates have been developed and is based on the dehydroxylation of hydroxyapatite, to obtain a material with a microstructure composed

of an alpha-tricalcium phosphate (α -TCP) matrix with nucleated tetracalcium phosphate (TTCP) grains, in coexistence with oxyapatite and amorphous calcium phosphate for the regeneration of severe trauma injuries. (Comesaña, Lusquiños et al. 2011). Unfortunately, the high temperature process don't allow the use of living cells during the manufacturing process, and a procedure as the one presented in this work, should be implemented.

Biodegradable implants have been reported decades ago for medical applications (Kulkarni et al., 1966; Kulkarni et al., 1971). The applications of biodegradable implants in orthopaedic surgery have been mandated from the need to eliminate implant removal operations. These materials are mainly polymers but also ceramics, are biocompatible and degrade after a period of time producing non-toxic compounds that can be metabolized by the organism. Biodegradable polymers can be classified depending on their natural or synthetic origin.

The first study concerning biodegradable materials used in implantation was presented in 1966 (Kulkarni, Pani et al. 1966) in which the biocompatibility of poly-L-lactic acid (PLLA) in animals was studied. The material proved to be non-toxic and gradually degraded. Nowadays, materials such as Poly(ortho esters) (POEs), Polycaprolactones (PCLs), Polyhydroxyalkanoates (PHAs), Polydioxanones (PDO, PDS), as well as Poly(lactic acids) (PLAs), Poly(glycolic acids) (PGAs) and their copolymers PLGAs are available for being used in implantation (Kontakis, Pagkalos et al. 2007). Furthermore, Pseudo-Poly(aminoacids) or polyaminocarbonates show promising properties (An, Woolf et al. 2000). Using copolymers made from the different types we can tune the degradation and physical properties.

The introduction of a porous structures has been reported to enhance both cell proliferation and albumin production of cell-laden hydrogels using HepG2 cells in

porous alginate hydrogels (Hwang, Sant et al. 2010). Previous works demonstrated good *in vitro* cytocompatibility of photosensitive gelatin methacrylamides for the encapsulation of fibroblasts, myoblasts, chondrocytes, endothelial cells, and cardiac cells (Nichol, Koshy et al. 2010; Schuurman, Levett et al. 2013).

Manufacturing composites structures can help to overcome the drawbacks of current available biomaterials. The combination of rigid scaffolds, hydrogels and fibres can increase the mechanical performance of the manufactured parts. A review show the various methodologies and approaches currently undertaken to create composite structures and their intended applications (Bosworth, Turner et al. 2013). The combination of scaffold architectures, that is one of the main advantages of using an AM technology, is showing potential with regards to therapeutic use within the TE community.

Although a lot of efforts have been made in the science of biomaterials, there is still a lot of things to do mainly adapting current manufacturing technologies to the manufacturing process of biomaterials in order to offer a reliable and safe way to regenerate tissue injuries.

2.1 Scaffolds

The most commonly followed TE approach involves transplantation of cells onto scaffolds. The scaffold attempts to mimic the function of the natural ECM, providing a temporary template for the growth of tissues. Scaffolds should have suitable architecture and strength to serve their intended function and provide a 3D environment that is desirable for the production of tissues (Yeong, Chua et al. 2004). They can be manufactured as: i) a rigid structure using ceramics and polymers with a well-organized

structure or as a sponge; ii) as a soft structure using hydrogels and biopolymers, and iii) with a mesh structure using fibres. A scaffold should: i) promote cell viability, differentiation, and biological ECM production, ii) have directed and controlled degradation, iii) adhere and integrate with the surrounding native tissue, iv) allow for the vascularisation, the diffusion of nutrients and waste products and v) provide mechanical integrity depending on the defect location span amongst others (Chung and Burdick 2008).

Polymers are the most common material used in scaffolds for RT due to their wide range of properties. Polymers can be classified as natural or synthetic (Paterson and Kennedy 1991). Scaffold architecture also plays a major role in the cellular behaviour. Computer aided design (CAD) libraries of scaffolds have been developed and will be an useful tool for researchers that want to find the optimal structure for its application. Different pore size to beam thickness can be tailored to develop structure with tailor made mechanical properties. These properties can be evaluated using finite element (FE) models (Chantarapanich, Puttawibul et al. 2012). Scaffolds with different properties and controlled architecture have been reported in the literature. Complex hierarchical scaffold designs can only be built using AM fabrication processes (Hutmacher, Sittinger et al. 2004; Tsang and Bhatia 2004).

Scaffolds structures have also been used in the regeneration of nerves comparing different kinds of biomaterials such as PLGA, poly(caprolactone fumarate) (PCLF), a neutral oligo [(polyethylene glycol) fumarate] (OPF) hydrogel, and a positively charged oligo[(polyethylene glycol) fumarate] (OPF+) hydrogel with a PCLF sleeve (Daly, Knight et al. 2013). The use of scaffolds from PCLF seeded with cells have also been investigated for intra-articular ligament injuries which are difficult to treat because of their poor regeneration potential. The use of these novel polymers to form a

“neoligament” seeded with progenitor cells, and GF show a high potential to regenerate native ligament tissue (Wagner, Bravo et al. 2013). Other widely used rigid biopolymers scaffolds for AM based RT are: PLA, PLGA, PGA, PCL, PHAs, PDO and PD.

Scaffolds in RM are also made of minerals and metals, mainly titanium and tantalum. These materials not always allow the regeneration of the tissue but promote the integration with the surrounding tissues and device integration, recovering the functionality (Pina, Canadas et al. 2017). Commercially-pure titanium (cp-Ti) and the titanium-aluminum-vanadium alloy (Ti6Al4V) used in custom made manufacturing of orthopaedic implants and prosthesis have also been used as scaffold in cell based therapies (de Peppo, Palmquist et al. 2012). β -tricalcium phosphate (β -TCP) has also been used as a scaffold showing a relatively good cell–scaffold interaction (Santos, Silva et al. 2012). This metal is not biodegradable but the printed mesh structure and the tissue grow through it can avoid the negative effects of shielding.

Some researchers prefer synthetic polymers because the mechanical properties and chemistry can be controlled. The use of scaffolds from cadaveric bone has also been reported in the bibliography. MSCs have been also using with allograft bone to produce a living composite in application as a technique of impaction bone grafting (IBG) in total hip reconstruction (THR) (Bolland, Tilley et al. 2007). The use of Starch based polymer powders as corn starch, dextran and gelatine for AM based RT have also been reported (Lam, Mo et al. 2002).

3D microstructures and nanotopographies on cellular functions, including cell adhesion, proliferation, morphogenesis and differentiation play an important role in TE. Recent development of fabrication methods to produce 3D fibrous scaffolds with microporous structures and nanotextures have been reported (Ng, Zang et al. 2012).

Physicochemical features of a cell nanoenvironment may exert important influence on SC behaviour. Engineering of functional biomimetic scaffolds that present programmed spatio-temporal physical and chemical signals to SC holds great promise in SC therapy (Das and Zouani 2014).

Moving to the area of cartilage regeneration, some natural polymers that have been explored as bioactive scaffolds for cartilage regeneration include the hydrogels: alginate, agarose, fibrin, hyaluronic acid (HA), gelatine, chitosan, chondroitin sulphate; and fibres of collagen and cellulose. Synthetic polymers currently explored for cartilage repair include: polyesters, fumarates, and polyurethanes (Chung and Burdick 2008) (Chung et al., 2008), PLA and PGA (Cui, Wu et al. 2009) amongst others.

Adapting current manufacturing technologies or developing new ones for the manufacturing of novel scaffolds that support cells and delivery signalling molecules it is necessary to improve the results towards manufacturing *in vitro* tissue like parts that regenerate injuries.

Using 3D bioprinting we can develop strategies for creating multicomponent constructs composed of synthetic and natural polymers taking advantage of the benefits of both kinds of materials.

2.2 Hydrogels

As said before the scaffold structure can be rigid, using rigid polymers, or non-rigid, using biomaterials as hydrogels and other biopolymers (Dhaliwal and Lopez 2018; Francis, Greco et al. 2018). Hydrogels can also be used as bioinks. Even when the scaffold is rigid it is necessary the use of hydrogels, containing cells, to be printed

attached to the mesh of the scaffold. This makes hydrogels to be an important part of the game in TE.

The term hydrogel relates to water-containing gels, consisting on polymer networks that are insoluble in water, where they swell to an equilibrium volume but retaining their shapes. Hydrogels are composed of a network of polymer chains that are hydrophilic, sometimes found as colloidal gels in which water is the dispersion medium (Baroli 2007). It is also possible to produce hydrogels containing a significant portion of hydrophobic polymers (Peppas 1992).

Hydrogels can be classified as natural or synthetics; degradable or non-degradable; physical or chemical; neutral, cationic, anionic, amphiphilic; amorphous or semi-crystalline amongst other (Baroli 2007). Hydrogels are highly absorbent, they can contain over 90% water. Hydrogels also possess a degree of flexibility very similar to natural tissue, due to their significant water content. One of the main disadvantages of processing hydrogels is the difficulty to shape them in predesigned geometries. Some 3D printing technologies are available or can be adapted to print some hydrogels. Hydrogels can be printed with a rigid scaffold structure or can serve as the scaffold structure itself, mainly in the application of soft TR. The combined potential of hydrogels and 3D printing is very interesting towards developing bioprinting solutions that can mimic the behaviour of living tissues. Hydrogels can also be used in hard TR as a component attached to the rigid mesh containing cells or other signalling molecules. Rapid prototyping techniques have shown a high potential for the production of scaffolds with the purpose of cell seeding and/or cell encapsulation (Billiet, Vandenhaute et al. 2012).

There are many different types of hydrogels on the market, and many of them have been investigated for being used in TE and RT. A list of different hydrogels, in a concise but

inclusive review of hydrogel applications, synthesis, properties and characterization can be found in the literature (Baroli 2007). Some of them can be already be used in AM based RT (Billiet, Vandenhaute et al. 2012).

One of the most widely used hydrogel for cartilage regeneration is sodium alginate solution mixed with a CaCl_2 solution (Schuurman, Khristov et al. 2011). Alginate is a fairly nontoxic and non-inflammatory polysaccharide derived from brown seaweed. Alginate has been approved in some countries for medical applications. Alginate is biodegradable, has controllable porosity, and may be linked to other biologically active molecules (Jia, Richards et al. 2014). Alginate has been explored for use in liver, nerve, heart, and cartilage TE. Unfortunately, some drawbacks of alginate include mechanical weakness and poor cell adhesion (Glicklis, Shapiro et al. 2000).

Microdeposition of alginate and models to characterize the process have been developed using FE diffusion models (Tirella, Orsini et al. 2009). The characterization of hydrogels using mathematical models is necessary in order to better understand the processes behind for optimization.

Some of the widely used hydrogels, in the printing technologies area, that use a laser beam as a source of power (laser based printing technologies) that produce the solidification of the hydrogels are composed of the following components: i) gelatine, methacrylate; ii) gelatine, methacrylamide (Billiet, Gevaert et al. 2014); iii) HA, methacrylate; iv) cystein, modified agarose; v) PEG, D(M)A (Liu and Bhatia 2002); vi) Alginate, Acrylated-TMC TMP; vii) gelatine, methacrylamide; viii) PEG, DA; ix) gelatine, methacrylamide; x) Fibronectin; xi) Bovine serum albumin (BSA), PEG-DA. Polyhydroxyethylmethacrylate (monomer HEMA) (Billiet, Vandenhaute et al. 2012) .

Some of the hydrogel materials explored in the printing technologies area that use a nozzle (nozzle-based printing technologies) to deposit material during the printed process are composed of the following components: i) gelatine, hyaluronan; ii) alginate, fibrinogen, chitosan; iii) collagen, chitosan, hydroxyapatite; iv) gelatine, ethanolamide methacrylate; v) hyaluronan, methacrylate (Toh, Lee et al. 2010); vi) PCL hybrid with alginate; collagen; vii) PCL, PLGA hybrid with acetocollagen; viii) gelatine or HA; ix) matrigel; x) Agarose; amongst others (Khalil and Sun 2007; Billiet, Vandenhaute et al. 2012; Saravanan, Vimalraj et al. 2018).

Some compounds that can be manufactured using other 3D printing technologies are composed of the following components: i) starch, cellulose, dextrose; ii) starch, cellulose fiber, sucrose, maltodextrin; iii) corn starch, gelatine, dextran; iv) starch, polyurethanes, PEG; v) PEO, PCL; vi) PLLGA, Pluronic F127; vii) HA, Cellulose, Starch; viii) PEG, Collagen, PDL; ix) Collagen; x) Alginate, Gelatine; xi) Fibrin (Billiet, Vandenhaute et al. 2012).

HA is also a compound widely used as an hydrogel because of its high biocompatibility and low immunogenicity (Ding, He et al. 2012). But its low mechanical strength limits its use to low mechanical performance tissues.

Physical hydrogels are receiving a great attention because they are produced without any chemical reaction. This make them suitable for cell and sensitive molecule (e.g., cytokine) encapsulation, avoiding the use of toxic or extremely reactive molecules, that have to be removed, used to initiate chemical crosslinking reactions (Baroli 2007).

Degradability is an important feature of hydrogels for TE. In fact, from the perspective of an ideal regeneration, initial support of implanted matrices/scaffolds should be substituted by the ingrowth of native ECM produced by the regenerated tissue.

Consequently, ideal matrices/scaffolds should degrade at the same rate of regenerated tissue growth.

The use of hydrogels has been severely limited due to swelling under physiological conditions, that cause a decrease in their mechanical properties. Kamata et al. (2014) have reported the synthesis of injectable “nonswellable” hydrogels from hydrophilic and thermoresponsive polymers, in which two independently occurring effects (swelling and shrinking) oppose each other. The suppression of swelling helps retains the mechanical properties of hydrogels under physiological conditions. Next steps are to tune these hydrogels to be printable and cell friendly (Kamata, Akagi et al. 2014).

Adapting current manufacturing technologies or developing new ones for the manufacturing of novel hydrogel with enhanced characteristics for AM based RT that support cells and delivery signalling molecules it is necessary to improve the results towards manufacturing *in vitro* tissue like parts that regenerate injuries (Hinton, Jallerat et al. 2015).

3 Growth factors

GFs are human body’s substances capable of stimulating cellular growth, proliferation, healing, and CD. Usually it is a protein or a steroid hormone. GFs are important for regulating a variety of cellular processes and typically act as signalling molecules between cells. GFs often promote cell differentiation and maturation, for example, bone morphogenetic proteins (BMPs) stimulate bone cell differentiation, vascular endothelial

growth factors (VEGFs) and fibroblast growth factors (FGFs) promote blood vessel differentiation and angiogenesis ².

With the attempt of mimicking the body environment, matrices are more often designed not only as a 3D support for cells, but also as a delivery system of tissue-inducing substances as cytokines, growth factors, exosomes, matrix metalloproteinases, genetic material. The main strategies of delivery are: i) entrap cells that normally produce the substance(s) of interest; ii) entrap cells that were genetically modified to produce the substance(s) of interest; and iii) entrap or co-entrap the molecule(s) of interest. However, the latter strategy is more challenging than it seems. In fact, tissue-inducing substances are generally fragile and sensitive ones, and may be negatively affected by encapsulation methods, which in turn may produce the delivery of a partially or nonactive molecule, or worse trigger immune responses (Singh and Singh 2003).

Some interesting publications about the various hydrogel technologies that have been proposed to control the release of bioactive molecules of interest for TE applications can be found in the literature (Censi, Di Martino et al. 2012). Delivery regimes and release kinetics are very important parameters to be taken into account to avoid unwanted side effects and toxicity and get the optimal results (Chen, Shelton et al. 2009).

There are many other GFs commonly used in TE are:

- EGF, epidermal growth factor
- FGF(s), fibroblast growth factor(s)
- IGF(s), insulin-like growth factor(s)
- KGF, keratinocyte growth factor
- NGF, nerve growth factor

² en.wikipedia.org/wiki/Growth_factor

- OP-1, osteogenic protein-1
- PDGF(s), platelet-derived growth factor(s)
- TGF- β , transforming growth factor- β
- TGF- α , transforming growth factor- α

For example BMPs have been extensively studied and 20 members of the BMP family have already been identified. Some of them approved for clinical use (Smoljanovic, Bojanic et al. 2009). The effect and the correct use of GF have to be deeply investigated in order to benefit from their advantages and avoid their drawbacks.

A number of GFs like TGF- β , FGF, BMP, and IGF, along with other soluble factors like HA, chondroitin sulphate, and insulin, have been explored for their effects on cartilage TE (Sheyn, Mizrahi et al. 2010). Members of the TGF- β family are commonly used to induce chondrogenesis in embryonic (Hwang, Kim et al. 2006) and adult MSCs (Iwasaki, Nakata et al. 1993), to increase cartilage ECM synthesis (Kim, Park et al. 2003), and to enhance proliferation of chondrocytes (Vivien, Galera et al. 1990).

However, there are some disadvantages with the use of GF and the safety in the clinical use has to be investigated deeper to allow clinical use.

A better strategy might be to construct scaffolds which are able to deliver differentiation factors directly to the cells embedded in the scaffold. These materials will lead to limitless possibilities for cartilage regeneration. However, they require further investigations for clinical use (Koga, Engebretsen et al. 2009).

GFs and other additives may be added to culture media *in vitro* or incorporated into scaffolds for *in vivo* delivery to control CD and tissue formation (Lopez-Ruiz, Jimenez et al. 2018). Further efforts in the design or optimization of materials with minimal tissue response, sufficient stiffness, appropriate degradation and release profiles are needed in order to make the translational step between academia and clinics successful.

Current AM technologies have to be enhanced in order to efficiently deliver these biomolecules that are a key factor for the success of AM based RM.

4 Additive manufacturing technologies for RM

3D printing or AM are a wide range of technologies that allow to create a 3D object from different materials, using a 3D model or other electronic data source through additive processes (Grimm 2004). In the eighties one of the earliest patents involving AM was awarded to Chuck Hull who founded in 1986 3D Systems Corp. Hull invented the process nowadays known as stereolithography employing ultra violet lasers to cure photopolymers³. Hull also developed the Standard Tessellation Language (STL) file format widely accepted by 3D printing software, as well as the strategies of slicing a 3D object. During the eighties another AM technologies were developed but this time using metals such as Selective laser sintering (SLS) and Direct Metal Laser Sintering (DMLS), although they were not yet known as 3D printing or AM at the time. In 1990, the plastic extrusion technology most widely associated with the term "3D printing" was commercialized by Stratasys under the name of fused deposition modelling (FDM). Some years later the company called Z Corporation commercialized an MIT-developed additive process under the trademark 3D printing, referring at that time to a proprietary process inkjet deposition of liquid binder on powder⁴. The fields of applications of AM started to grow reaching even the field of RM. Several 3D tissue fabrication techniques based on methods for scaffold fabrication, cellular assembly, and hybrid hydrogel/cell have been described in the literature. Some based on a heat source, others on a light

³ Hull CW. (1986). Apparatus for production of three-dimensional objects by stereolithography. Patent US4575330 A. Published 11 March 1986.

⁴ en.wikipedia.org/wiki/3D_printing

source, some that use adhesives and even others that indirectly fabricate a mold (Tsang and Bhatia 2004). In the next sections we will briefly describe the different AM technologies reported and their advantages and limits to be used in RM.

There are many different types of technologies used to print multimaterial parts composed of hydrogels containing cells, scaffolds and fibers (Melchels, Domingos et al. 2012). Another methods of printing based in robotics arms have also been developed and include the design of a new concept of printing head (Ozbolat, Chen et al. 2014).

4.1 Types of AM technologies

Many different classifications of AM technologies have been reported. Based on the technology used to create the layers, Billiet et al. (2012) have classified the technologies into **laser based systems**, **nozzle based systems** and **printer based systems** (Billiet, Vandenhoute et al. 2012). i) Laser-based systems benefit from the laser beam energy to melt powder material to fabricate rigid scaffolds or to photo polymerize a liquid as a basis to fabricate cross-linked polymeric TE scaffolds. The use of heat limits the biomedical application of the technology in cell-based therapies. Some improvements in the manufacturing process mainly in the software have to be implemented in order to be suitable to manufacture cell seeded scaffolds. ii) Nozzle based technologies generally melt polymers before depositing it in a bed and involves elevated temperatures, which are undesirable from the perspective of scaffold bioactivity. Again, improvements in the manufacturing process have to be implemented in order to be suitable for direct cell dispensation AM technologies. iii) Printer based systems works with powder beds and

deposition of a binder that fuses the particles, or directly depositing material using inkjet technology.

Some of the most interesting technologies for biomedical applications are:

Fused deposition modelling (FDM): by this process, a nozzle with a heater melts a thermoplastic filament and deposits it in a surface, drawing the outline and the internal filling of every layer. After one layer has been printed, the z-axis moves and a new layer is printed (Figure 10).

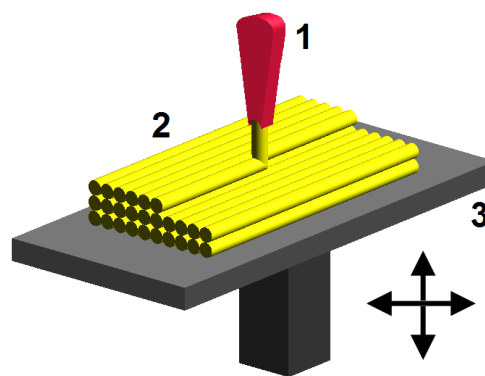


Figure 10 FDM working principle (source Wikimedia Commons)

FDM is an AM technology commonly used in modelling, prototyping, and production applications. FDM works on an additive principle by laying down material in layers⁵. With this technology we can do cheap models that can give us a real 3D idea of the model. FDM can be used in RM due to the possibility of manufacturing biopolymers as PLA (Figure 11), the capacity to print internal meshes and the roughness of the external shapes, due to layer deposition inaccuracies, that improve cell adhesion (Zein, Hutmacher et al. 2002).

⁵ en.wikipedia.org/wiki/Fused_deposition_modeling

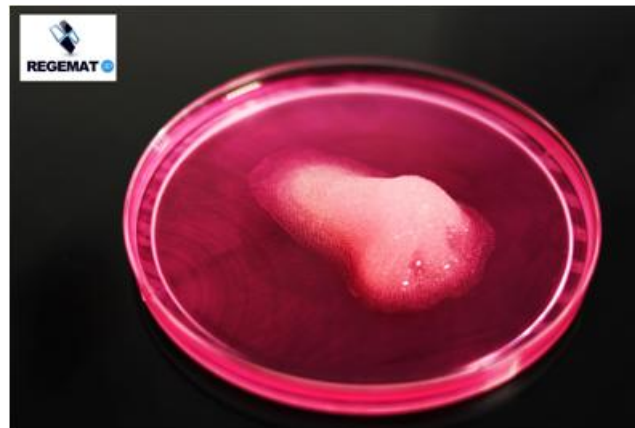


Figure 11 FDM model of a nose (courtesy of REGEMAT3D)

Stereolithography (SLA): this process uses a selective photo-initiated cure reaction of a polymer layer by layer with a continuous movement of the z-axis (Figure 12). This technology as many others in AM requires the use of supporting structures.



Figure 12 An SLA model of a medical an ultrasound device (courtesy of END Lab University of Granada)

Selective laser sintering (SLS): this technique uses a laser emitting infrared radiation, to selectively heat powder material just beyond its melting point. The laser traces the shape of each cross-section of the model to be built, sintering powder in a thin layer. After each layer is solidified, the piston over the model retracts to a new position and a new layer of powder is supplied using a mechanical roller (Melchels, Domingos et al. 2012) (Figure 13) (Figure 14).

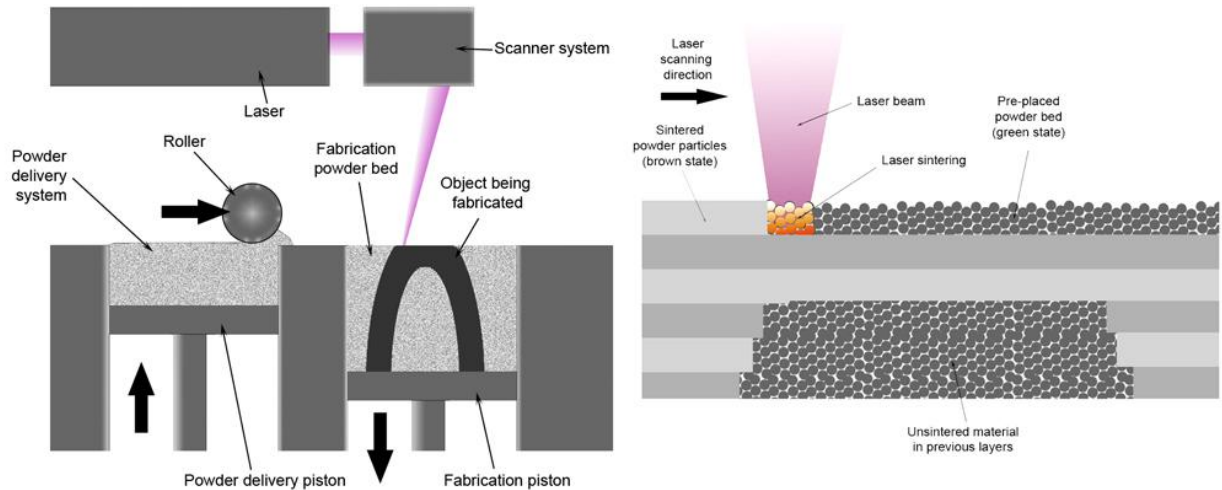


Figure 13 SLS working principle (source Wikimedia Commons)



Figure 14 SLS skull patient specific biomodel (courtesy of BRECA Health Care)

Selective laser melting (SLM) is similar to SLS but the material is fully melted rather than sintered. **DMLS** developed by EOS, it is similar to SLS but differ in technical details. **Electron beam melting (EBM)** is a type of AM for metal parts that was developed by Arcam AB in Sweden. It is similar to SLM, the main difference being that EBM uses an electron beam as its power source. EBM technology manufactures parts by melting metal powder layer by layer with an electron beam in a high vacuum (Figure

15). Unlike in the sintering techniques of SLS and DMLS, parts produced by the melting techniques of EBM and SLM are fully dense, void-free, and extremely strong. These metal printing technologies have been successfully used in the customization of medical devices (Ferrís-Oñate, Morales-Martín et al. 2010). Wiria et al. (2007) used SLS to fabricate TE scaffolds consisting of PCL and hydroxyapatite. Optimal sintering conditions for the powders were achieved by varying parameters such as laser power and scan speed. Studies of the sintered specimen morphology were performed by scanning electron microscopy (SEM) (Wiria, Leong et al. 2007).



Figure 15 EBM hip prosthesis stem(Ferrís-Oñate, Morales-Martín et al. 2010)

Adhesive Inkjet printing (AIP): this process uses a binder material that is deposited over the surface of a powder bed, joining particles together where the object is to be formed. A piston lowers the powder bed so that a new layer of powder can be spread over the surface of the previous layer and then selectively joined to it. The process is repeated until the 3D object is completely formed (Lam, Mo et al. 2002).

Laser cladding (LC): is an alternative technique for production of real functional parts from an electronic drawing of the part. This technique utilizes a laser as energy source to stack successive layers of a desired material following the pattern given by the

layered electronic design. The precursor material is feed in the form of powder which is injected into the laser focal spot and subsequently molten and solidified (Figure 16). Instead of just sintering the forming particles as in SLS, LC produces much stronger parts by complete melting of the precursor particles (Comesaña, Lusquiños et al. 2011).

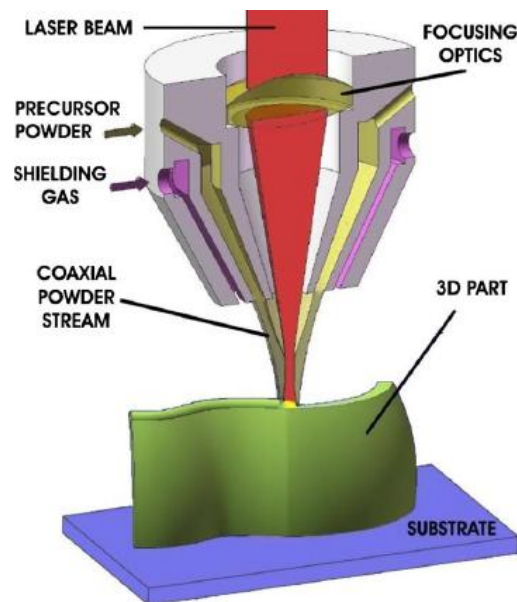


Figure 16 LC working principle (Comesaña, Lusquiños et al. 2011)

Two-photon polymerization (2PP): involves nearly simultaneous absorption of ultra-short laser pulses for selective curing of photosensitive materials. This process has recently been used to create small-scale medical devices out of several classes of photosensitive materials, such as acrylate-based polymers, organically-modified ceramic materials, zirconium sol-gels, and titanium-containing hybrid materials (Ovsianikov and Chichkov 2012). This technology has been used in parallel with **Laser-Induced-Forward-Transfer (LIFT)**. LIFT is a direct-writing technique allowing the deposition of tiny amounts of material from a donor thin film through the action of a pulsed laser beam. Although LIFT was originally developed to operate with solid films, it has been demonstrated that deposition is also viable from liquid films. In this case the transferred material is not vaporized; rather, a small amount of liquid is directly ejected

from the film to the receptor substrate, where it deposits in the form of a microdroplet. This makes LIFT adequate for biosensors preparation, since biological solutions can be transferred onto solid substrates to produce micrometric patterns of biomolecules (Ovsianikov, Gruene et al. 2010).

Some AM different technologies can be used simultaneously with SC therapies in order to produce custom made multimaterial components for TR. Basically, these layering methods fall into three basic types: liquid based, solid-based and powder-based RP systems (Peltola, Melchels et al. 2008).

One printing technology very interesting for the manufacturing of complex organs with vascularisation is the **Inkjet printing technology (IPT)**. IPT is based on propelling droplets or a continuous ejection of ink onto paper, plastic, or other substrates. IPT offers many advantages when the aim is to print complex organs (Nakamura, Kobayashi et al. 2005). IPT can control all of the small ink droplets, whose sizes are almost the same than individual cells, eject the droplets in their correct position, printing individual cells safely and controlling density, and their arrangements (Arai, Iwanaga et al. 2011). The advantages of IPT have also been reported by other groups (Boland, Xu et al. 2006). There are different IPT as **droplets on demand (DOD)** (Figure 17): with an electromechanical actuator, a thermal actuator or actuated by electrostatic vacuum; or **continuous ejection (CE)**. Using different hydrogels as ink we can use this technology for RT. This continuous 3D dispensing process is the basis of the system known as 3D-Bioplotter, introduced by Landers and Mülhaupt in 2000 at the Freiburg Research Centre (Landers and Mülhaupt 2000). The technique was specifically developed to produce scaffolds for soft TE purposes, and simplifying hydrogel manufacturing.

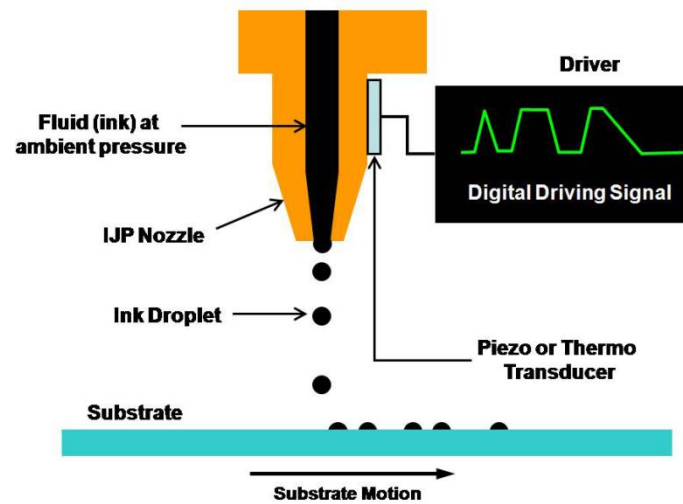


Figure 17 A typical setup for DOD IPT. From Xu et al. (2007)

Arai et al. (2011) have reported a piezoelectric inkjet head system, which can eject ink materials by a mechanical force without generating high heat, so that living cells and biological raw materials can be ejected without significant damage or denaturation. Some of the problems that can be found in IPT are related to the nozzle obstruction that occurs as the cell density of bio-ink is increased (Arai, Iwanaga et al. 2011).

There are many different AM technologies available. RM researchers face the challenge of using these technologies to create human like tissues. In order to successfully do that, new improvements have to be made to be able to manufacture biological complex composite structures. In many cases the simultaneous use of different AM technologies together is going to be a key factor, in other cases indirect AM strategies will be needed to produce the desired results. There is still a long way to go but some results have already been achieved.

4.2 Application of AM technologies to RM approaches

AM has already shown his huge potential to save lives, offering some advantages impossible to be implemented with other manufacturing technologies (Chang, Park et al. 2014; Gomes, Rodrigues et al. 2017; Zhang and Wang 2018). Not all the AM techniques are suitable for the generation of hydrogel printed parts. Billiet et al. (2012) give an overview on the different rapid prototyping techniques suitable for the processing of hydrogel materials (Billiet, Vandenhoute et al. 2012).

It has been confirmed that cell responses due to the mechanical and chemical microenvironment tend to differ between 2D cell culture models and 3D microenvironments (Shachar and Cohen 2003). AM technologies can help RM researchers to move from 2D cultures to 3D. From the beginning of the 21st century some successful cell printing trials have been undertaken. Boland et al., (2006) presented the results of inkjet printing experiments with two different cell types (Boland, Xu et al. 2006).

But the application of AM is not just limited to the creation of new tissues. The potential to accommodate various physico-chemical, pharmacokinetic and pharmacodynamic characteristics of drugs makes this manufacturing technology an interesting one for drug delivery applications (Sastry, Nyshadham et al. 2000).

Each AM technology has its own unique advantages and disadvantages in producing TE scaffolds. Now it is time to further develop these technologies and adapt it to a specific TE application towards the clinical application of the technology (Roseti, Parisi et al. 2017). It has also been demonstrated the possibility to manufacture multicomponent construct with mechanical tailored stiffness (Schuurman, Khristov et al. 2011). This aspect is very important for the manufacturing of hard tissues to mimic the

physiological conditions. Cells are more likely to create tissues under physiological conditions.

The parameters of the biopolymer deposition process play an important role and can affect the structural, mechanical and cellular TE properties of AM scaffolds. Some models have been described in the literature (Khalil and Sun 2007; Billiet, Gevaert et al. 2014). An important characteristic feature of every technique will be its resolution. Every technique is subdued to a lower technical limit size of the smallest details producible. This so-called lower limit shows a clear relationship with the feasible scale of the object: the higher the resolution of the smallest details, the smaller will be its maximum object size (Melchels, Feijen et al. 2010).

Nanotechnology is going to play an important role in the future success of AM in creating very complex high resolution organs (Garreta, Gasset et al. 2007; Peran, Garcia et al. 2012).

Some success has already been achieved. In 2003, Dr. Atala and his colleagues published a paper in *Nature Biotechnology* showing that miniature kidneys could be engineered, and these experimental kidneys were shown to be functional; able to filter blood and produce and dilute urine. Wake Forest is now using a 3D bioprinter to engineer more sophisticated prototypes of these miniature kidneys. The goal is to make larger functioning kidneys and other solid organs like hearts and livers (Wang, Yan et al. 2007). PLGA scaffolds with feature sizes of 10–200 μm , have been also developed using microdeposition and soft lithographic approaches (Vozzi, Flaim et al. 2002). Metabolic syndrome models have been developed *in vitro* using Adipose-derived stem cells (ASCs) and AM techniques (Xu, Wang et al. 2010). Calcium phosphates for bone defects (Ginebra, Espanol et al. 2010) printing systems have also been developed with application in craniomaxillofacial surgery (Klammert, Gbureck et al. 2010). Another

groups have developed a low temperature process printing system based on a Z Corp machine (Gbureck, Hölzel et al. 2007; Gbureck, Hölzel et al. 2007; Gbureck, Vorndran et al. 2007). Klammert et al.(2009) investigated the cytocompatibility of this low-temperature direct 3D printed calcium phosphate scaffolds *in vitro* (Klammert, Reuther et al. 2009).

In order to mimic the composition of living tissues it is also very interesting to include fibers. Different types of fibers as collagen are found in many of the tissues that form an organ. Electrospinning is one technology that can be used to convert liquids into fibers. Printed hybrid scaffolds including fibers have demonstrated enhanced mechanical properties compared to printed alginate or fibrin–collagen gels alone. The electrospinning technique has been well reported and there are a number of excellent reviews, which cover the fundamentals and effects of variable parameters, the range of electrospinnable materials and the variety of fibre collector methods developed (Bosworth, Turner et al. 2013).

One of the key factors in order to successfully print complex tissues is to recreate the vascularisation. Some interesting approaches for fabricating engineered tissue constructs replete with vasculature, multiple types of cells, and ECM have been reported (Kolesky, Truby et al. 2014). Vascular conducts are primordial in order to transport nutrients to the cells and remove the waste compounds (Schmidt-Nielsen 1994). Some techniques to print vascular conducts have been developed in the last decade (Mironov, Boland et al. 2003). Other have printed vascular tissue eliminating the need of an scaffold (Norotte, Marga et al. 2009). Unlocking the full biological potential of SC (*in vitro* or *in vivo*) necessitates an environment similar to that present during native development. It has been described the self-assembly-based technology as an interesting approach for the formation of vascular trees, one of the main unsolved problems in TE

(Jakab, Norotte et al. 2010). Effective vascularisation of tissue engineered constructs is a key to build larger tissues or organs (Nerem and Seliktar 2001).

One of the advantages on focusing on AM based cartilage regeneration, apart from the big prevalence and market of cartilage injuries, is the lack of vascularisation. This make cartilage regeneration a very interesting starting point for AM based RT as it is closer to the clinical application than other TR, also because it does not need a complex bioreactor system to create the tissue which can be created *in vivo* after implantation.

5 Bioreactors and ultrasounds in RM

A bioreactor is an engineered device or system that supports a biologically active environment. Bioreactors play a crucial role in the final properties of engineered tissues. The bioreactor environment directly affects the uniformity of cell seeding into 3D scaffolds as well as the maintenance of the cell phenotype and characteristics of the tissue (Bueno, Bilgen et al. 2004). A bioreactor should provide *in vivo*-like physical stimulation to the growing tissues to promote secretion of ECM and tissue formation (Lin, Hsu et al. 2009).

There are many different types of bioreactors as conventional spinner flasks (Freed, Vunjak-Novakovic et al. 1993), rotating wall vessels (Freed and Vunjak-Novakovic 1995), concentric cylinders (Saini and Wick 2003), and perfusion bioreactors (Carver and Heath 1999). Differences in the parameters of maturation of the growing tissue constructs highly affect tissue structure (Vunjak-Novakovic, Freed et al. 1996). Depending on the needs and characteristics of every tissue engineered construct a type of bioreactor have to be selected.

Different stimulating procedures have been used in order to enhance the formation of new tissues in RM as GFs and additives, gene therapy, hydrostatic pressure, dynamic compression, and bioreactors (Chung and Burdick 2008). Bioreactors are devices in which biological and/or biochemical processes are manipulated through close control of environmental and process-bound factors such as pH, temperature, pressure, nutrient and waste flow (Martin, Wendt et al. 2004). Bioreactors also play a key role in TE as they are used in expanding the cell population, tissue formation and maturation of tissue. The bioreactor environment directly affects the uniformity of cell seeding into 3D scaffolds as well as the maintenance of the cell phenotype and, therefore, the characteristics of the tissue. Bioreactors are responsible for providing the right mass transfer conditions for nutrients and waste to be exchanged between the culture medium and the cells, and for scaffolds to degrade simultaneously with tissue production. Ideally, the bioreactor itself provides *in vivo*-like physical stimulation to the growing tissues, either by mechanical or hydrodynamic loading, enhancing the secretion of ECM and tissue formation (Bueno, Bilgen et al. 2004).

Lin et al. (2009) developed a scaffold-bioreactor system for growing TE trachea and investigated the effect of fluid flow on producing trachea-like neotissue (Lin, Hsu et al. 2009). Zhu et al. (2010) reported the use of Taylor–Couette flow-based bioreactor to culture bone marrow stroma cells-sponge constructs. Taylor–Couette flow consists of a viscous fluid confined in the gap between two rotating cylinders. The results indicated that moderate shear stresses (0.02–0.19Pa) generated in the bioreactor improved the proliferation of rBMS cells to around 1.3 times of the static control with well-maintained calcium deposition ability of the cells. Relative larger shear stresses (0.24Pa) helped to improve the calcium deposition ability of the cells but inhibited their proliferations. Larger shear stress (40.24 Pa) inhibited the proliferation of the cells as

well as weakened the ability of cell membrane to preserve calcium ions (Zhu, Arifin et al. 2010).

Other studies have reported the benefits of using ultrasounds to promote the proliferation of cells, matrix deposition and the formation of tissue. Hsu et al., (2006) used pulsed ultrasound (1 MHz, 67 mW/cm² Ispta, and 10 min/day). Besides they compare the use of ultrasounds with the use of a rotating bioreactor. The scaffolds were made of polyester composites as described below and seeded with human chondrocytes obtained from the knee joint cartilage of three patients. The better performance in either ultrasound-exposed or bioreactor group was believed to be associated with the lower concentration of nitric oxide (NO). NO released may inhibit matrix synthesis in chondrocytes. The study concluded that ultrasound had a positive effect on neocartilage formation in the human chondrocytes seeded, type II collagen-modified polyester composite scaffolds. Nevertheless, the positive effect of ultrasound tended to decay after 28 days of culture while that of bioreactors last for 42 days (Hsu, Kuo et al. 2006). Scheven et al. (2009) investigated the use of low frequency, low intensity ultrasound in dental applications. They postulate that low intensity ultrasound may stimulate endogenous coronal tooth repair by stimulating dentine formation from existing odontoblasts or by activating dental pulp SC to differentiate into new reparative dentine-producing cells. Ultrasound therapy promoting dentine formation and repair may also have the potential benefit of alleviating dentine hypersensitivity by inducing occlusion of dentinal tubules (Scheven, Shelton et al. 2009).

Furthermore, ultrasounds can be used as a non-destructive analytical technique to provide real-time online assessments of matrix evolution in cell hydrogel constructs used in TE. Rice et al. (2008) used ultrasounds to measure the mechanical properties and matrix accumulations during 9.5 weeks of *in vitro* culture of chondrocytes,

encapsulated in poly(ethylene glycol) hydrogels. Gel degradation was manipulated to provide conditions with varying distribution of the large cartilage ECM molecule, collagen (Rice, Waters et al. 2009).

A recent publication of our team also presents a bioreactor based on ultrasonic monitoring for the non-destructive evaluation of 3D culture human engineered cartilage. Non-destructive tissue quality assurance procedures to ensure that the tissue formed from the bioprinted scaffolds and the biological components meet the regulatory specifications are needed. Ultrasound evaluation is presented as an interesting candidate to ensure the quality and functionality of the formed tissue as it is an accurate non-invasive procedure that can be automatized, this will help to get the clearance of the bioprinted treatments by the regulatory agencies and move from lab to bed. Furthermore, ultrasounds can also be used as a way on interacting with the biological components producing local effects that may improve the quality of the formed tissue. (Melchor, López-Ruiz et al. 2018)(Figure 18).

Graphical abstract

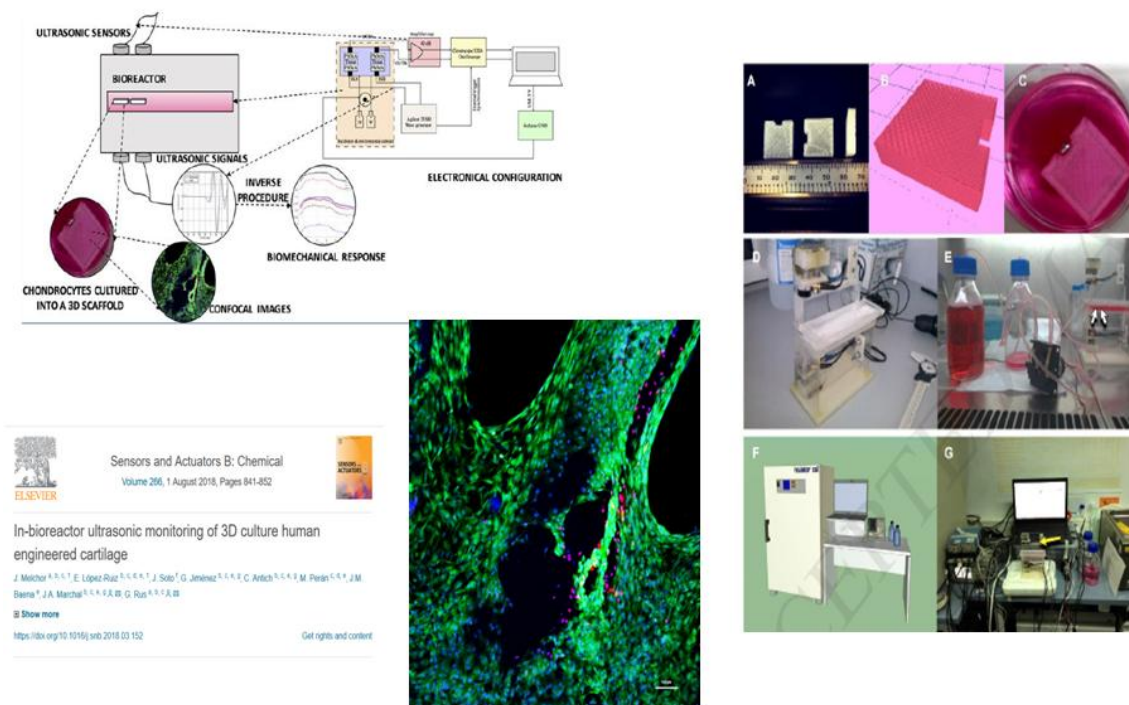


Figure 18 In-bioreactor ultrasonic monitoring of 3D culture human engineered cartilage. J. Melchor, E. López-Ruiz, J. Soto, G. Jiménez, C. Antich, M. Perán, J.M. Baena, J.A. Marchal, G. Rus. Sensors and Actuators B:Chemical 266 (2018) 841-852

Cartilage TE bioreactors environment directly affects the uniformity of cell seeding into 3D scaffolds as well as the maintenance of the chondrocyte phenotype and, therefore, the cartilaginous characteristics of the tissue. Bioreactors are responsible for providing the right mass transfer conditions for nutrients and waste to be exchanged between the culture medium and the chondrocytes, and for scaffolds to degrade simultaneously with tissue production (Schulz and Bader 2007). It has been reported that chondrocyte-laden scaffolds grown in perfusion culture increase cell proliferation and biochemical content compared to static culture (Xu, Urban et al. 2006). For long-term *in vitro* culture, low shear stresses stimulate ECM synthesis and deposition, yielding greater tissue formation, while high shear stresses suppress sulfated glycosaminoglycans (GAG) deposition, a characteristic component of cartilage ECM. In general, higher seeding densities have enhanced GAG content, potentially due to cell–cell interactions (Freed,

Marquis et al. 1994), while scaffolds seeded at low cell densities fail to elicit a response in bioreactor culture. Bioreactors currently being investigated for cartilage TE include: a parallel-plate bioreactor (Gemmiti and Guldberg 2006), rotating wall bioreactor (Freed, Hollander et al. 1998), and a concentric cylinder bioreactor (Saini and Wick 2003).

Bueno et al. (2004) reported a novel wavy walled bioreactor designed to enhance mixing at controlled shear stress levels and it was used to culture chondrocytes in suspension. Characterizing the wavy walled bioreactor's hydrodynamic environment and its effects on cartilage cell/tissue culture can help establish direct relationships between hydrodynamic forces and engineered tissue properties (Bueno, Bilgen et al. 2004). Janjanin et al. (2008) reported the use of spinner flask bioreactors obtaining constructs that exhibited hyaline cartilage histology with desired thickness and shape as well as favourable tissue integrity and shape retention, suggesting the presence of elastic tissue. Both culture conditions showed significant time-dependent increase in sulfated glycosaminoglycan and hydroxyproline contents. TGF-1/ IGF-I-treated samples were significantly stiffer; with equilibrium compressive Young's modulus values reaching 17 kPa by Day 42 (Janjanin, Li et al. 2008).

It has been demonstrated that bioreactors and ultrasounds can be used to enhance the results of producing tissues for RM therapies. In order to successfully produce *in vitro* functional tissue, one bioreactor have to be able to mimic the physiological environment; the temperature, Ph, Oxygen, carbon dioxide, and mechanical stimuli amongst other parameters. The maturation of the 3D bioprinted constructs is key. More developments have to be done to provide to the researcher new tools to *in vitro* create functional tissues.

6 Cartilage injuries

Joint cartilage is a specialized connective tissue that contains a single cell type, the chondrocyte, and a highly hydrated ECM composed mainly by collagens and glycosaminoglycans. It is sub-classified into three different types: elastic, hyaline and fibrocartilage. The composition and histological architecture of joint cartilage ensures the transmission and distribution of mechanical loads through the joint (Merceron, Vinatier et al. 2008). Cartilage itself lacks both vascularisation and innervations and healing processes are therefore slow and the resulting scar tissue most often lacks the necessary mechanical properties and physical durability of the original articular cartilage (Vachon, Bramlage et al. 1986). Articular defects can be limited to the superficial layer of cartilage or can extend deeper, also affecting the underlying subchondral bone, this injury is known as osteochondral injury. The degree of injury ranges from a small defect to a piece of the bone breaking off inside the joint. These defects can be of many sizes and depths and can stay attached to the area that was injured or become loose inside the joint. This injury is more common in adolescents and young adults and typically occurs at the knee, ankle or elbow. The effects that causes osteocondral injuries are not yet understood. Compressive trauma and the lack of blood supply may be one of them. Certain defects, such as those resulting from osteochondritis dissecans (OCD), may in fact start in the subchondral bone, only secondarily affecting the overlying cartilage. Other joint pathologies involving the subchondral bone include osteonecrosis and osteochondral fractures (Gomoll, Madry et al. 2010).

A meniscus is a fibro-cartilaginous structure present in humans in the knee, the acromioclavicular, sternoclavicular, and temporomandibular joints, as well as the radio-

carpal joint. The term 'meniscus' often refers to the cartilage of the knee, either to the lateral and medial menisci. Both are cartilaginous tissues that provide structural integrity to the knee when it undergoes tension and torsion. The meniscus of the knee are two pads of fibrocartilaginous tissue which serve to disperse friction in the knee joint between the lower leg (tibia) and the thigh (femur). They are concave on the top and flat on the bottom, articulating with the tibia. They are attached to the small depressions (fossae) between the condyles of the tibia (intercondyloid fossa), and towards the center they are unattached and their shape narrows to a thin shelf (Gray 1918). The blood flow of the meniscus is from the periphery (outside) to the central meniscus. Blood flow decreases with age and the central meniscus is avascular by adulthood leading to very poor healing rates. The two menisci in each knee are crescent-shaped pads of cartilage tissue. The main functions of the menisci are tibiofemoral load transmission, shock absorption, lubrication of the knee joint and to improve the stability of the knee joint.

The mean annual incidence of meniscal tears is about 60-70 per 100,000 (Maffulli, Longo et al. 2010). According to the International Statistical Classification of Diseases and Related Health Problems 10th Revision (ICD-10) there are 5 main types of meniscus pathologies: traumatic; congenital as discoid meniscus; degenerative as chondropathy and parameniscal cysts; metabolic as chondrocalcinosis; inflammatory as gouty arthritis and rheumatoid arthritis.

The need for effective cartilage repair strategies has been rising continuously, as the increase in life expectancy in humans also leads to a major increase in rheumatoid arthritis and OA. It is estimated that more than 39 million people in the European Union and over 20 million Americans have OA and it is anticipated that by the year 2020, these numbers will have doubled. In Germany, OA has major economic consequences,

creating direct and indirect costs of 8 billion Euros per annum (Csaki, Schneider et al. 2008).

Treatment is variable depending upon the size of the defect, age and activity level of the patient. It also depends on whether the fragment is loose in the joint. Current surgical treatments of articular cartilage injuries are: bone marrow stimulation (Johnson 1986), mosaicplasty (Matsusue, Yamamuro et al. 1993) and ACT. These treatments have not been as effective as thought then new approaches are being adopted (Koga, Engebretsen et al. 2009).

In ACT, autologous chondrocytes are applied on the damaged area during a knee surgery in combination with a membrane. Problems of ACT are: donor-site morbidity; chondrocyte dedifferentiation during *in vitro* culture, especially during monolayer culture; and fibrocartilage formation after cell implantation instead of defect healing (Brittberg, Peterson et al. 2003).

MSC are a promising research area for the regeneration of osteochondral and meniscus injuries (Csaki, Schneider et al. 2008; Koga, Engebretsen et al. 2009; Mobasheri, Kalamegam et al. 2014). Pastides et al. (2013) have reviewed the studies that focus on the clinical application of SC therapy in treating cartilage defects in skeletally mature human subjects (Pastides, Chimutengwende-Gordon et al. 2013).

ASCs are emerging as good candidates for achieving cartilage regeneration. New solutions in this area have to be developed to induce and control the differentiation of adipose-derived MSC into chondrocytes and to prevent the development of a hypertrophic phenotype responsible for tissue mineralization. Furthermore, it is needed to develop matrices that exhibit the mechanical and biological characteristics of joint cartilage. Research on these two complementary aspects of cartilage engineering must continue (Merceron, Vinatier et al. 2008). AM can help in the development of effective

solutions for the regeneration of cartilage and meniscus injuries. It is necessary to develop specific bioprinting solutions in cartilage and meniscus regeneration as a tool for cartilage TE researchers (Lopez-Ruiz, Jimenez et al. 2016).

7 Use of bioprinting in the development of new drugs.

As a way of manufacturing tissue like 3D constructs, bioprinting can find multiple applications in health care. *In vitro* produced tissues can be used to test new drugs, speeding up the development time and reducing the need of preclinical and clinical trials (Fang and Eglen 2017). 3D bioprinting is a powerful tool that can help in areas where traditional animal models and 2D cell culture methods are not allowing pharmaceutical companies to make good progress.

3D human microtissues models have been utilised to evaluate the toxicology of nanomaterials in the liver (Kermanizadeh, Lohr et al. 2014). In the majority of the 3D cell culture approaches, improved liver specific functionality and metabolism over longer time periods is achieved as compared to classical monolayer cultures. 3D microtissue models have also been used in drug development against osteosarcoma (Rimann, Laternser et al. 2014).

Although the use of microtissues is an advance in comparison to the use of individual cells, the lack of a well-developed structure is a disadvantage in comparison than using animal models. Bioprinting is called to be the tool to go from microtissues to 3D tissues. Some studies have used 3D printing to manufacture the device containing the microtissue, known as microchip (Huang, Qu et al. 2014). But the technology has still to be further developed to be able to manufacture bigger and more human-like tissues and organs.

Furthermore, bioprinting can be used in the development of neoplasm models to develop new anti-tumoral drugs. Neoplasm, commonly referred to as a tumor, is an abnormal growth of tissue in 3D. A malignant neoplasm is widely known as cancer. Anti-cancer drug development is inefficient, the high fail rate is partly due to the lack of predictive models or the inadequate use of existing preclinical test systems. Using 3D AM we can create 3D structures containing tumoral cells and tissues that can better simulate the native 3D tumor microenvironment that favours tumor growth and progression. An overview of available *in vivo* and *in vitro* 3D models of cancer can be found in the literature (Unger, Kramer et al. 2014). A comparison between 2D and 3D models for HeLa cells and hydrogels to construct *in vitro* cervical tumor models have been reported, showing over 90% cell viability (Zhao, Yao et al. 2014).

These models can help to understand the interaction between tumoral cells groups and health cells and to test new drugs finding the most effective molecules. These models will likely be of significant use in understanding the biological mechanisms that govern the pathological abnormalities observed in cancer and to act in the different pathways of the processes involved.

In this introduction we have summarize the main technologies and state of the art of TE and AM. All these strategies require the development of specific biofabrication systems, which is the aim of this project, and bioreactors.

Hypothesis

The recent advances in different technologies presented above make think that we are facing a new era in the treatment of pathologies where the only limit is going to be our imagination. Nevertheless, there are still a lot of limitations, but these limitations can be overcome, some in the short term, others increasing the research in the area. Our hypothesis is based in the following points:

- I. Using 3D AM it is possible to layer by layer manufacture meshed functional multimaterial constructs with different external geometries and internal mesh structures and from different materials avoiding the restrictions shown in the bibliography(Kim and Cho 2009; Kundu, Shim et al. 2015; Scaffaro, Lopresti et al. 2016).This can be done developing new algorithms, electronics and hardware.
- II. The constructs can be seeded with cells during the printing procedure. An improved process can be developed to enhance cell survival and distribution in the construct as a precursor of a functional tissue to regenerate an injury (Chang, Nam et al. 2008).
- III. Defining the right strategy, ingredients and procedure, we can create a 3D construct where cells behave as they do *in vivo*. More specific, we hypothesize that chondrocytes can be bioprinted with high viability and they won't dedifferentiate in the scaffold and will create the right ECM (Bonaventure, Kadhom et al. 1994).

In the present work we will develop the system, the procedure and the trials to show that it works for the specific case of cartilage injuries. We hypothesize that cells can grow and create ECM avoiding the dedifferentiation as a precursor of a functional tissue.

These constructs can be used to regenerate tissue injuries. New meshed structures can help cells to interact in a more physiological condition increasing cell viability and tissue formation. Besides new biomaterials with improved properties for SC therapies can be developed and adapted to be 3D printed.

Objectives

The main objectives are:

- I. To develop a bioprinting system with algorithms, electronics and hardware to layer by layer manufacture meshed functional multimaterial constructs with different external geometries and internal mesh structures and from different materials
- II. To develop an improved process that can print with cells and to enhance cell survival and distribution during the manufacture of the constructs and show its effectiveness using chondrocytes as a precursor of a functional tissue to regenerate an injury.
- III. To create a 3D construct with chondrocytes where cells behave as they do *in vivo*, with high viability, avoiding dedifferentiation and creating the right ECM as a precursor of a functional living tissue.

Materials and methods

In this section we present the process of development of the Bioprinting system, the software and the electronic control unit (ECU), as well as the printing procedure and trials that confirm our hypotheses.

From the GUI to the software algorithms and the hardware of the bioprinter, the development is explained in this section. Furthermore, the different printing trials, configuration and laboratory assays to obtain the results and the validation of the system are described.

A description of the assembly and the components is provided but maintaining the compulsory confidentiality due to the private source of funding of the project and the industrial application of the system and the obtained results. After the design and the building of the system, we have validated it and proved that bioprinting is an effective way to produce cell laden scaffolds to be used in RM. In order to show this effectiveness, we have undergone laboratory trials to prove the potential of bioprinting in RM and TE consisting on an *in vitro* living 3D model to regenerate cartilage injuries using state of the art materials and an improved process based on Volume-by-Volume (VbV) Bioprinting and Injection Volume Filling (IVF) to enhance cell survival and distribution to regenerate the injuries.

The main parts of the systems are: i) the structure, composed of the profiles and the covering; ii) the 3D axis composed of the stepper motors, the guides and the threaded bars; iii) the printing unit or head; iv) the ECU; v) the sensors and actuators; vi) the user interface and the software that send the information to the ECU. The following paragraphs show the different steps in the development of the system and its validation.

1 Bioprinting system development

1.1 Concept design of the system

The development of an electronic medical device is a multidisciplinary task that requires the use of different technologies and expertise. Product design by means of CAD, mechanical validation by means of FE analysis, computational fluid dynamics (CFD) simulations, electronics and computer science amongst others, as well as a deep understanding on the regulation, the standards, the quality assessment and the different manufacturing technologies and building methods.

The system presented in this thesis is a complex one, which has been developed by a multidisciplinary team, joining biologist know how, chemistry and engineering. The first step in the project development is the general concept design of the work station by means of a diagram that shows the different sub projects that have to be developed (Figure 19).

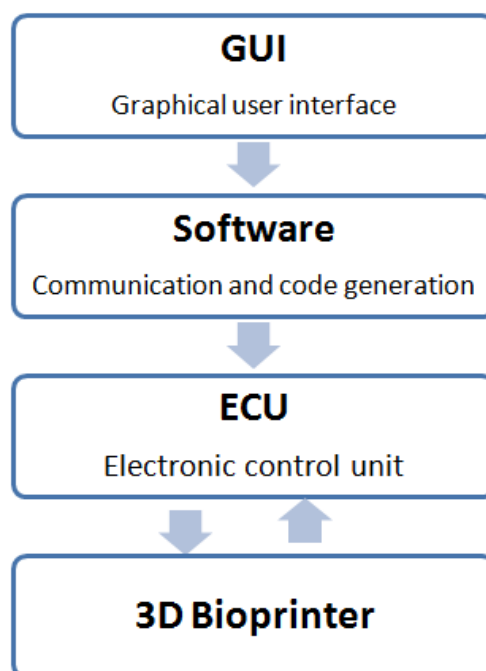


Figure 19 Sub projects in the development of the work station.

All the sub projects have a special importance in the final results of the system. The 3D Bioprinter subproject can be subdivided into the different parts (Figure 20):

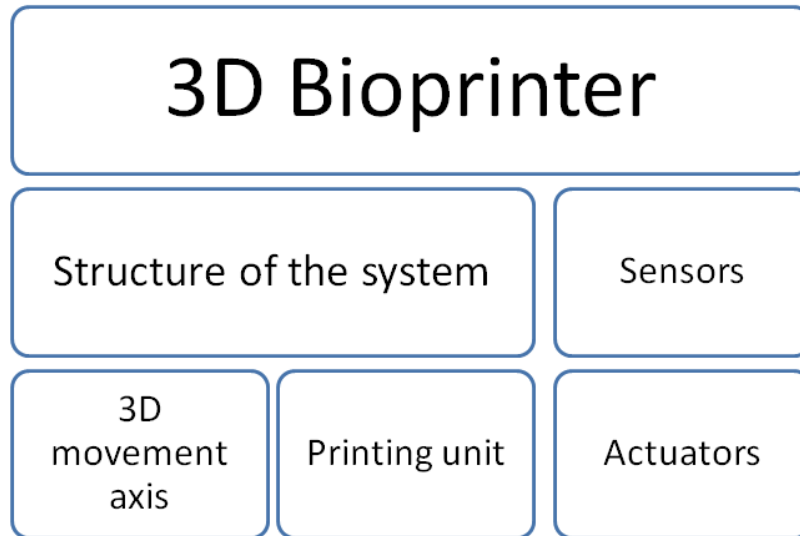


Figure 20 Sub parts of the 3D bioprinter.

After the CAD design of the different parts of the prototype it is very interesting to assembly it in order to check the positioning and configuration of the different components. After the first prototype is built, dynamic trials on the movements and the assembly are performed to proof that the system works as desired. The election of the different components, surface finish and tolerances and suppliers of the system has been carefully conducted. This process involves some degree of trial and error and is a very important part of the development. 3D printing prototyping technologies can help a lot in this procedure, being nowadays easier to move from the virtual CAD design to a functional prototype.

1.2 Development of the bioprinting unit

The 3D bioprinting unit or printing head is one of the main parts of the system as it draws the different trajectories of the layers, deposit the material on the manufacturing platform and apply the different power sources to the material in order to transform it from the raw state to the solidified geometry. This part is going to limit aspects as the resolution of the manufactured parts and the mesh structure size.

The head is depositing different kinds of materials coming from the 3 different sources:

- A thermoplastic polymer as PLA (scaffold)
- Mono or multi phase bioinks containing cells
- The medium or some other additive compounds
- Viscous pastes as nanocellulose or other biomaterials

The thermo plastic polymer is deposited using FDM. The multiphasic hydrogel is deposited using IPT based on CE. One of the phases may be laden with cells and the other one activates a polymerization process that gel and attach to the scaffold structure. The printing head have been designed using computer aided design and mechanically validated using FE analysis. The distribution of the different parts has been designed in order to optimize the printing area. This head has been designed by means of parametric computer aided design trying to maximize the manufacturing area and setting the different material reservoirs in the optimal positions.

1.3 ECU, Sensors and actuators of the work station

The hardware of the system has to accomplish the instructions that come from the code generated by the software after receiving the printing parameters and the geometries from the GUI. The actuators are the components that controlled by the ECU, transform code into physical signals and perform the needed actions. Besides the system has to measure some values and send the information back to the ECU that will recalculate the new signal to be applied. This is done by the sensors of the system.

The REGEMAT3D biprinter ECU receives data from the GUI, processes it, identifies the G commands, and executes the actions associated with that command. G-code⁶ is the common name for the most widely used numerical control programming language. It is used mainly in computer aided manufacturing (CAM) for controlling automated machine tools.

The power supply provides from the electricity of the network, 12V direct current (DC) and up to 30A for powering the electronic system. The different parts that integrate the electronic system⁷, are:

The processing core consists of an Arduino Mega platform, with its ATMEGA2560 microcontroller. Arduino is an open-source computer hardware and software project and user community that designs and manufactures kits for building digital devices and interactive objects that can sense and control the physical world⁸. This platform is programmed for reading the data that arrives in the serial receiving port, identifies the G command and verifies it by means of an error control procedure. After the verification, the actions associated this G command are executed.

⁶ <http://en.wikipedia.org/wiki/G-code>

⁷ The system has been continuously evolved during the last years and some of the component described may have been replaced

⁸ <http://arduino.cc/en/guide/introduction>

Furthermore, another electronic modules have been designed and manufactured in order to integrate all the functions needed to run the bioprinter. These modules consist of:

- Power Indicator
- Voltage reference supply
- Heater control
- Temperature monitoring
- Fan control
- I²C⁹ communication
- Stepper motor drivers' control
- End-stops
- Emergency stop

The heater control is controlled by the microcontroller by means of Pulse-width Modulation (PWM) signal. PWM is a technique used to encode a message into a pulsing signal. It is a type of modulation. Although this modulation technique can be used to encode information for transmission, its main purpose is to allow the control of the power supplied to electrical devices, especially to inertial loads such as motors¹⁰. For a more accurate regulation of the hot end temperature, a proportional-integral-derivative (PID) control has been implemented into the firmware. Firmware is the combination of persistent memory and program code and data stored in it. A PID¹¹ is a control loop feedback controller mechanism widely used in industrial control systems. A PID controller calculates an error value as the difference between a measured process variable and a desired set point. The controller attempts to minimize the error by adjusting the process through use of a manipulated variable.

⁹ <http://en.wikipedia.org/wiki/I%C2%B2C>

¹⁰ http://en.wikipedia.org/wiki/Pulse-width_modulation

¹¹ http://en.wikipedia.org/wiki/PID_controller

The main actuators of the system are:

- Stepper motors NEMA that rotate a precision screw in order to move the different axis.
- Stepper motors that move each syringe for the injection of the materials.
- A fan to improve the cooling process of the thermoplastic material used in rigid scaffolds

The main sensors of the system are:

- Endstops
- Heater resistance
- The temperature of the hotend of the FDM nozzle is reordered using Negative Temperature Coefficient (NTC) sensors.

In the ECU we have also implemented an enhanced process for data reception and error control, and G command management. An improved process for head reference and printing area limits and a precise head movement to the printing points have also been developed.

1.4 Software and graphical user interface

The development of a own software to control the work station is one of the biggest challenges in the development of a bioprinting system. Mainly all the low-cost 3D printing developments come from the same open source code. In the early beginning of the project we identified that to have an own code, and graphical user interface (GUI) was a key factor in the success of our development. Understanding the code and being able to implement new algorithms to control new hardware was crucial for a project as REGEMAT 3D that aims at offering a modular work station adaptable to different

materials and testing conditions. Besides the user experience and usability is very important for us, as the user background is more biological than technical¹².

The first step is the development of the GUI that is the platform to interact with the user. In the first version we identified the basic options that need to be on it and in a second version, after acquiring the feedback of potential users we have added some new features. The code has been structured to be able to easily add any instruction, option or control code to add any device required in a specific research application.

The first version of the GUI is quite simple and has been implemented to choose the different files needed for the printing (geometry in STL, and printing parameters) and to create a G-code. The GUI have been developed using Qt Creator 3.1.0¹³. Qt Creator is a cross-platform C++, JavaScript and QML integrated development environment which is part of the SDK for the Qt GUI Application development framework

REGEMAT3D bioprinter has the ability to build a scaffold (using thermoplastics, photo curable or viscous pastes biomaterials) with a specific geometry through scaffold material deposition layer by layer, also allowing the delivering of the material contained in the syringes (which can be cells embedded in a medium, biomaterials and biopolymers, or other biological materials) in selected layers, in order to control the whole bioprinting process. The bioprinter's validation has been focused in printing cartilage cells using FDM technology with resorbable polymer filament as PLA and a hotend (at high temperatures) which melts the filament and generates a thin thread, but also it is possible to print a determinate biomaterial placed in a syringe, at normal temperature. Currently we also have in the system individual temperature control (cooling and heating) in every syringe.

¹² The Software has been continuously evolved during the last years adapting it to the different biomaterials and developed procedures

¹³ http://en.wikipedia.org/wiki/Qt_Creator

Once the G code has been generated, the next step is to begin the communication between the interface and the ECU. After the initiation of the communication G commands are received from serial input data by the ATMEGA2560 and checked for errors. Once a G command, has been verified, the command is executed, through the search of its type and the set of instructions associated.

We have developed some improvements in order to enhance the printing process. We have implemented a novel process of point mesh generation from the STL and layer mesh infill that allows to print complex pore structures using different layers. Furthermore, a process to infill the pores have been implemented in order to deposit cell laden hydrogels and other biomaterials in the different layers, once the temperature of the filament has decreased enough to ensure the survival of the cells.

2 Validation of the work station

In this section we explain the validation of the system as explained in the publication.

TE is a wide scientific area with a lot of solutions to be develop. All the developments that have been enumerated in the precedent sections have the aim of using the advantages of 3D printing in TE. In order to validate the system, we have selected the application of cartilage. 3D printing can help to print customized 3D meshed structures that contain chondrocytes and biomolecules, to anatomically reproduce a cartilage injury and the characteristics of living cartilage. Besides 3D bioprinting can be used to print human like 3D living structure to test new drugs and evaluate the interaction between damaged tissues and healthy tissues. Besides all the manufacturing process can be automatized, controlled and traced towards an industrial clinical application.

For the validation of the system we have used a proprietary process that we have developed for this specific application (VbV and IVF).

AM techniques are based on the principle of adding material layer-by-layer allowing to manufacture complex external and internal shapes with a mesh structure (Pham and Gault 1998; Wong and Hernandez 2012; Frazier 2014). The use of biopolymers for AM technologies have emerged during the last years (Melchels, Domingos et al. 2012; Ozbolat, Moncal et al. 2017). Parameters of the biopolymer deposition process and the structure of the mesh play an important role and can affect the structural, mechanical, biodegradation time, and cellular properties of AM scaffolds (Cui, Wu et al. 2009). Among different options, thermoplastic polymers can be easily printed using the 3D printing technology known as FDM. This technology consists of a nozzle with a heater that melts a thermoplastic filament and deposits it in a controlled and organized manner, layer-by-layer, on a surface. After one layer has been printed, the z-axis moves and a new layer is printed (O'Brien, Holmes et al. 2015) . In this way, scaffolds are manufactured as a mesh, being rigid enough, at the same time flexible, to ensure the maintenance of the required structure.

The use of already clinically approved thermoplastic polymers presents a promising approach in treating cartilage defects (Chia and Wu 2015; FDA 2016). However, the high manufacturing temperatures of thermoplastic polymers decrease cell viability and also limit the scaffold geometry due to the need to avoid direct cell contact with the printed filaments. In order to solve these problems, low temperature biomaterials and novel printing procedures have been explored (Kim, Jang et al. 2016), but new biomaterials need a long time and procedure before they can be used in patients.

Therefore, new procedures based on currently approved biomaterials have to be investigated. The aim of this trial for the validation of the system, was to implement a novel bioprinting method for high melting temperature thermoplastics, such as PLA, that allows high cell viability and without shape and mesh restrictions. This method consists on a VbV 3D-biofabrication process with an algorithm that divides the printed part in different volumes and injects the cells after each volume has been printed, once the temperature of the printed thermoplastic fibers has decreased. This 3D-bioprinting method has the main objective to avoid thermal damage of the cells. Moreover, it allows to manufacture scaffolds with the desired biodegradation time and stiffness to enhance the performance and outcomes of the treatment. The biological feasibility of the printing process was assessed by printing bioinks of human chondrocytes together with PLA fibers and testing cell viability, distribution and proliferation.

2.1 Bioprinter and software configuration

We have configured a bioprinter system with 3 syringes and one FDM extruder (REGEMAT 3D, Granada, Spain), consisting in a hardware, the software Designer (REGEMAT 3D, Granada, Spain) containing the algorithms that allow the configuration of VbV, and an ECU that connects the software to the hardware were used in the experiments (Figure 21).

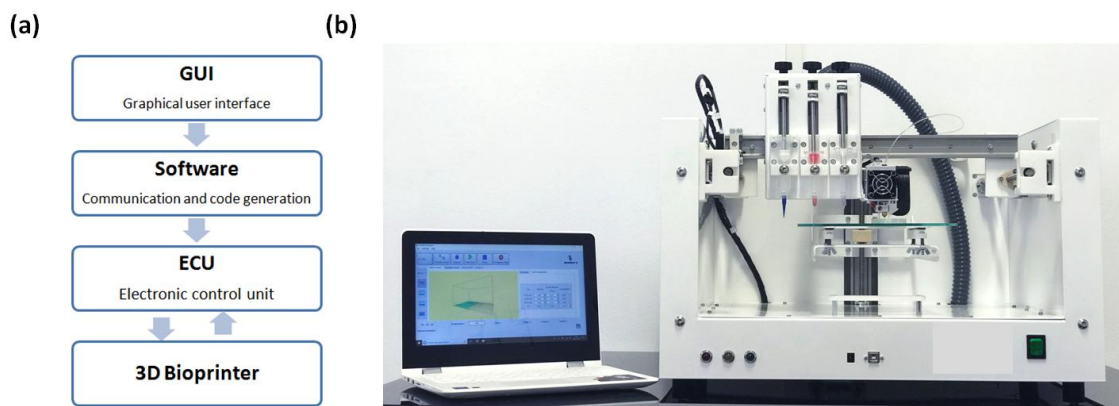


Figure 21 Bioprinter characteristics, hardware and software of the bioprinting system. Process flow of bioprinting system (A). System and bioprinter images (B) (Extracted from the publication of the author)

The bioprinting system was configured for PLA and used two syringes with needles of different diameters to inject alginate with chondrocytes embedded and a calcium solution. The position and distance between the FDM extruder and the syringes were configured to optimize the procedure. The software Designer can be set up using a simple GUI to print anatomical structures, selecting how and when the bioinks are deposited.

In order to avoid cell contact with the high temperature thermoplastic printed parts, VbV allows the deposition of x layers of the thermoplastic and afterwards filling the resulting volume ($x \cdot A_n$, being A_n the area of the layer n) with chondrocytes. All the data acquisition parameters have been programmed and integrated in the software's GUI for the configuration of the VbV printing procedure.

The configuration of the VbV process is quite straightforward. The number of layers printed before filling the resulting volume have to be set. Once the layers have been printed the syringe containing the cell-loaded hydrogel solution will penetrate into the scaffold in different points (N points), filling it up uniformly. Afterwards, a second

syringe will inject the solution that will gel the hydrogel keeping the desired distribution of the cells in the scaffold. After that, the system prints the next volume layers that will be filled in a similar way. Following the configuration of the scaffold and syringes parameters, the next step is to generate the associated G code. The G code with the G commands control the printer system and will build the geometry from the GUI defined specifications. Once the G code is generated the printing can be started.

2.2 Chondrocytes isolation and characterization

In this experiment that is part of the publication presented, articular cartilage was obtained from patients with knee OA during joint replacement surgery. Ethical approval for the study was obtained from the Ethics Committee of the Clinical University Hospital of Málaga, Spain, following the regulations on this matter. Informed patient consent was obtained for all samples used in this study. None of the patients had a history of inflammatory arthritis or crystal-induced arthritis, following our project's inclusion criteria. Human articular cartilage was obtained from the femoral side, selecting the non-overload compartment: lateral condyle in varus knees and medial condyle in the valgus cases. Only cartilage that macroscopically looked relatively normal was used in this study. Human articular chondrocytes were isolated as previously described (Lopez-Ruiz, Peran et al. 2013). Chondrocytes were grown in Dulbecco's modified eagle's medium (DMEM)–high glucose (Sigma) supplemented with 10% FBS (Gibco), 50 µg/µL of 1-ascorbic acid 2-phosphate (Sigma), 1% penicillin-streptomycin (Sigma) and 1% ITS (Gibco) in a 25-cm² cell culture flask. Cells were incubated at 37°C humidified atmosphere containing 5% CO₂ and expanded in a monolayer for 7–10 days before the experiment.

Chondrocytes seeded on glass coverslips were fixed and stained with 0,4% toluidine blue staining for 15 min and then were rinsed with distilled water. For immunohistochemical analysis, fixed monolayers were blocked for 1 hour at room temperature (RT) with 5% BSA, 5% FBS in phosphate buffered saline (PBS) and, then, incubated with Col I (SC25974, St. Cruz) and Col II (SC52658, St. Cruz) overnight at 4°C. The next day, samples were washed thrice with PBS and incubated with the secondary antibodies (Alexa) for 1 hour at RT and finally, were washed thrice with PBS and mounted with mounting medium with DAPI. Photographs were taken with a Leica DM 5500B (Solms, Germany) microscope.

2.3 Volume-by-volume printing of 3D hybrid scaffolds

In this experiment that is part of the publication presented, the biofabrication technique comprises two processes for every volume: first, the fused deposition of the thermoplastic polymer to obtain the scaffold and second, the injection of the bioink and CaCl₂ solution to fill the printed scaffold. Firstly, commercial non-medical grade PLA (1,75 mm filament) was used and it was melted at 210°C in a nozzle extruder and deposited, at rate of 1,4 mm/s, in a layer-by-layer manner to generate a previously designed matrix (600 µm pore size, cylinder-type structure of 10 mm diameter and 10 mm height). After printing 4 layers of the scaffold (0,35 mm thickness), the bioink (25µl; 1 × 10⁶ cells ml⁻¹ encapsulated in alginate, 2% w/v) was injected into the scaffold in the selected points (speed: 8 µl/s; 21G nozzle). Then, cell-loaded alginate solution was chemically cross-linked by following with an injection of 100 mM CaCl₂ (40µl; speed: 8µl/s). All these processes were repeated until the target dimensions of the

constructs were fulfilled. Finally, all cell-laden scaffolds were cultured in medium, as previously described, at 37°C in 5% CO₂ atmosphere.

2.4 Confocal microscopy

In this experiment that is part of the publication presented, chondrocyte viability after the bioprinting process was assessed at 24 hours and 7 days using confocal microscopy. For this purpose, samples were washed two times with PBS and incubated for 15 min at 37°C with Cell Tracker Green/CMFDA (CTG)(Invitrogen). Afterwards, samples were washed twice with PBS, fixed with 4% paraformaldehyde in PBS for 20 min at RT and stained with DAPI. Cells were photographed by confocal microscopy (Nikon Eclipse Ti-E A1, USA) and analyzed using NIS-Elements software.

2.5 Apoptosis evaluation

In this experiment that is part of the publication presented, chondrocytes cultured within the printed constructs were evaluated for apoptosis signals just after impression (0 min), 30 min and 2 hours after the printing process. Cell apoptosis was checked in four different conditions in order to analyze any effect over cells: (i) control cells before the printing process, (ii) cells embedded in alginate, (iii) printed cells with alginate, and finally (iv) printed cells with alginate over PLA fibers.

Cells were isolated using ammonium citrate (55 mM) and analyzed with Annexin V-fluorescein isothiocyanate detection kit (eBioscience Inc.) by a FACS CANTO II (BD

Biosciences) using the FACS DIVA software, according to the manufacturer's instructions.

2.6 Cell proliferation assay

In this experiment that is part of the publication presented, Alamar blue assay (Biorad) was used as a measurement for the determination of cell viability. Cell growth was analyzed at different time points: 0, 1, 2, 5 and 7 days. Scaffolds were incubated with 10 μ l of Alamar blue solution per each 100 μ l of media and incubated for 3 hours. At this time, fluorescence intensity was measured at an excitation wavelength of 530 nm and emission of 590 nm (Synergy HT, BIO-TEK.).

2.7 Statistical analysis

In this experiment that is part of the publication presented, results were processed using GraphPad Prism 5.0 software for Windows (Graphpad Software, La Jolla California USA). All graphed data represent the mean +/- the 95% confidence interval (95% CI) from at least three experiments. Differences between treatments were tested using the two tailed Student's T test. Assumptions of Student's T test (homocedasticity and normality) were tested and assured by using transformed data sets [$\log(\text{dependent variable value} + 1)$] when necessary. P-values < 0.05 (*) and P-values < 0.01 (**) were considered statistically significant in all cases.

3 New meshes structures, scaffolds and bioink formulations

In this section we explain the validation of the system for printing different biomaterials for the scaffolds (with different properties as stiffness, melting point, transparency...) and different matrix geometries. The geometry of the mesh and the biomaterial composition is going to affect the stress transferred to the cells and its distribution, this will have a big influence in the no dedifferentiation of the cells and ECM formation, the biodegradation time and dynamics of the biodegradation as well as the mechanical behaviour of the construct. In order to proof the effectiveness of the developed system to print different biomaterials and mesh structures we have selected a number of different thermoplastics (no all biodegradable) that has been printing, configuring the system to the properties of extrusion. The list of the biomaterials printed can be seen in the following table.

Sample	Material	Geometry			Extrusion parameters							
		Size (mm)	Pore size (mm)	Layer height (mm)	Temperature (°C)	Travel (units)	Height change (mm)	Flow speed (mm/s)	Perimeter speed (mm/s)	Infill speed (mm/s)	Retract speed (mm/s)	
#1	E.P.	5x15	4	0,3	200	1	0	1,4	10	10	10	
#2	E.P.	5x15	4	0,3	200	15	2	1,4	10	10	10	
#3	E.P.	5x15	4	0,3	200	15	0	1,4	10	10	10	
#4	BOUN	5x15	4	0,3	210	15	0	1,4	10	10	10	
#5	GLACE	5x15	4	0,3	220	15	0	1,4	10	10	10	
#6	PLA 3D870	5x15	4	0,35	210	15	0	1,4	10	10	10	
#7	PLA 3D870	5x15x15	0,8	0,3	220	15	0	1,4	10	10	10	
#8	PLA 3D870	5x15x15	0,8	0,25	210	15	0	1,4	10	10	10	
#9	PLA 3D870	5x15	4	0,25	210	15	0	1,4	10	10	10	
#10	PLA 3D870	5x15	4	0,35	210	15	0	1,4	5	5	10	
#11	SUPPORT	5x15	4	0,35	240	15	0	1,4	10	10	10	
#12	FLEX	5x15	4	0,3	240	15	0	1,4	10	10	10	
#13	FLEX	5x15	4	0,3	230	15	0	1,4	10	10	10	
#14	SUPPORT	5x15	4	0,3	240	15	0	1,4	10	10	10	
#15	FLEX	5x15	4	0,3	230	10	0	1,4	10	10	15	
#16	FLEX	5x15	4	0,3	230	10	0	1,4	5	10	15	
#17	FLEX	5x15	4	0,4	230	10	0	1,4	5	10	15	
#18	FLEX	5x15	4	0,3	240	10	0	1,4	5	10	15	
#19	FLEX	5x15	4	0,3	240	1	0	1,4	5	10	15	
#20	FLEX	5x15	4	0,3	240	1	0	1,45	5	10	15	
#21	FLEX	5x15	4	0,3	230	1	0	1,45	5	10	15	
#22	FLEX	5x15	4	0,3	230	10	0	1,45	5	10	15	
#23	ABS	5x15	4	0,3	250	10	0	1,4	10	10	10	
#24	PETG	5x15	4	0,3	240	10	0	1,4	10	10	10	
#25	PETG	5x15	4	0,3	240	2	0	1,4	10	10	10	
#26	PP	5x15	4	0,3	220	2	0	1,4	10	10	10	
#27	TPU HARDNESS +	5x15	4	0,3	220	2	0	1,4	10	10	10	
#28	TPU HARDNESS +	5x15	4	0,3	220	10	0	1,4	10	10	10	
#29	TPU HARDNESS +	5x15	4	0,3	220	15	0	1,4	10	10	15	
#30	TPU HARDNESS +	5x15	4	0,3	220	10	0	1,4	10	10	15	
#31	TPU HARDNESS +	5x15	4	0,3	210	15	0	1,4	10	10	15	
#32	TPU HARDNESS +	5x15x15	0,8	0,3	210	15	0	1,4	10	10	15	

#34	NYLSTRONG	5x10x10	1	0,3	250	2	0	1,4	5	5	10
#35	NYLSTRONG	5x15x15	1	0,3	250	5	0	1,4	7	10	10
#36	NYLSTRONG	5x15	4	0,3	250	-	-	-	-	-	-
#37	CO-POLYESTER TEMPERATURE +	5X15	4	0,3	250	10	0	1,35	10	10	10
#38	SUPPORT	5X15	4	0,3	240	10	0	1,4	10	7	10
#39	SUPPORT	5X15	4	0,3	240	5	0	1,4	10	9	10
#40	BIO PS	5X15	4	0,3	155	10	0	1,4	10	10	10
#41	BIO PS	5X15	4	0,3	160	10	0	1,4	5	5	10
#42	BIO PS	5X15	4	0,3	160	10	2	1,4	5	5	10
#43	BIO PS	5X15	4	0,3	160	10	0	1,5	10	10	10
#44	BIO PS	5X15	4	0,3	170	10	1	1,4	5	5	10
#45	BIO PS	5X15	4	0,3	170	15	0	1,4	5	5	10
#46	BIO PS	5x15x15	1	0,3	170	15	0	1,4	6	6	10
#47	BIO PS	5x15x15	1	0,3	170	15	0	1,4	6	5	10

Table 1 Types of thermoplastics and printing parameters

Besides we have shown the effectiveness of our software and hardware to print different geometries and mesh structures. In order to do that we have selected the honeycomb configuration and different pore size for the mesh structure of the scaffold.

To conclude we also show the effectiveness of our developed system for printing different biomaterials as a scaffolds for different geometries as a meniscus printed using PCL and non-thermoplastics as nanocellulose (Chinga-Carrasco 2018) and novel bioinks as methacrylate modified pectin bioink which shown very interesting results in the clinical application of skin (Pereira, Sousa et al. 2018).

With all these experiments we proof the versatility of the system to work with a wide range of biomaterials either for the scaffolds and bioinks. This will help to accelerate the development of protocols and procedures that can generate cell laden constructs that mimic the structure of living tissue and can help to produce, after the maturation in a bioreactor, functional tissues to regenerate injuries.

Results

1 Bioprinting system

The buildup of a bioprinter is a complex process that includes many different tasks from the screwing of the bolts to the welding of the connections of the stepper motors, the sensors and actuators and its connections to the ECU. In Figure 22 we can see some of the relevant parts of the building and assembly of the REGEMAT 3D Bioprinter. A more detailed information on all the task undertaken is out of the scope of the present work and is part of the intellectual property of the company.

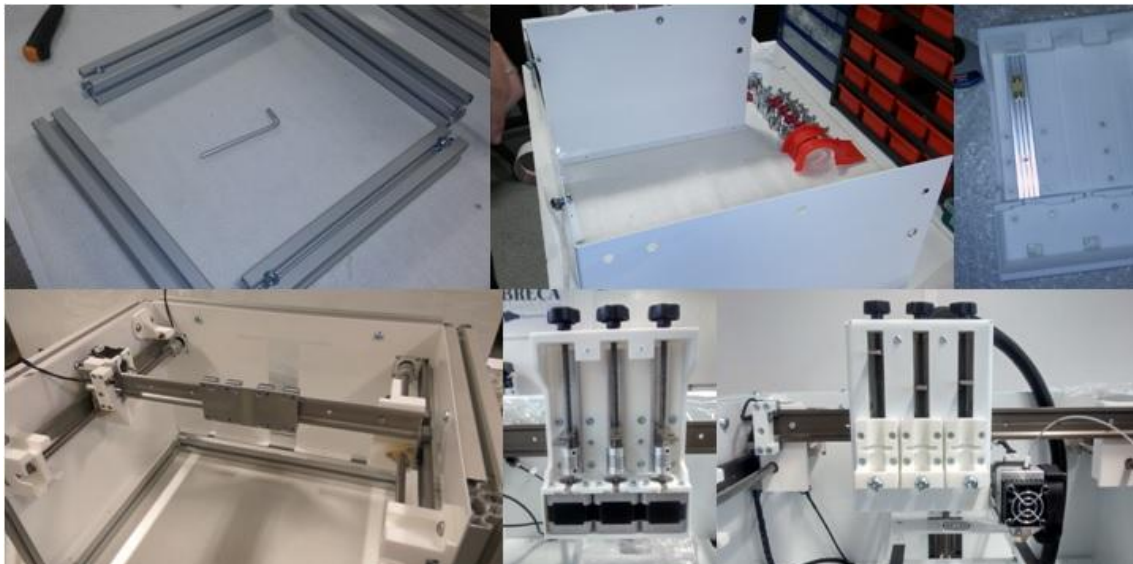


Figure 22 Build-up and assembly of the system

3D printing technologies allows us to manufacture a real prototype that is very interesting in order to detect failures and redesign it. It also allows testing the movements and the electronics as well as the communication between software and ECU. The 3D AM system developed consists on a 3 axis movement system including a printing head or 3D printing unit.

In Figure 23 it is shown a picture of the BIO V1 as shown in the 2018 commercial brochure of the company.

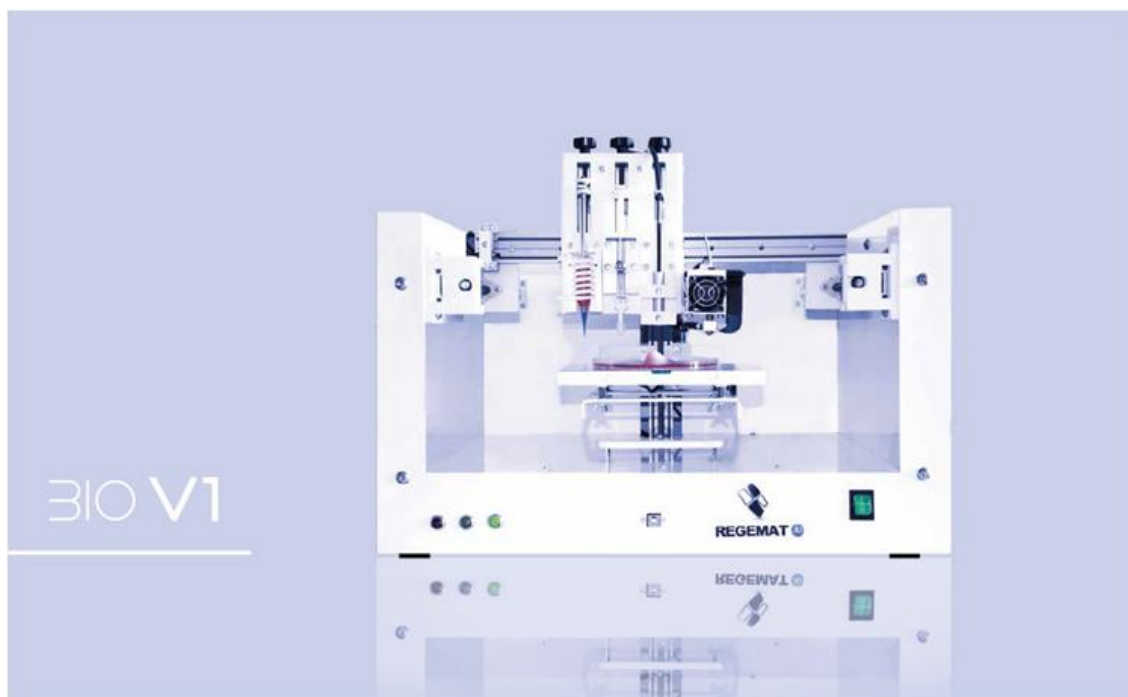


Figure 23 REGEMAT 3D V1

1.1 Bioprinting unit

As one of the main results of the present work, we have developed an innovative concept of printing head. In our optimized process, presented in the section of validation of the system, we have 2 different kind of printing procedures:

- One using a rigid thermoplastic scaffold in which high temperatures of the melting process makes essential to deposit the cell laden hydrogel after the temperature has decreased.
- Another that uses as a scaffold a hydrogel which deposition process don't involve high temperatures.

The configuration that we have developed takes these 2 different processes into account, and the distribution of the parts has been designed to increase the effective area of printing. However, the developed modular bioprinting system can be configured for many other different printing procedures and include different bioprinting technologies that can be seen in the next figures. The tools can be easily replaced and the configuration can be done in a simple way using the tool tab of the software.

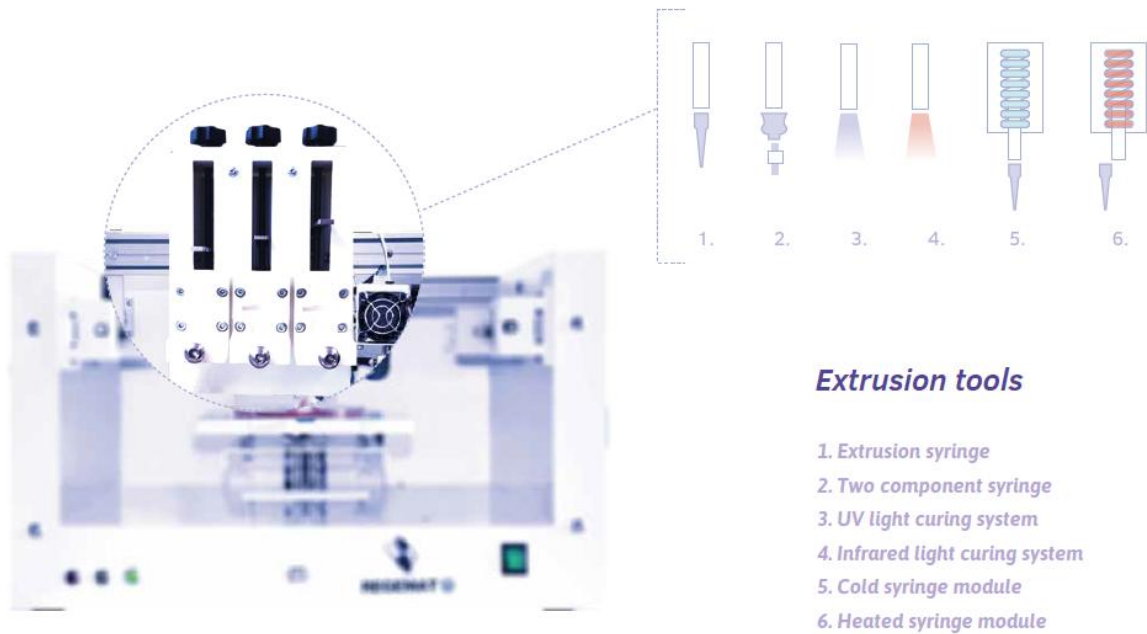


Figure 24 Head extrusion tools

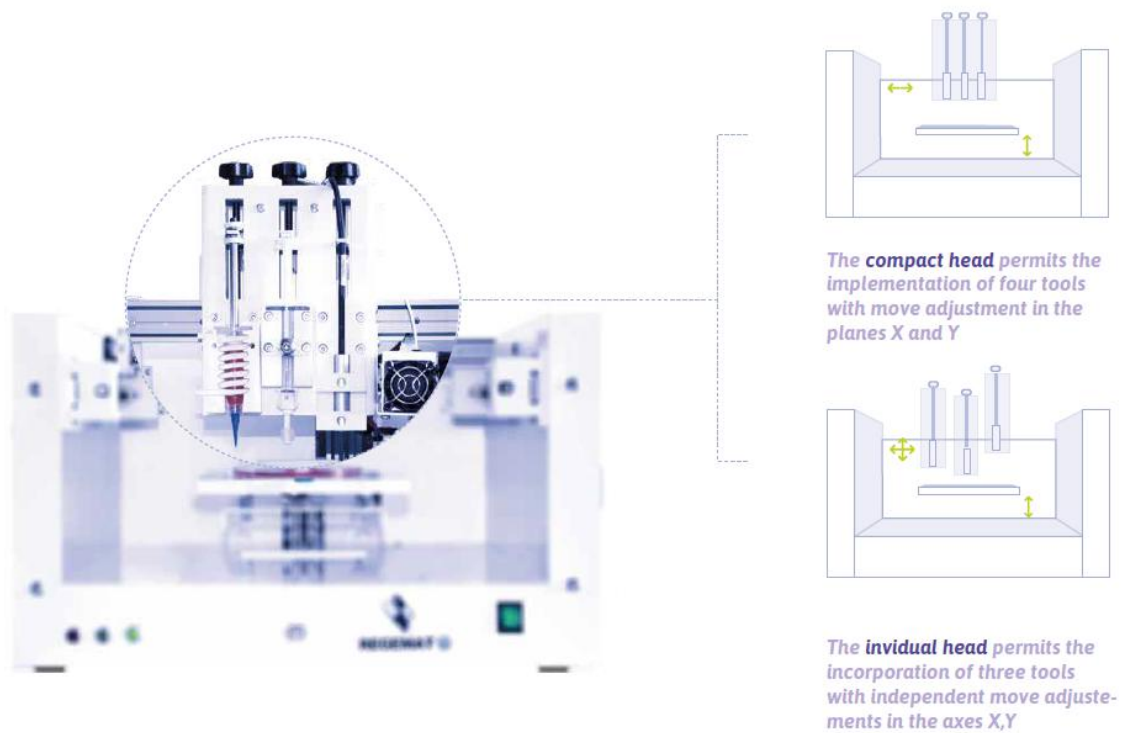


Figure 25 Head options, compact or individual Z-axis for each tool

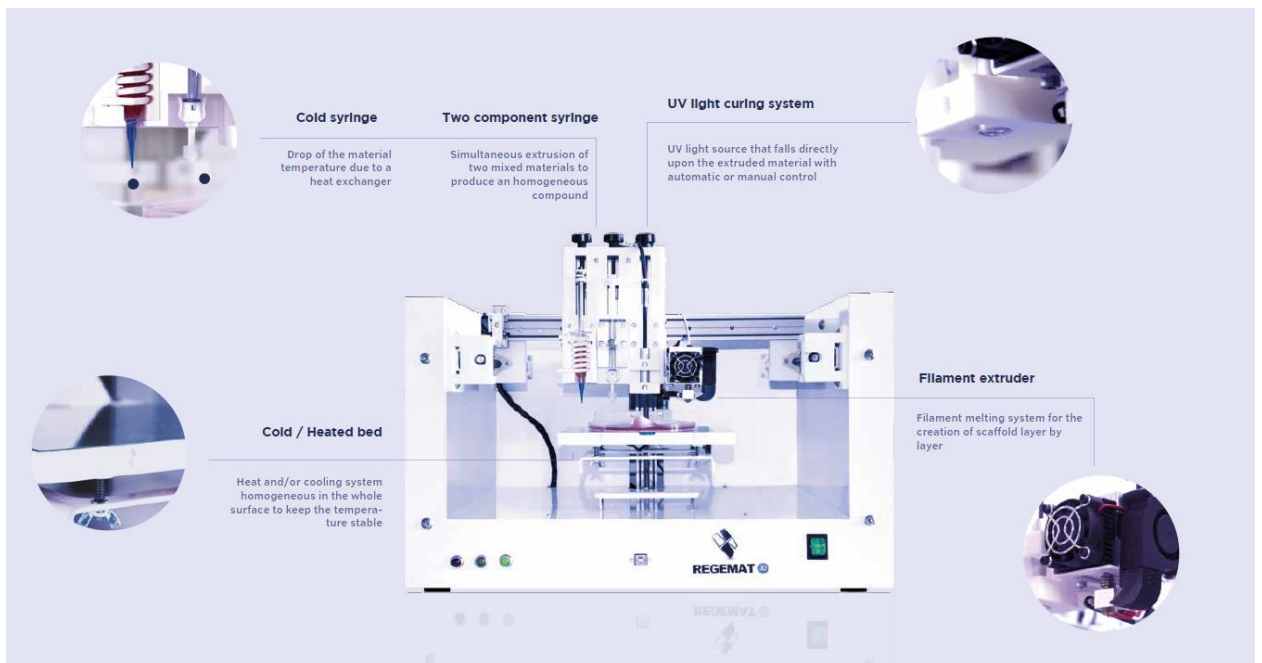


Figure 26 Some options of the printing head

A central unit connected to the sliding bars have been designed. All the different syringes containing the materials to be printed using IPT based CE are easily removable and inserted to the central unit. The FMD nozzle is also incorporated to the central unit. This central unit gives the printing head the necessary rigidity in order to be able to print with a filament resolution of 0,3mm. The material is printed using a heating resistance and a thermometer that heat the extreme of the nozzle. A stepper motor located in the structure, produce the force that move the filament towards the heated zone, melting the material and depositing it in the manufacturing area.

The distance between the syringes and the FDM is the minimum as possible, so we have placed the stepper motors in line. In future designs of the bioprinter, we may need to use more syringes and stepper motors, so in order to maximise the effective printing area we may have to use a parallel configuration of the stepper motors, increasing the distance between the syringes and the FDM nozzle. These changes will have to be configured in the software.

Figure 27 shows the 3 main manufacturing modes that can be used. The first one has already been described (FDM) m the second one is a proprietary algorithm that injects the cells in the different pores of the scaffold. This can be done point by point or continuously injecting the bioink. The last one and the one used in the experiment for the validation of the system is the IVF of the volumes printed.



Figure 27.3 Main manufacturing modes that can be used in the system

In addition to these printing modes the system can also print using photocurable polymers with UV lights.

1.2 ECU, Sensors and actuators

The result of the different modules that have been integrated to the ECU to control the different sensors and actuators of the system are:

-Processing and control platform: Figure 28 show the connections of the different pins of the ATMEGA2560 microcontroller used to read the instructions from the software and to control the drivers of the stepper motors and the different sensors and actuators.

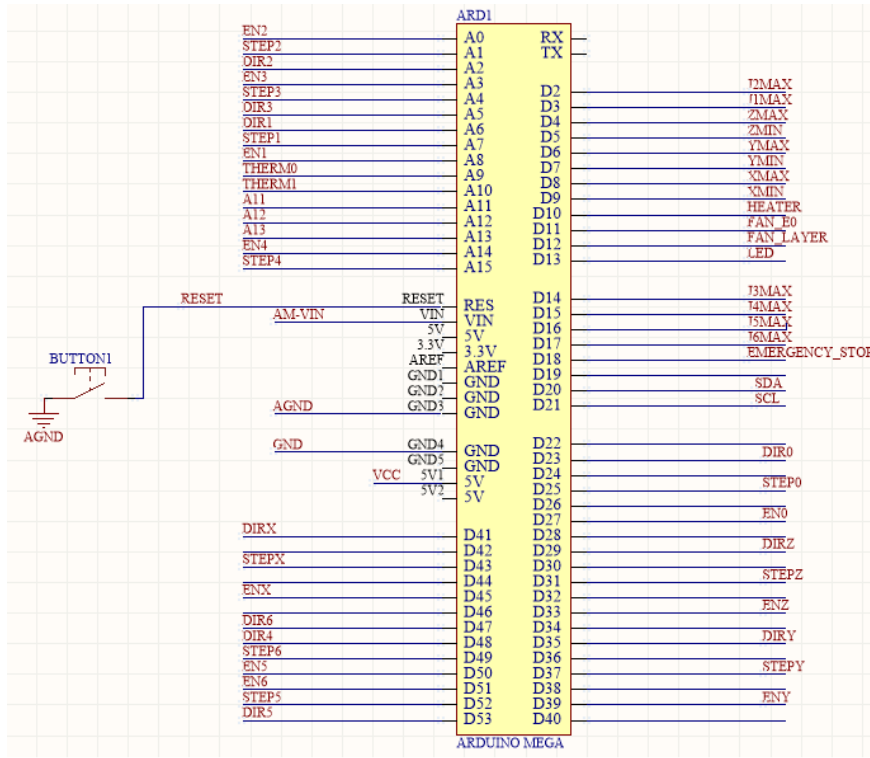


Figure 28 Arduino Mega microcontroller

-**Power Indicator:** This led shows that the processing platform is on (Figure 29).

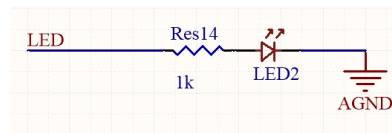


Figure 29 Power indicator sketch

-**Voltage reference supply:** The power supply is directly connected with this circuit, that filters and protects the rest of the components from high current and voltage peaks (Figure 30).

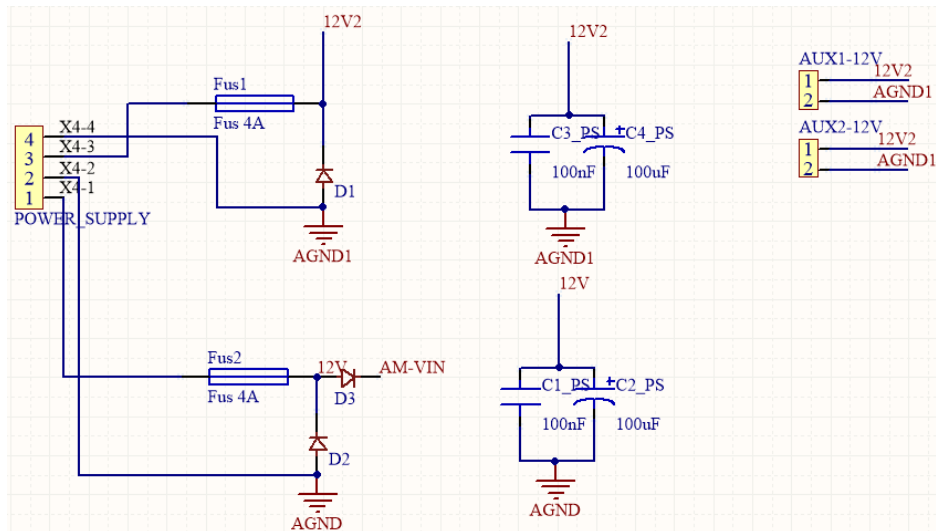


Figure 30 Voltage reference supply sketch

-Heater control: This circuit is controlled by the microcontroller by means of PWM signal, and allows to control the current inside the resistor that heats the hotend where the filament extrusion happens. For a more accurate regulation of the hotend temperature, a PID control has been implemented into the firmware (Figure 31).

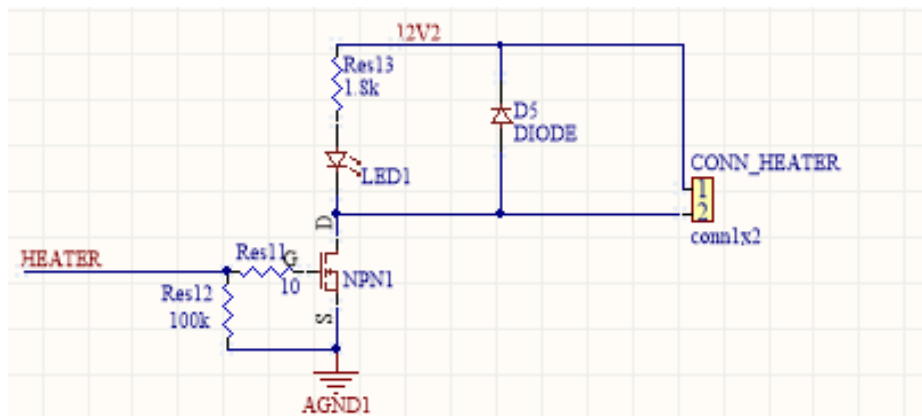


Figure 31 Heater control sketch

-Temperature monitoring: The system counts with two inputs for NTC sensors, in order to measure and monitor with a high accuracy the hot end temperature (Figure 32).

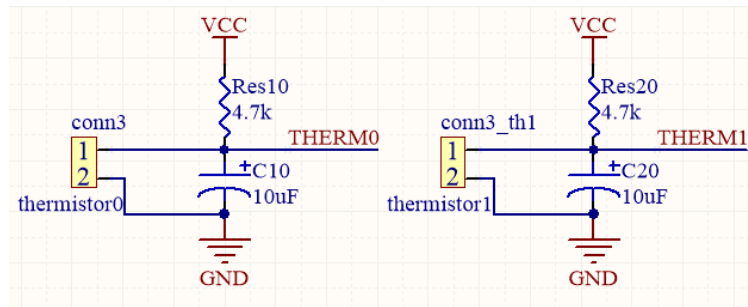


Figure 32 Temperature monitoring sketch

-Fan control: As the heater control, the system also regulates the fan force through the current flow which depends of a PWM signal. There are two fans, one for heater cooling and one for scaffold cooling (Figure 33).

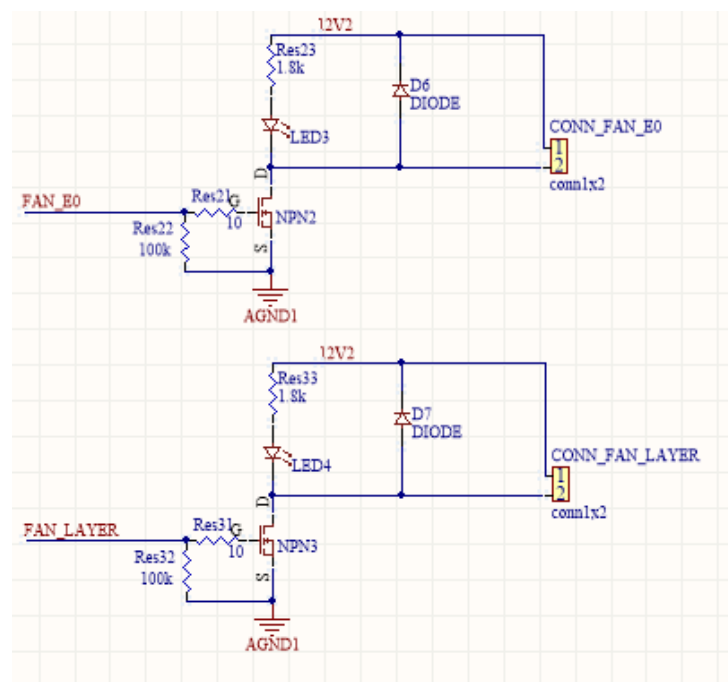


Figure 33 Fan control sketch

-I²C communication: An I²C port has been integrated for the communication between an I²C device and the processing core (Figure 34).

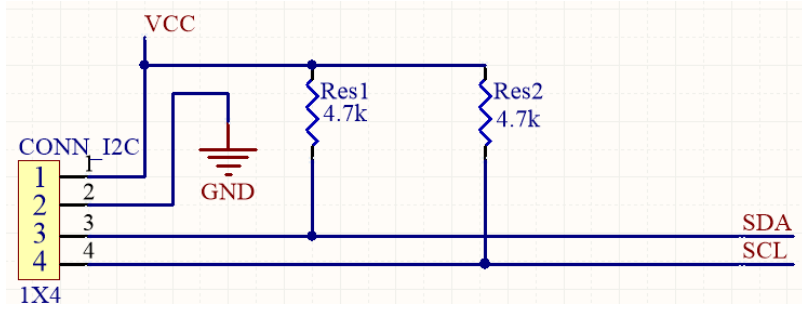


Figure 34 I²C communication sketch

-Stepper motor drivers' control: The accurate movement of the stepper motors is achieved using current drivers which are controlled by the processing core. For a single driver, the microcontroller calculates the needed steps for reaching a particular point in this axis, it activates the driver and selects the direction, and then sends pulses to the driver that moves the stepper motor. The drivers are configured for working under microstepping mode, allowing to achieve high accuracy movements (Figure 35).

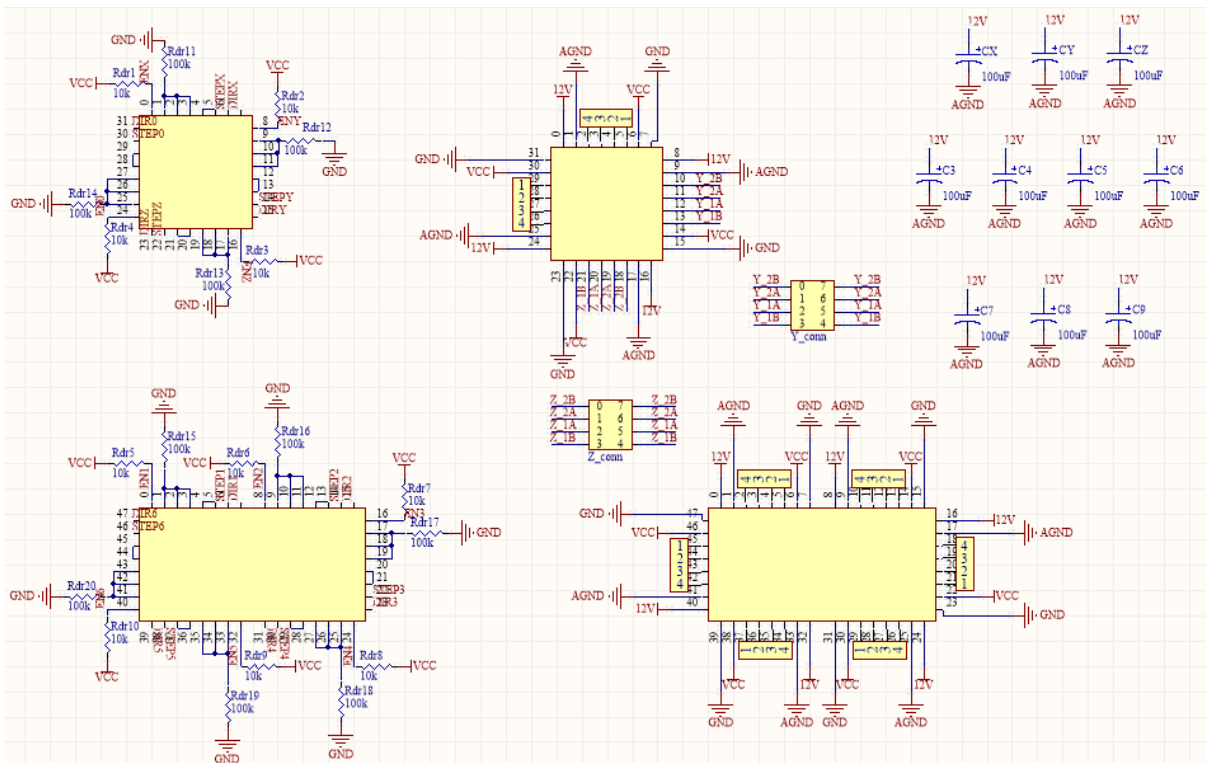


Figure 35 Stepper motors drivers sketch

-End-stops: Each axis has two sensor which are placed in the opposite sides and are used to limit the printing volume in such a way that the printing head cannot exceed these limits. They alert to the processing core, which stops the movement in that direction. The syringes have also a sensor that indicates when the syringe is empty (Figure 36).

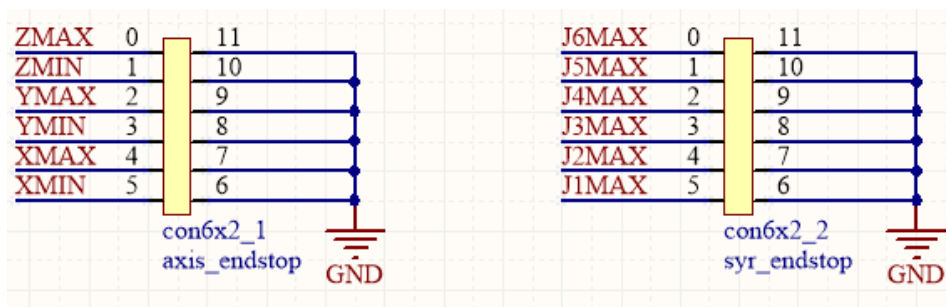


Figure 36 End stops sketch

-Emergency stop: The embedded system counts with an emergency button that can be pushed by the user when there are errors or undesired behaviours of the machine, getting into a state of emergency (Figure 37).



Figure 37 Emergency stop sketch

Figure 38 shows the distribution of the different components in the ECU of the bioprinting system.

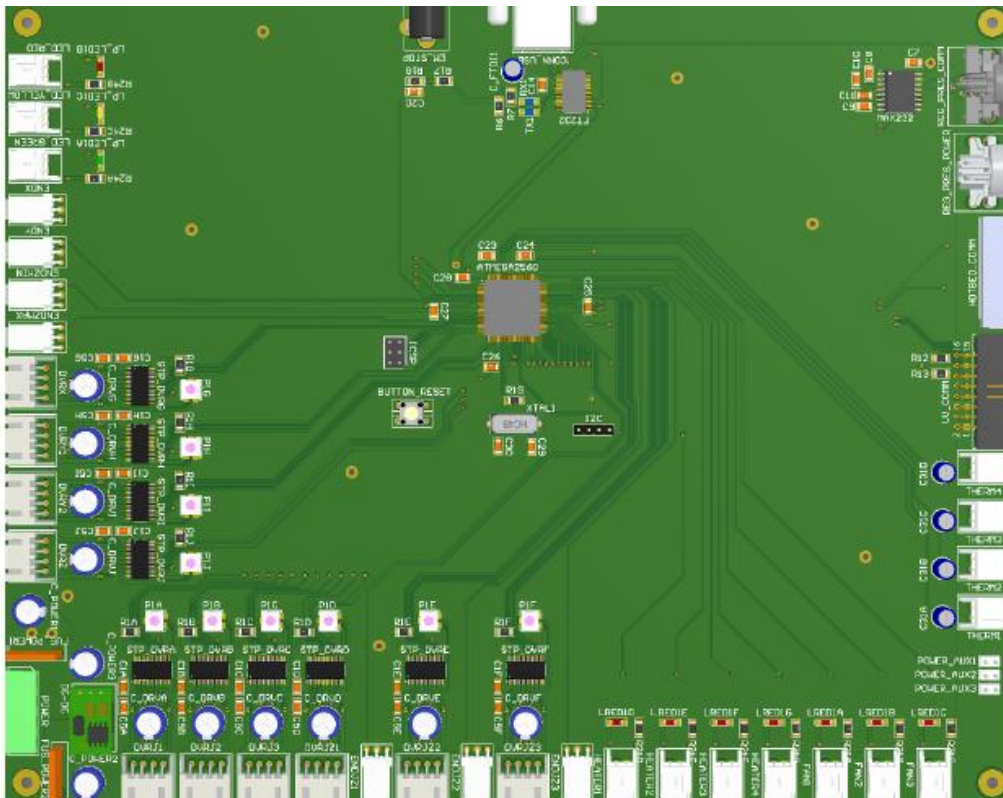


Figure 38 ECU Sketch render

Figure 39 shows a block diagram which identifies the main function of the firmware. When there are no commands in the input serial buffer, the system executes tasks for checking its state (if there are movements of the printing head) and for maintaining the last programmed heater temperature.

If the interface sends some G commands, the system detects that there is some information in the serial input buffer, characters are read until the identification of the command. The next step is to verify the integrity of the command (through an error checking) and if some command has been lost (through line number checking). Finally, if the verification is correct, the associated instructions are executed, whereas in the opposite case, the system asks for receiving again the same command.

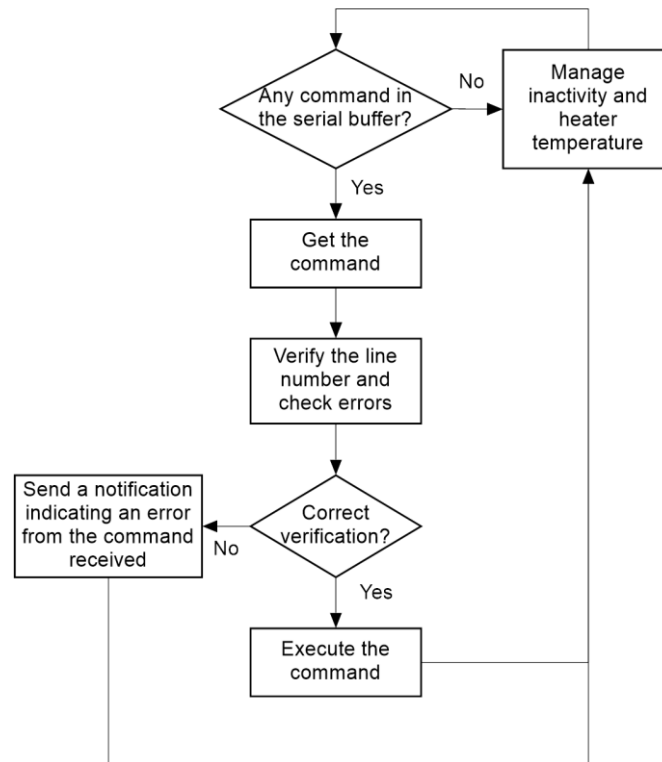


Figure 39 Diagram of the main functions of the firmware.

The firmware includes three types of instruction: i) type G, for actions associated to printing head movements; ii) type T, for selecting the extruder or a syringe for delivering; iii) and type M, for other instructions as heater temperature selection, fan control and so one. Table 2, Table 3 and Table 4 below reflect the G-commands supported (Type G, M and T).

<i>Type G</i>	
G1	Movement of the printing head from the current position to the destination position selected by the command
G4	Pause of the printing head movement during a certain time selected by the command
G28	Homing: Movement of the printing head to the

	initial position of reference → point (0,0,0)
G92	Change of the value of a coordinates to a value selected by the command

Table 2 Types of G instructions and function

<i>Type M</i>	
M104	Set a targeted temperature of the hotend
M105	Read the hotend temperature
M106	Turn on the layer fan
M107	Turn off the layer fan
M109	Set a targeted temperature of the hotend and wait until it is reached
M112	System goes to emergency state
M113	System returns from emergency state
M600	System saves the current position and goes to pause state
M601	System returns from pause state and it is positioning in the last position before of the pause state

Table 3 Types of M instructions and function

<i>Type T</i>	
T	Systems selects the extruder or a syringe as current delivering system. The next delivering commands are related to it.

Table 4 Types of T instructions and function

Apart from G-commands reception and verification, the most important functions of the firmware are the movement of the stepper motors and the hotend temperature control. With regard to the first, the pulses are sent using the timer 1 interrupt and configuring the interruption in order to obtain the desired speed; for the second, temperature is read using timer 2 interrupt and managed in the main function.

1.3 Software and GUI

GUI and G code generation

The developed interface allows that any user uploads a 3D model, locate it in a concrete position into the printing volume, and start to print, after setting the parameters of the scaffold and the materials of the syringes.

The first step for printing a desired geometry of the scaffold, is to **upload the STL file** which codifies the shape of the piece as a set of triangles, each one with three vertices and a normal vector (Figure 40). The interface allows to work with predefined geometries (their STL files are included in the software library), as for example, a cube, a cylinder, a plane with a small thickness, ... ; or to upload a STL file generated from a 3D design built with any CAD software. In the figure below, the bottom used in load a predefined or designed STL is shown, as well as the geometry inserted into the printing volume (in this case, a cube has been loaded).

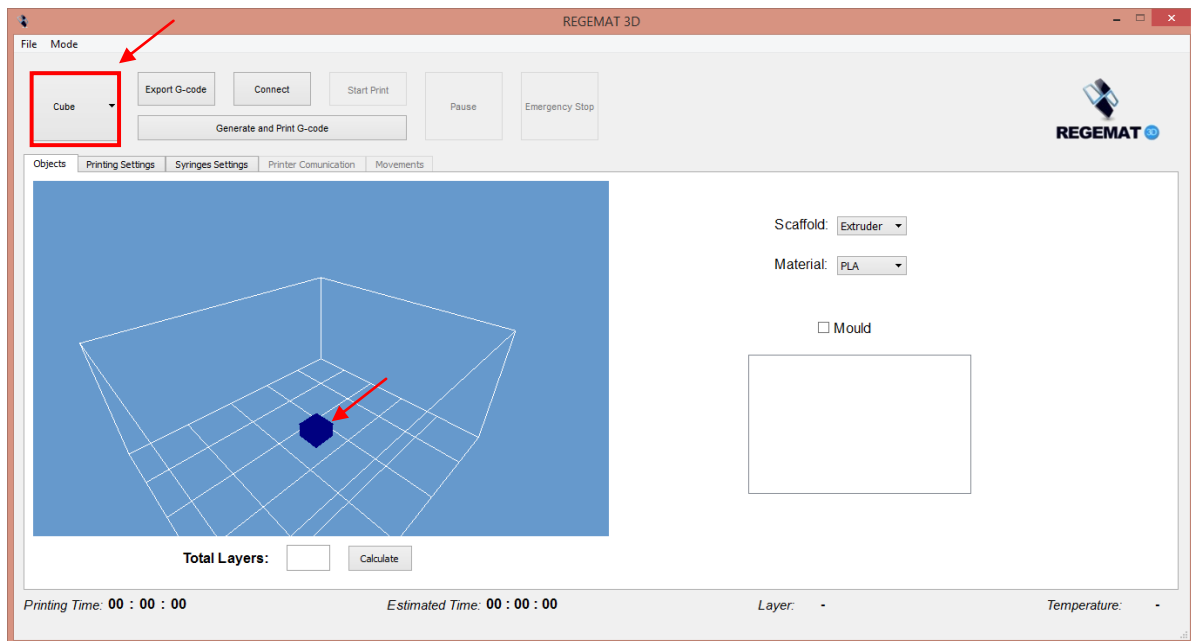


Figure 40 Loading a predefined ST

The printing volume refers to the effective volume of the bioprinter REGEMAT3D, where any geometry can be printed using all delivering systems of the printing head explained in the precedent sections. Once the geometry appears, it is possible to move it around this volume to a desired place where it will be printed. The GUI also allows the user to print different geometries in the printing area and to position them.

Other important consideration is the scaffold material. As the figure below shows, the interface allows to extrude a thermoplastic polymer filament, such as PLA, through a hotend nozzle in order to obtain a thin thread; or to use a syringe of the printing head with a fluid biomaterial. Both possibilities can be the structure of the scaffold. The syringes can also be used to fill the rigid scaffold pores if we use the thermoplastic polymer as scaffold.

Scaffold settings (Figure 41) includes the configuration of several parameters related to scaffold porosity, layer height, hotend configuration (as nozzle size, temperature, ...), speed of the printing head, number of perimeters and “skirts”, and fan cooling of the

scaffold. Although these settings are very focused on generating a scaffold using the extruder and a polymer filament, a correct selection of each parameter allows the printing of the structure using other biomaterials or polymers placed in the syringe which has been selected for being the scaffold builder.

Once all the parameters have been set, the configuration can be saved in a file for future prints with the same configuration. This option, which is shown in the figure below, can be also used in loading a configuration that previously has been saved.

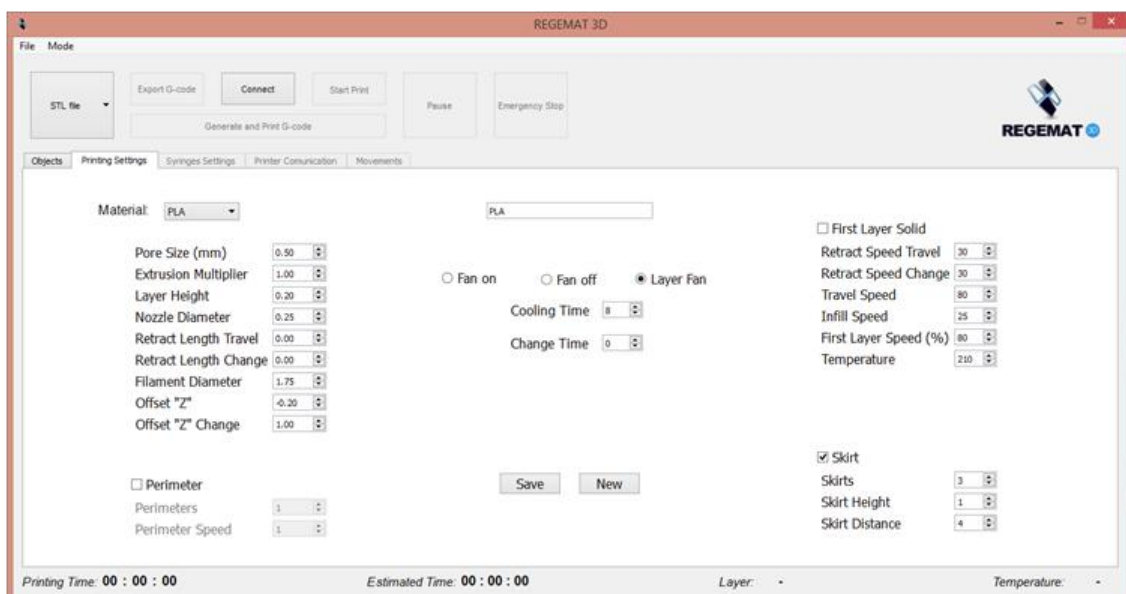


Figure 41 Scaffold settings

In the Figure 42 the possibilities of **syringe settings** are shown. The user should identify the material that each syringe contains, and then configure the amount of each material per layer and the layers where it will be dropped. Also, special syringe behaviour for adapting to the material properties can be configured, as well as an internal control for avoiding an incorrect configuration in which the system has to deliver more material than there is in a syringe.

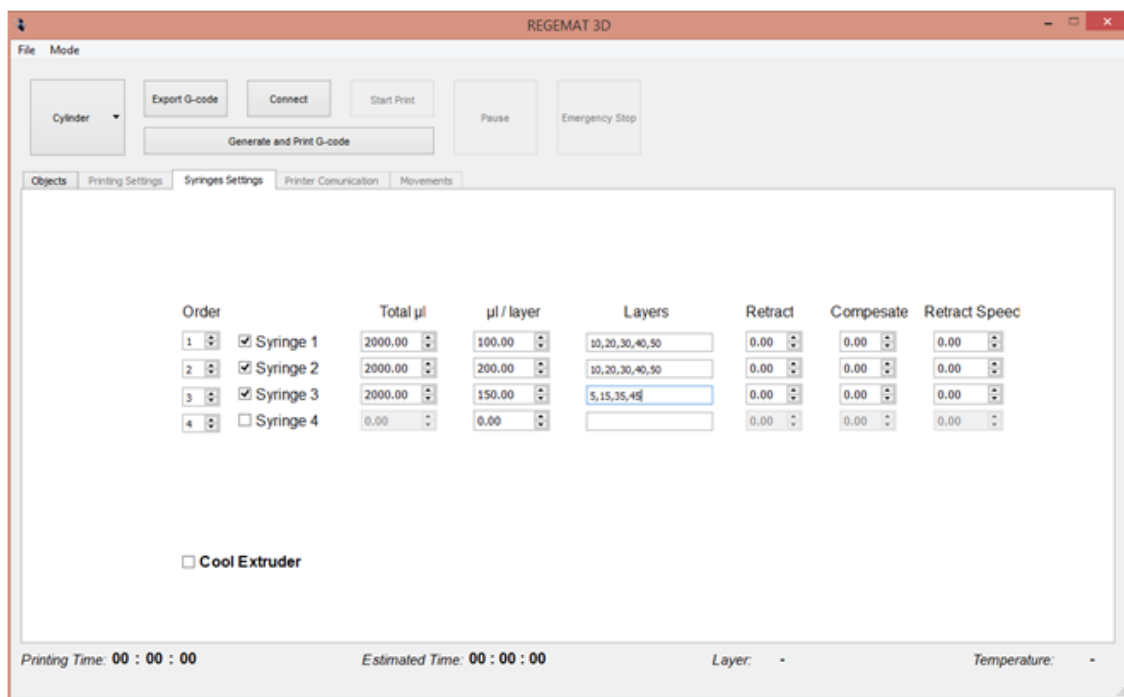


Figure 42 Syringes settings

After the insertion of the geometry and the configuration of the scaffold and syringes parameters, the next step is to **generate the associated G code**. A G code with the G commands will control the bioprinter system and manage it for building the geometry with a determined characteristic. To obtain the G code the information about the geometry codified by triangles in a STL file is processed by several algorithms until obtaining a structure that contains layer by layer, the points that have to follow the printing head for building the perimeter and the internal mesh, and for filling the mesh pores with specific materials.

Once the whole route is known, the information of points is formulated as movement commands, integrating them into G command structures. Finally, these movement instructions are completed with others related to fan and temperature control, and tool management.

The result is a set of commands that the microcontroller knows how to interpret them, and identifies specific actions for their execution. In the Figure 43, an example of a G code obtained from a particularly scaffold and syringes settings is presented.

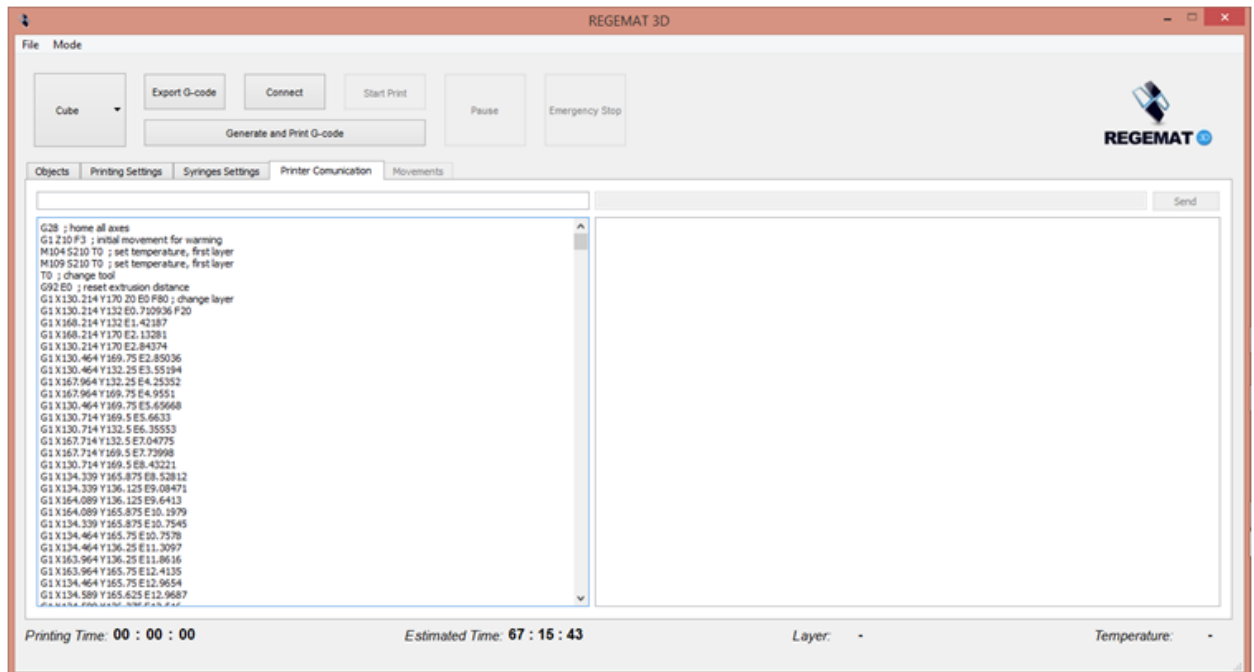


Figure 43 Generation of G code

Figure 44 and Figure 45 show the software in its final version. Figure 44 shows the upload of a distal femur geometry and the trajectories for printing after the configuration of the printing parameters. Figure 45 shows some of the printing parameters to be configured.

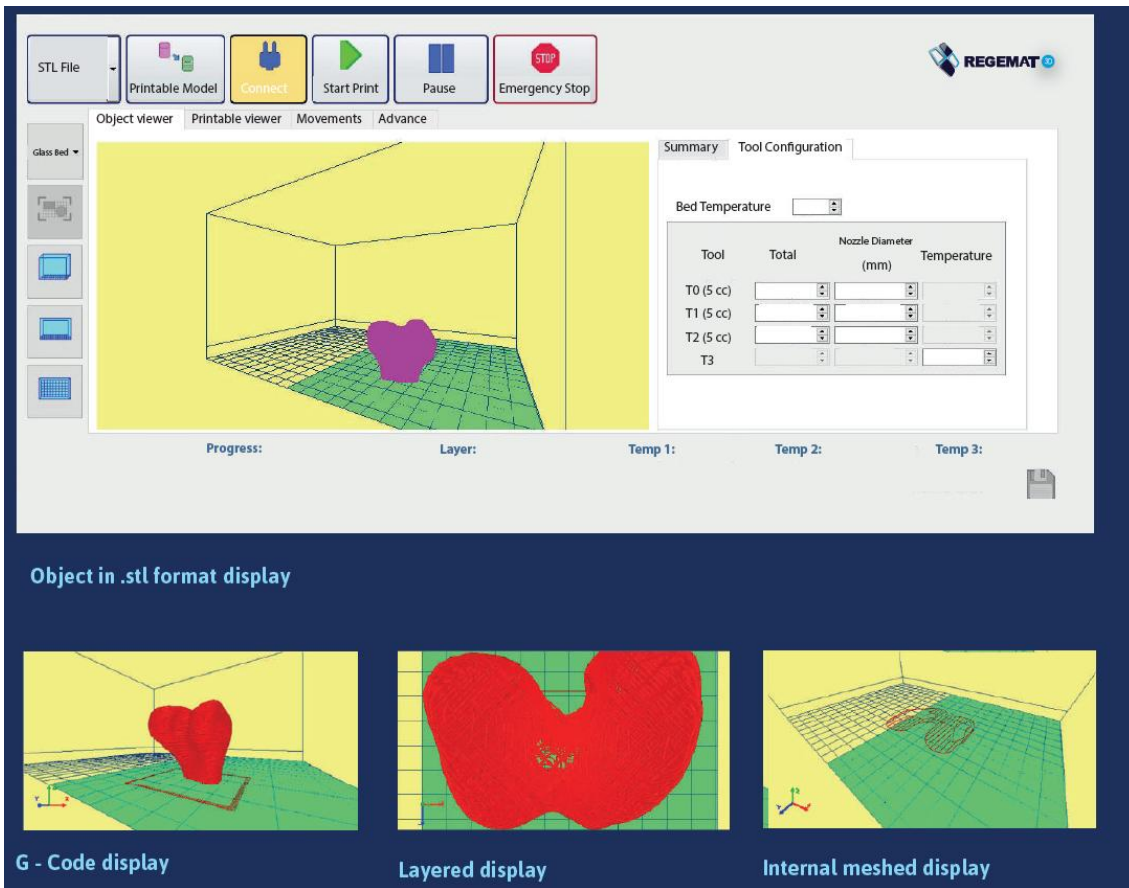


Figure 44 Distal femur section printing trajectories

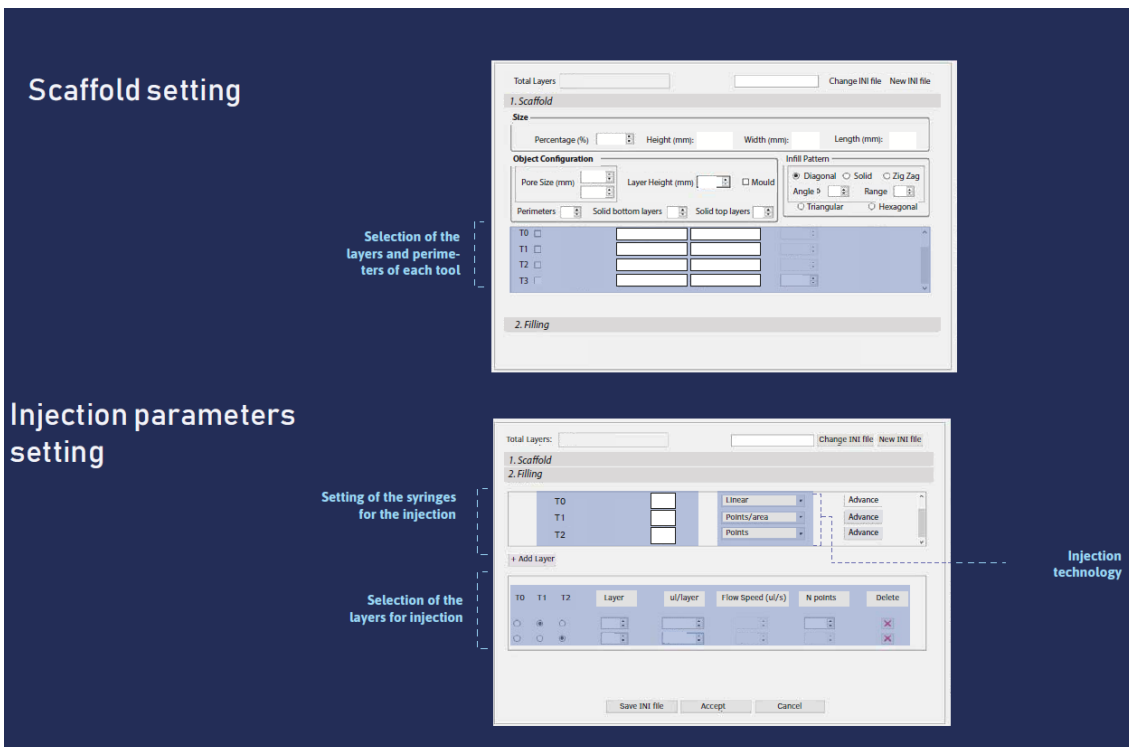


Figure 45 Printing parameters configuration

Software and ECU communication

The first step for establishing the communication between the interface and the printing system, is the configuration and connection through the serial port. The information about this connection (port name, baud rate, parity bit, ...) are preconfigured. Once the G code has been generated, the next step is to initiate the communication between the interface and the printer. As the internal configuration of the communication has been programmed in both sides, the user starts this communication pushing the button of “connect”. As the interface is the master, it is the responsible of configuring the connection for enabling the communication, as well as the finalization and closing of the ports.

When this communication is enabled, the first transmitted messages are from the slave (the printing system), that contains general information and the connection.

The next steps in the communication between the developed software and ECU are the **G command reception and error checking from serial input data and the execution of actions associated to the received G command.**

In the G command reception and error checking from serial input data, the receptor of the G commands transmitted by the software is the microcontroller ATMEGA2560 integrated in the ECU. Before the data is processed the line number of the command and the checksum have to be verified in order to confirm that the commands are executed in the correct sequence. If any command is sent by the software without the line number, the printer system is able to process it if the checksum is correct, this is the case when the user is acting over the printer without sending a G code. When an individual command is sent by the interface without line number, the printer system is also able to

process it if the checksum is correct; this happens when the user is doing concrete actions over the printer, instead of send the G code generated.

In the execution of actions associated to the received G command, once the data related to a G command has been verified, the command is executed, through the search of its type and the set of instructions associated. If the selected command exits, a confirmation with the same line number is sent to the transmitter, in order to enable the arrival of new commands. Otherwise an error notification is sent.

A special case is the emergency management, represented by M112 and M113 commands, for activating and deactivating the emergency state, respectively. When a M112 is received, the system ignores any received command but M113, which makes the system returning to a functional state.

1.4 Improvements and technical contributions in the printing process

Some of the improvements in the algorithm of code generation and the printing process are:

a) Point mesh generation of the volume perimeter from an STL file

STL files contain vertices and normals, which define triangles (three vertices and a normal vector) (Figure 46). A 3D printer is an additive machine, so the main step, in order to get a G-code file, is to convert a triangle mesh into a layer mesh.

```

solid cubo
  facet normal -1.000000e+000 -1.156482e-016 0.000000e+000
    outer loop
      vertex 1.821377e+001 0.000000e+000 2.000000e+001
      vertex 1.821377e+001 3.000000e+001 2.000000e+001
      vertex 1.821377e+001 0.000000e+000 0.000000e+000
    endloop
  endfacet
  facet normal -1.000000e+000 -1.156482e-016 0.000000e+000
    outer loop
      vertex 1.821377e+001 0.000000e+000 0.000000e+000

```

Figure 46 STL file code with the normal vectors and the vertex

The description of the operations applied to obtain the perimeter mesh, is shown in Figure 47. The software saves all the triangles from the STL file. From each z point and the parameter "layer height", layers are formed with the triangles points that touch this layer. Based on these layer's points, segments are created. All these segments define the scaffold perimeter that the user loads from the interface.

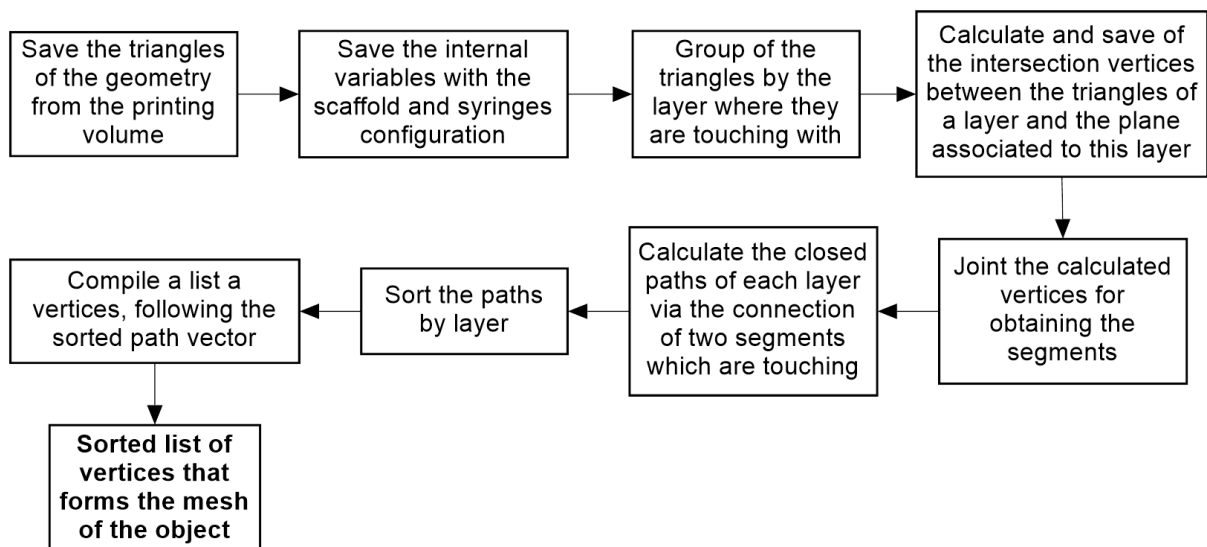


Figure 47 Operations applied to obtain the perimeter mesh

b) Layer internal mesh calculation

The infill of the scaffold is a geometrical pattern that defines the inner volume for the perimeter mesh obtained from a STL file. Particularly, for obtaining square pores, the

infill pattern is a set of rectilinear paths, whose direction in an even layer is perpendicular to odd layer, shaping a grid pattern. The scaffold porosity is defined from the infill as well.

Perimeter segments are used as reference system for building the infill segments. There are two important parameters which the algorithm uses for calculating and building the grid mesh: the nozzle diameter and the pore size. Both of them are obtained from the printing GUI, where scaffold printing parameters are configured (Figure 48).

The screenshot displays the 'Printing Settings' window for 'Syringes Settings'. The material is set to 'PLA'. The left column contains parameters for Pore Size (1.00 mm), Extrusion Multiplier (1.10), Layer Height (0.20 mm), Nozzle Diameter (0.25 mm), Retract Length Travel (0.00 mm), Retract Length Change (0.00 mm), Filament Diameter (1.75 mm), Offset 'Z' (0.00 mm), and Offset 'Z' Change (1.00 mm). The middle section includes radio buttons for 'Fan on', 'Fan off', and 'Layer Fan' (selected), along with 'Cooling Time' (20) and 'Change Time' (30). The right column features 'First Layer Solid' (checked) with sub-parameters: Retract Speed Travel (30), Retract Speed Change (30), Travel Speed (80), Infill Speed (20), First Layer Speed (%) (80), and Temperature (230). Below this is the 'Skirt' section (checked) with Skirts (3), Skirt Height (1), and Skirt Distance (6). 'Perimeter' is checked with 1 perimeter and a speed of 20. 'Save' and 'New' buttons are located at the bottom center.

Figure 48 Printing settings of the mesh infill.

A diagram with the process used in getting the internal grid mesh is shown in Figure 49. The square pores are achieved combining two layers. Each of these layers contains a set of segments, placed to a certain distance one another (grid space), that connects two points of the perimeters. The direction of this set of segments is orthogonal from a layer to the next one, in a way of superposing two of them, the internal mesh is formed by pores with the desired size.

Once the pore size and the nozzle diameter are set, the grid space is calculated as the sum of both of them. This parameter tells to the algorithm the distance between two parallel filaments extruded by the printing head, and defining the size of the pores. Also,

two orthogonal vectors, v_1 and v_2 , and two starting referential points, p_1 and p_2 are defined, and associated each other. A pair of the direction vector and referential points $\{v_1, p_1\}$ will be assigned to the odd layers, whereas the others $\{v_2, p_2\}$ will be for even layers.

For the first layer, a straight line parallel to v_1 that crosses the referential point p_1 , is traced. After that, it is checked if there are segments which have been intersected by the straight line. As this starting point is outside of the geometry perimeter, there are not intersected segments. Then, the referential point is moved, in the direction of v_2 and a distance equal to grid space, and a new straight line parallel to v_1 is traced. Now, it can happen that there are some segments intersected by the straight line, or there are none. In the second case, the referential point is displaced as before. In the first case, that means that the referential point is into the perimeter. The pair of intersection points are saved, and then the referential point is moved.

This verification is continually executing until the referential point is again outside of the perimeter, and there are no intersected segments by the straight line. At this point, the algorithm has a set of pairs of points that connects two points of the perimeters, and the segment formed by this joining is parallel to a vector v_1 . Finally, the connection of these segments will be the path that the printing head will follow for generating the infill of the geometry.

In the next layer, the process is the same that has been described, but using $\{v_2, p_2\}$ and moving the referential point in the direction of v_1 . As before, at the end of the process a path formed by the connection of parallel segments is obtained, but in this case, these segments are orthogonal in respect of the path segments of the previous layer.

When two consecutive layers are superposing, the result is a grid mesh which fill the internal part of the piece.

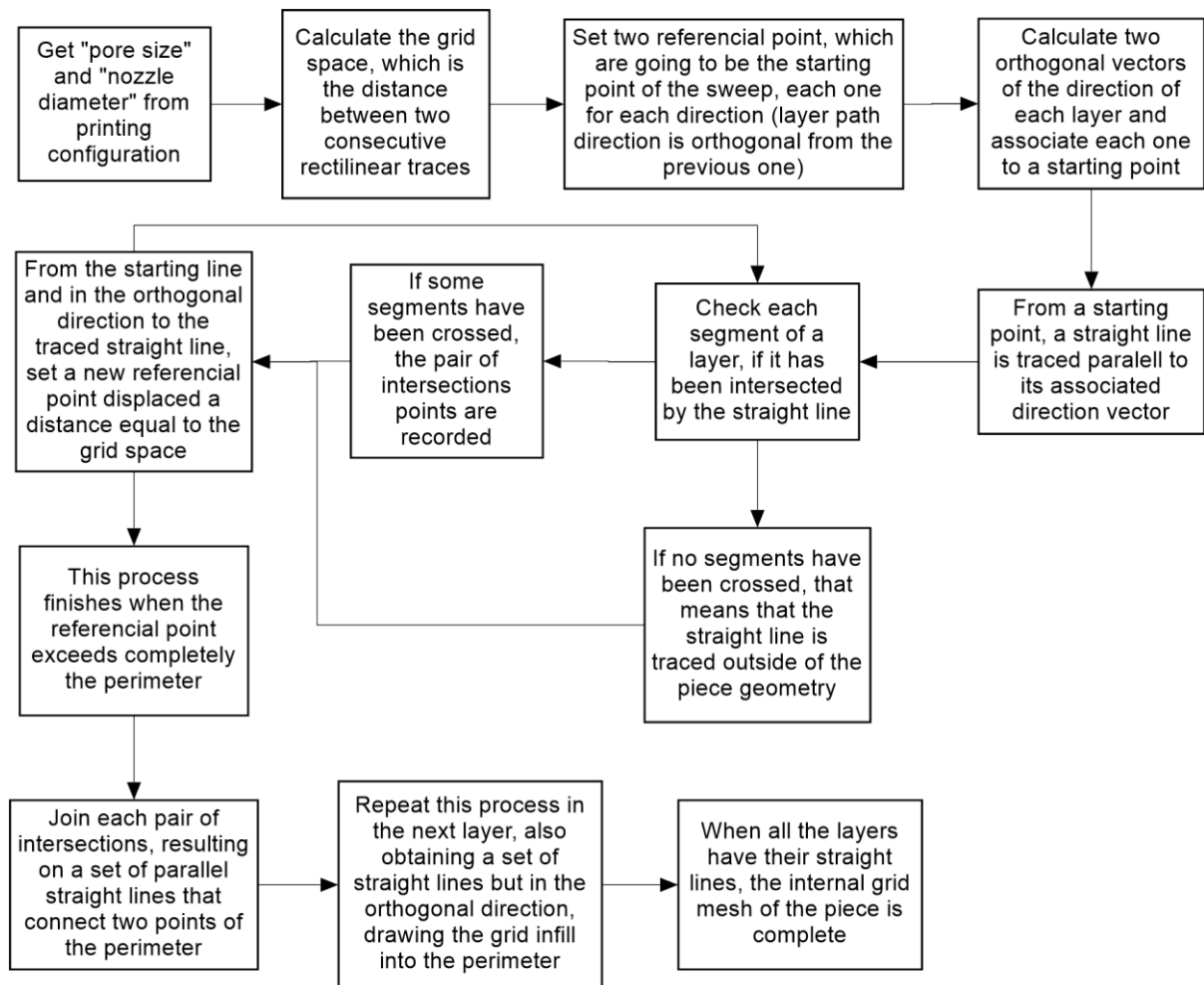


Figure 49 Operations applied to obtain the layer infill.

c) Porous filling calculation

The pores can be filled in two different ways, depending on whether a specific amount of material is individually delivered in each pore, or the delivering is continuous, travelling around the layer and dropping material in all the places where the printing tool is. The choice between these two modes can be done in the syringe configuration. We have enhanced the first process that we have named individually pore filling (IPF) to increase the viability and survival of the cells when working with high temperature thermoplastics.

At functional level, the difference between the continuous ejection mode and the single pore ejection mode, is in how the printing head moves and delivers material. In the continuous delivering mode, the printing tool travels between different points of the perimeter until fill all the pores of the layer. In the single pore mode, there is not delivering in the transition between two pores, instead of this the tool place above the pore, an amount of material is delivered and the tool is moved to the next pore, and then there is a delivering again, and so on, until all the pores are filled. This reduce de required quantity of cell laden hydrogel.

However, the movement of the syringe is equal in both modes, and the difference is that in the continuous mode, the movement is done between perimeter points, whereas in the single mode, the movement is done between different pores. An important consideration for the IPF is that, although the printing tool is moved between pores, its path pattern is a straight line that connects different points of the perimeter, and this is the same path that the printing tool follows in the continuous mode. In addition, the direction of the travel for both modes is the same than the vector v_1 which was used in defining a rectilinear pattern for generating the internal mesh of the scaffold. And consequently, all these paths generated are parallel or orthogonal (depending on the layer) to the internal mesh of the scaffold.

The basis of algorithm that is used in drawing the path which will follow the printing tool for filling the pores, is practically the same as the one used in generating the internal grid mesh, but it differs in that there is only a vector of direction (v_1), and the initial reference point is moved, in the direction of v_2 , a distance equal to the half of the grid space. This shift allows that the paths calculated by the algorithm are placed between the straight lines of the grid mesh, and therefore, the printing tool is moved exactly in the middle of a line of pores, enhancing the dropping of material into it.

From the parameters calculated for building the internal mesh, now $\{v_1, v_2, p_1\}$ are used. As in the grid mesh generation algorithm, v_1 identifies the direction of the paths for filling the pores, v_2 is used for defining the direction through the referential point is moved, and p_1 is the starting referential point, being the beginning of the sweep. In this case, the first operation is to shift this point, a distance equal to the half of the grid space and in the direction of v_2 .

The next steps are the same as before. The referential point is moved in the direction of v_2 a distance equal to the grid space; a straight line in the direction of v_1 is traced and its intersection point with the perimeter is saved. At the end of the sweep, the algorithm contains a vector with pairs of points that identifies the travel of the printing tool. Due to the shift, this tool will move above the middle of the pore, because this new travel lines are placed between the grid mesh lines.

d) Injection volume filling

IVF procedure allows the user to configure the numbers of scaffold layers, or material volume, to be printed before the volume filling takes place. The software uses the shape of each layer to calculate the volume to be filled with the bioink. The algorithms calculate this volume to be filled with the volume shape and the different points to inject the cell laden bioink.

e) Generation of a file that contains all the G commands

Once the algorithm generates a set of sorted points that defines, layer by layer, the external shape of the geometry and an internal grid mesh structure formed by pores of a determined size, the last step is the generation of commands which will be sent to the

machine and will define the movements of the printing head for building the scaffold and delivering the materials placed into the syringes.

Based on layer structure, syringes configuration and printing settings, the G-code file is generated (Figure 50). A G-code file contains: movements, temperatures commands, tool settings and machine instructions.

```
G28 ; home all axes
G1 Z10 F3
M104 S230 T0 ; set temperature, first layer
M109 S230 T0 ; set temperature, first layer
T0 ; change tool
G92 E0 ; reset extrusion distance
G1 X91.2138 Y134 Z0 E0 F80 ; change layer
G1 X91.2138 Y92 E0.864348 F16
G1 X133.214 Y92 E1.7287
G1 X133.214 Y134 E2.59305
G1 X91.2138 Y134 E3.45739
G1 X91.4638 Y133.75 E3.46467
```

Figure 50 G code segment generated by REGEMAT 3D

A movement is defined by a target point (X, Y, Z), amount of material printed (E) and a speed of the movement (F). All motion instructions start with "G1", the other values are optional, so if a value is not set the printer doesn't change this parameter.

The amount of material printed for a segment is calculated by the multiplication of the distance of this segment by a parameter that defined the amount of material with respect to the distance unit (millimeters). The operations applied to obtain this standardized value, is different, depending on whether the scaffold is building or the pores are filling. In the first case, the standardized value is proportional to the nozzle diameter and the layer size, whereas in the second case, it is calculated by the division of the amount of material per layer between the distance that the printing head travels for filling all the pores (continuous delivering); or between the number of pores of this layer (IPF).

The algorithm used in generating a file with the G command, is shown in the next diagram. The first instructions are referenced to the initial management of the

REGEMAT3D bioprinter, that includes a movement to a referential point, which will be the reference axis, and hotend temperature management.

Then, the process for each layer is always the same both perimeter and internal mesh and pore filling: moving the printing head to this layer, selecting all the tools which are used in this layer and printing the segment or into the pore with each of them. In the cases of the perimeter, the internal mesh and the continuous pore fill, the G1 instruction includes the destination distance and the amount of material to deliver. For IPF, it is necessary two G1 instructions per each pore: place the delivering tool in the pore and deliver the assigned amount of material (Figure 51).

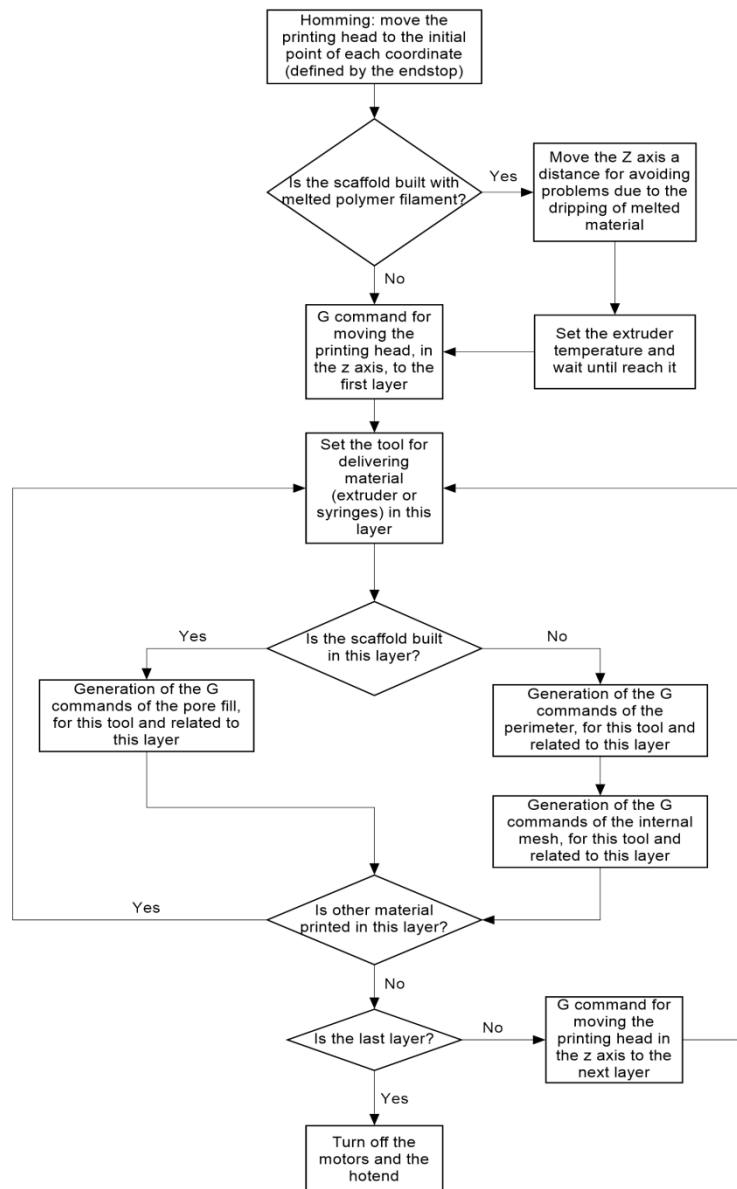


Figure 51 Operations applied to obtain the file

Also, there is a layer fan control, whose mode is configured in the scaffold settings and allows to use the fan in the whole printing, to not use it, or turn it on a specific time when there is a change from the hot end to another delivering tool for the same layer.

f) Individual commands

REGEMAT 3D software allows that the user directly sends some order to the printer without generating the G code. The interface has two methods for this aim, a basic mode and an expert mode.

The first one, is a special tab, "Movements", with some push buttons and selected buttons. The user can choose a tool (extruder or syringe) and move it or deposit material. Each row of buttons specifies movements in one coordinate (x, y, z) or extrusion (E). Every column controls the steps number or move the tool to the origin ("Home" button). The "Refill Syringe" button moves the syringe selected in other to get out the syringe and refill (Figure 52).

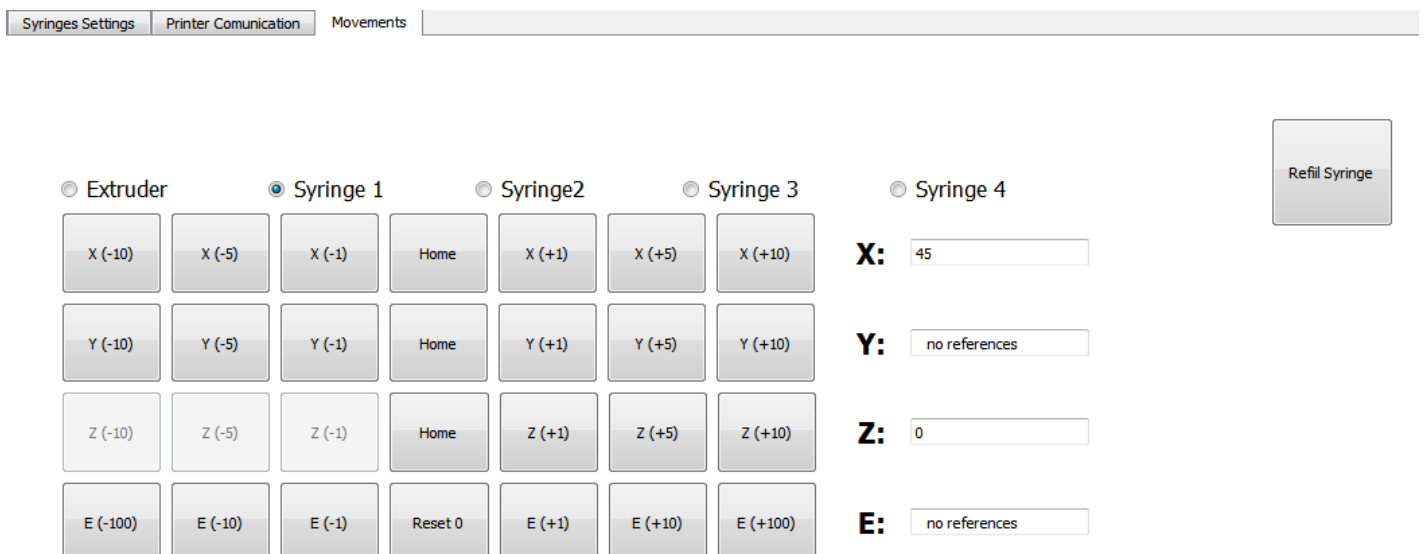


Figure 52 "Movements" tab

The second method, it is a command-line. The user is able to send individual G-code command and reads the results in the communication window (Figure 53).

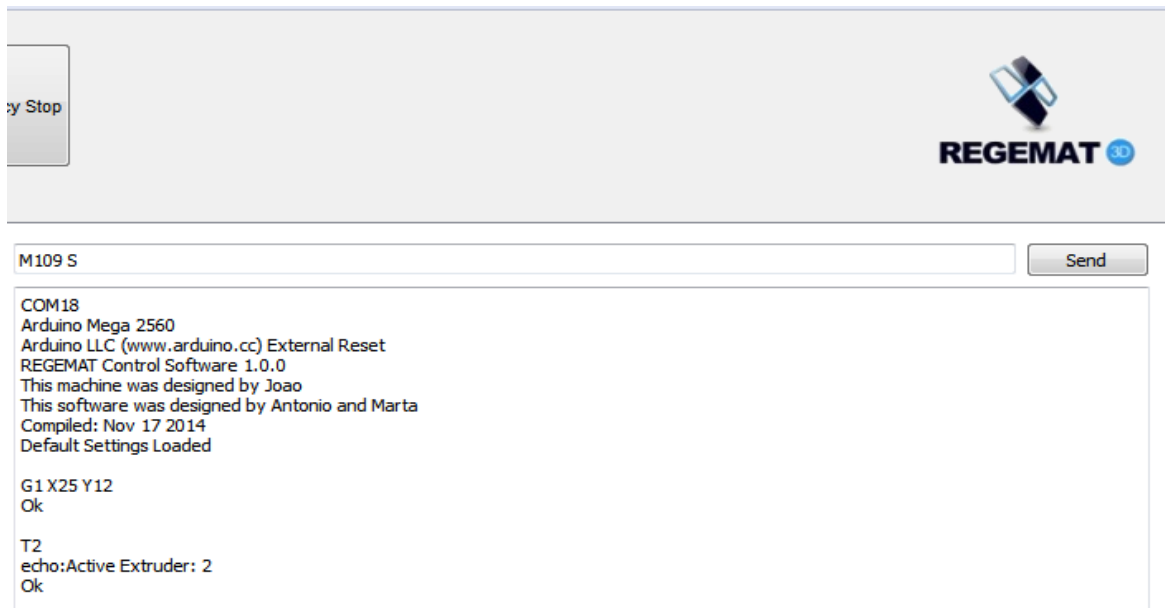


Figure 53 Command-line

g) Serial transmissions, error control and command resend

The G-code command transmission between the software and the 3D printer uses a serial communication. In this communication, the computer acts as the master, sending orders to the printer; whereas the printer acts as slave, answering the orders (Figure 54).

```
N3 G1 X104.214 Y131 Z0 E0 F80 *100
echo:Active Extruder: 0
Ok 1
Ok 2
Ok 3

N4 G1 X104.214 Y89 E0.864348 F16*31

N5 G1 X146.214 Y89 E1.7287*119

N6 M105*33
Ok 4

N7 G1 X146.214 Y131 E2.59305*116
Ok 5
```

Figure 54 Communication messages.

For controlling the data flow to the printer and managing errors in the communication, a sliding windows protocol has been implemented. The transmission window has a size of four commands, this is the number of commands which can be sent to the printer

without receiving any confirmation. When the window reaches its maximum size, the interface does not send any command and keeps waiting to receive the confirmation of some of the sent command.

Each G command has associated a line number (N) and a checksum (*), which are also sent with the command. Both elements allow for the verification of data integrity in the receptor. With the line number, the printer is able to execute the commands sequentially, and report to the interface errors in the order of command received or data integrity, identifying also the number of the command which is waiting. The checksum helps to detect errors in the bit read.

Checksum is a number obtained from a logical operation applied to the line of the command which is going to be sent, line number included. This number is calculated both at the emitter and receiver; the first introduces the number into the message and the second compare both checksum numbers. If they are equal, then the data received is considered as correct and it is executed; otherwise, the data received is incorrect and the receptor sends a request with the line number that waits to receive correctly (Figure 55).

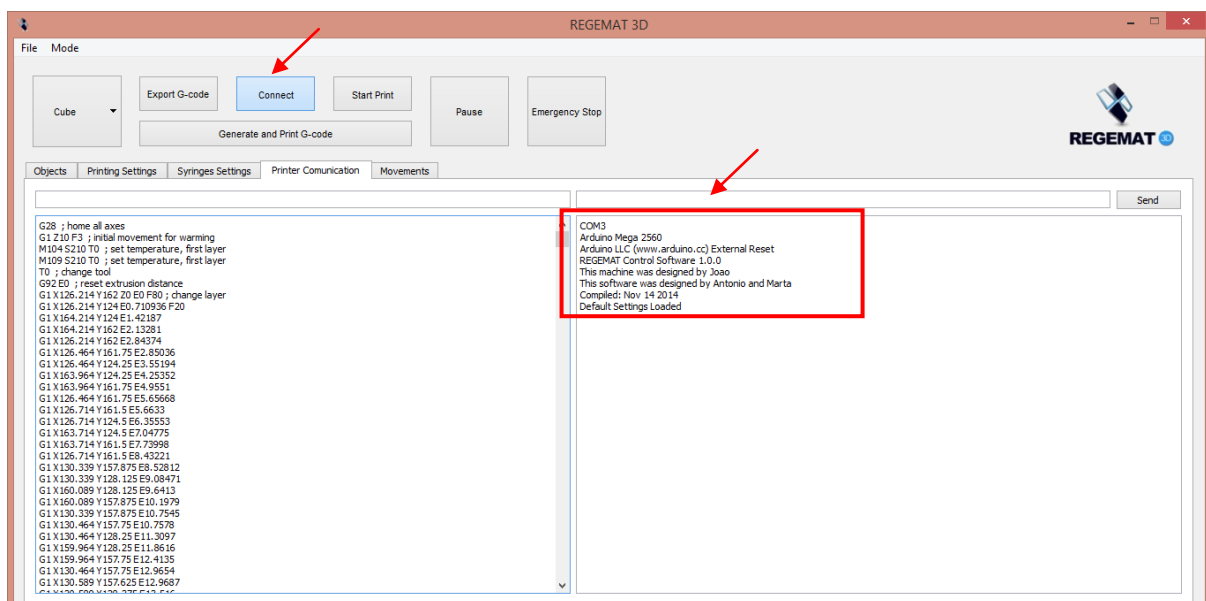


Figure 55 Initiation of the communication

Finally, once the connection has been carried out successfully, the only task that needs to be done, is the beginning of the printing, pushing the “Start Print” button. At this moment, the interface starts to send, in a rigorous order and using a sliding windows protocol for data flow control and error management, each of the G commands generated, and the printer executes each one of them, building the scaffold.

In Figure 56, it is also possible to see all the messages, both input and output, that are sending and receiving by the interface.

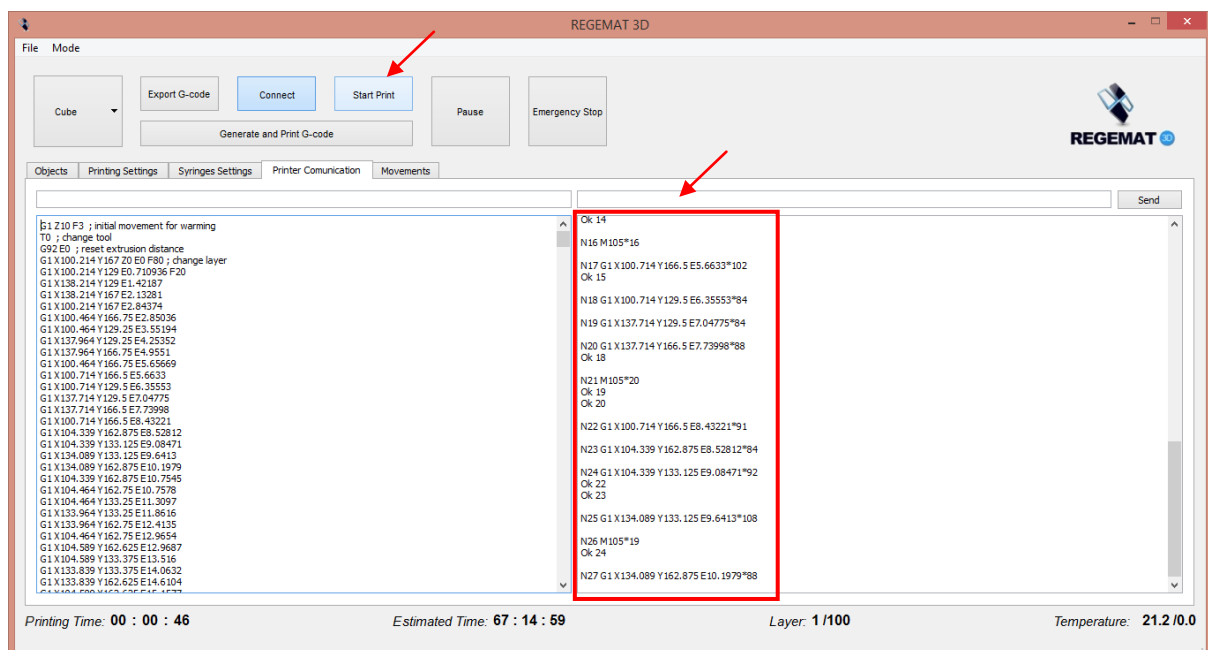


Figure 56 Start printing

1.5 Improvements and technical contributions in the ECU

a) Data reception and error control

As it has been explained before, the interface has implemented a sliding windows protocol that allows flow control and data integrity verification about the serial communication with the bioprinter platform, resending a specific command when it is requested by the printer. Due to the management of the communication is done by the

master (the interface), the tasks of the receptor (the microcontroller of the ECU) are reduced to check line number and checksum and send a confirmation of the command received or a request, asking for a specific command through its line number.

The diagram below shows the operations that are carried out by the receptor for identifying the command, checking and returning a message notifying about it.

The first step is to read bytes from the input serial buffer, saving them consecutively in a parameter type string, until identify a character corresponding with end of the line (generally, this character is normally the *line feed* “\n” or carriage return “\r”). When some of these characters are detected, the lecture of the buffer finishes and the string contains a G command.

Next step is to verify data integrity. The line number is the first parameter that is tried to read from the string, and then, it is checked if the line number coincides with the expected, which is the next command to the last that the microcontroller has received successfully. In the positive case, a confirmation is returned to the message; otherwise, there is a request to the master, reporting that the line numbers do not coincide, and indicating the line number of the command that is waiting. This verification allows a strict sequential execution of the commands, an indispensable condition for building correctly the scaffold.

Secondly, the checksum of the data is calculated in the receptor, and the result is compared with the checksum value of the received message. In the case where both values are equal, that means that apparently the command has been transmitted and read without errors. However, if they are different, the input string contains an error, and therefore, it must not be executed by the printer. In this case, the microcontroller reports an error due to a checksum mismatch, and requests a resend of the command associated to a specific number line

If both test, line number and checksum, have been validated, the string is processed, identifying the G command and executing its instructions (Figure 57).

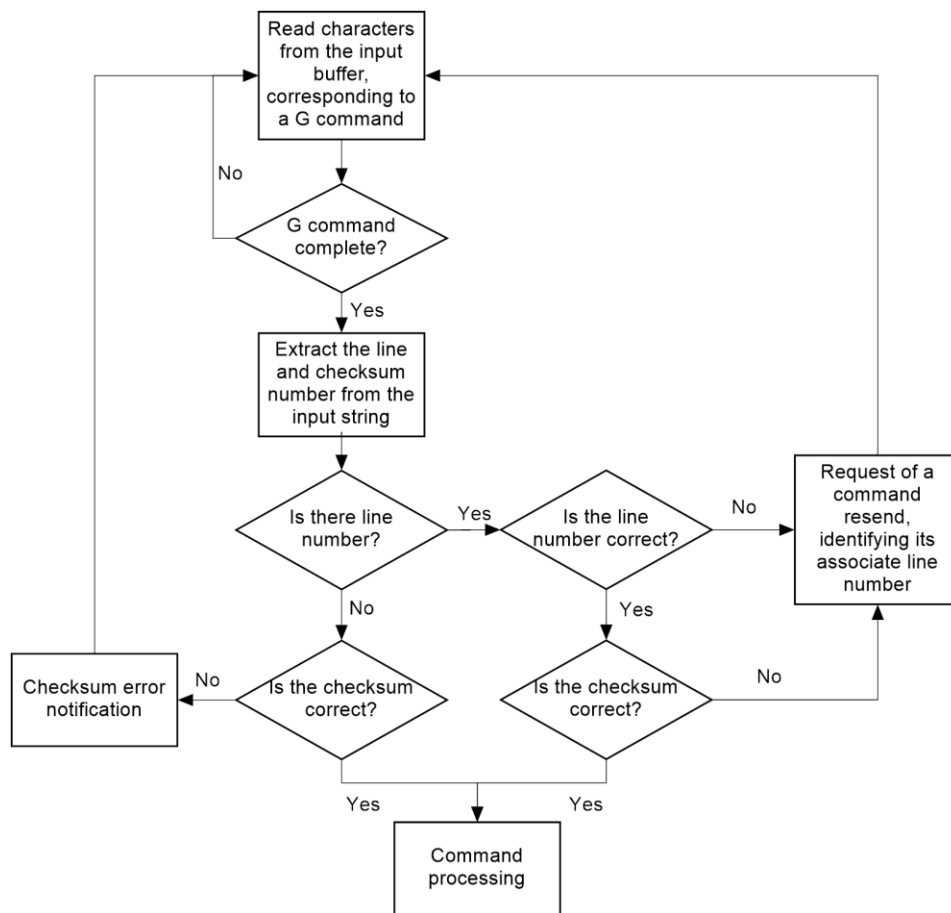


Figure 57 Operations that are carried out by the receptor for identifying the command, checking and returning a message notifying about it.

b) Received G command management

When the message has been verified using the line number and the checksum, the G command is ready for its execution. As explained before, there are two G commands, M112 and M113, which are used to manage the emergency state of the system. Specifically, the first leads the system to the emergency state, executing a specific set of instructions for disabling any action by the system, whereas the second is able to return the system to the normal state, where any command can be executed.

Through the interface or an external button, the user imposes that the printer changes its state to the emergency, mainly due to undesired behaviours of the printer or not correct

building of the scaffold. The emergency instructions include disabling the motors for stopping the movement, turning off the hotend for its cooling and the layer fan, clearing the buffer with the next movement commands and lead the system to a state where it keeps waiting a M113 command, ignoring any other. When this command is received, the system returns to a normal state, allowing the actions of the new received G commands.

When the system is in the normal state, a G command is received and verified, and if this is not M112, the instruction sections related to this command are executed. All commands are carried out in real time; therefore, for a command, it is sent by the interface, verified by the receptor and executed. However, the command G1, related to the movement of the printing head to a target point, calculates a lot of parameters which will be used in the displacement, but the structure with the parameters is placed into a sorted buffer. Then, this movement will take place when all the movements which have been stored before, have been executed by the printer (Figure 58).

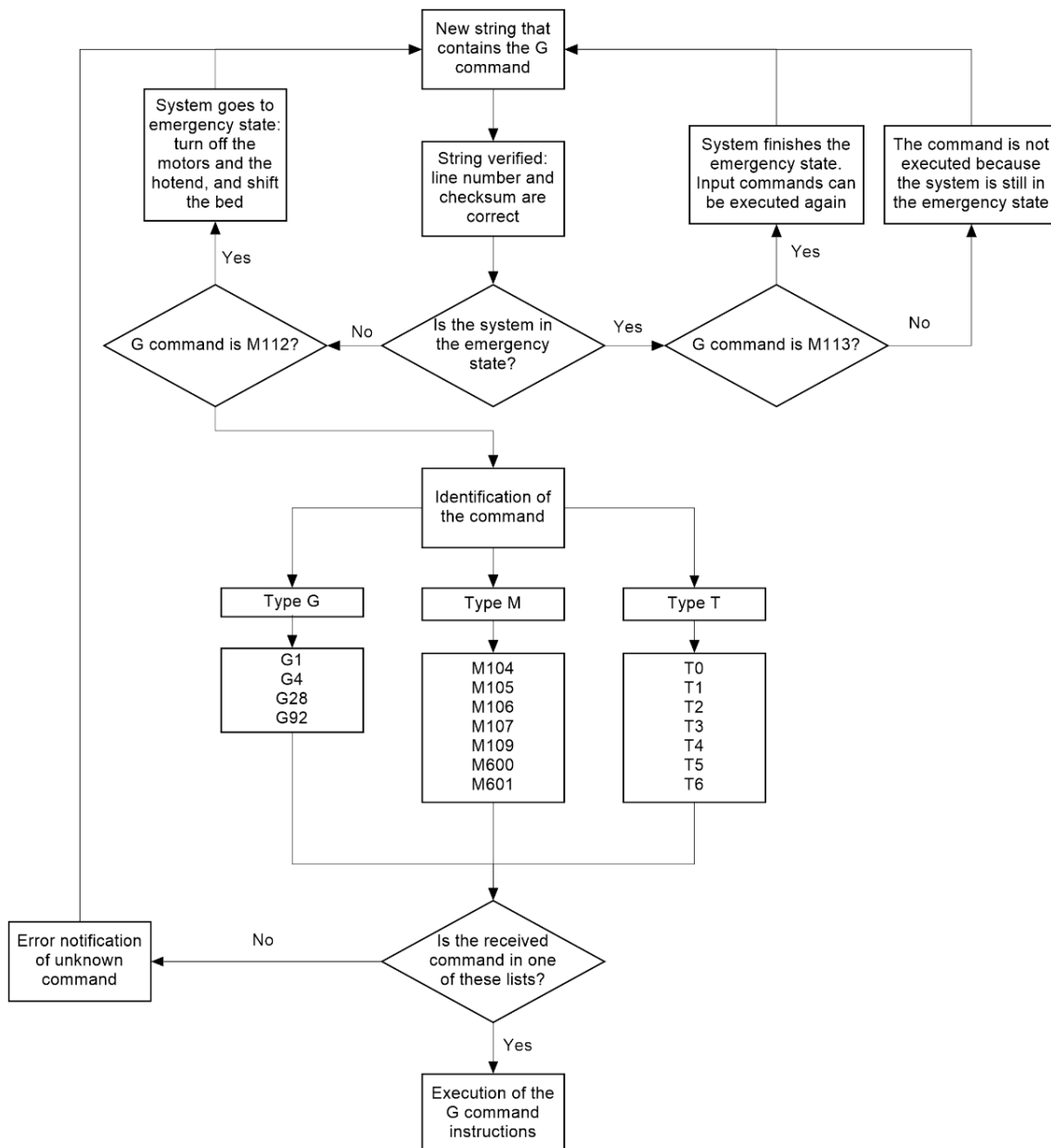


Figure 58 Operations applied to received G command management

c) Head reference and printing area limits

When the printer is turned on, by default, the microcontroller sets all the values of the current position to zero (X,Y,Z,E for all delivering tools). With this method, the origin of coordinates is not fix, but depends on where is placed the printing head at the beginning of the printing, and this is an unknown information. Consequently, there is a mismatch between the reference of the interface and the printer, because the origin point in both are in different places.

Depending on how the coordinates are referenced, there are two modes of operation of the machine: relative and absolute coordinate system. With the relative coordinates, the origin of the axis is the point where the printing head is located when the system is connected, possibly being different in each print. With the absolute coordinate's mode, the origin is a point defined by the endstop sensors, being always equal in each printing. For a success printing and scaffold location, the REGEMAT3D bioprinter has integrated 2 sensors per each axis, only for {X,Y,Z}, situated in opposite places and defining the minimum and maximum point that the printing head can reach in that axis. These sensors are popularly known as *endstop*, and basically, they work changing the output state value when they are touched. They are used in two different events: when a G28 command has been received, forcing a homing of the printing head; and as physical limits, avoiding that the printing head move out of the limits by error.

The aim of the G28 command is to move the printing head to a specific point, represented by the endstop sensor and where the origin of the coordinates is defined. Precisely, this motion is carried out individually to each axis (first Y axis, then X axis and at last, Z axis), in the direction of the minimum endstop, until the printing head touch it, changing the axis of the homming movement. At the end of this command, the printing head is positioning in an origin of coordinates, having contact with the endstops of each axis (in the minimum side).

Alternatively, when the system is using a relative coordinates mode, the endstops are not used in defining a predefined point as in the absolute coordinate mode, but they represent the physical limits of the printer, preventing that the printing head progress in the direction related when the endstop is touched.

d) Precise head movement to the printing points

In this case, all the processes involved in the printing head movement, are described. Specifically, this shift responds to the G1 command, and four steps are needed for carrying it out: capture the values of the destination point, calculate a set of parameters corresponding to a movement and the current state of the printer, store them as a structure into a buffer, and the execution of the movement using the stored structure with the interrupt timer of the microcontroller.

A G1 command includes information about a shift and / or speed. In a complete one, the three axis (X,Y,Z), the extrusion of the material (E), which refers both hotend and syringes, and the speed of the movement (F), contain a number of the targeted move in that direction, placed just after its corresponding letter. That allows an easy determination of the destination point. It is not necessary that all of them appears in the message for doing the movement in a concrete direction.

Once the destination point is known, the next phase involves the calculation of a set of parameters that describes the movements, helping to the system to enhance how the printing head is moved. All these parameters are parts of a data structure, which when is filled, is stored in a buffer of movements. These parameters are related with the current and destination point, its distance, the speed of the movement and its pattern, and acceleration profile, millimetres to motor steps conversion and timer interrupt configuration.

The microcontroller is running continuously the timer one, producing interruptions for checking if the buffer of movements is empty or not. In the first case, the interrupt routine does nothing, but in the second case, the interrupt routine capture the first element which has been stored, and with the parameters associated to the desired movement, it sends a small amount of pulses (steps) to the stepper motor drivers

involved in this shift, causing that the stepper motors of these directions starts to rotate in the selected direction and proportionally to the steps received. When these set of pulses have been emitted, the interrupt routine configure the timer with a time calculated on the basis of the speed and acceleration profiles, and which allows to control in each moment the speed of the movement. This is how the microcontroller regulates the speed.

e) PID control of the temperature

The accuracy control of the hotend temperature across the time is one of the most important tasks of the electronic system, as an incorrect regulation can cause that the temperature values oscillates around a targeted value, causing undesired behaviours of the hotend and in the delivering of polymer filament, preventing the scaffold from being successfully built.

The hotend temperature is generated by a heater, where the supplied current is dissipated. This current is controlled by a PWM signal from the microcontroller, that is applied to a power MOSFET transistor, allowing the regulation of the amount of current through the heater.

We have implemented in the microcontroller a PID control system, which through the error between the current and the desired temperature, it is able to adjust the power that is supplied to the heater in order to maintain the temperature in values as close as possible to the targeted temperature. This type of control comprises a proportional, an integral and a derivative parameter, through which the amount of power delivered to the heater is computed. Therefore, an appropriate real time control of the temperature involves two phases: the calculation of the PID parameters and the adjustment of the delivered power when a targeted temperature for the hot end is set.

For the computation of the PID variables, the classic method of Ziegler-Nichols¹⁴ has been programmed. Specifically, the oscillation method is proposed, in which the temperature signal shows an oscillating behaviour through an on/off supply of the heater, which is enabled (supplying all the possible power) when the measured temperature is lower than a targeted temperature, and disabled when it is higher. From the resulting wave two parameters are obtained, the critical gain and the oscillation period, through which the PID parameters can be computed. Both the empirical results of the two parameters and the calculation of the PID parameters are described in the method. Once they are solved, the internal configuration of the printer electronic system is completed with them.

Once the PID configuration has been finished, the PID control process of the hotend temperature is accomplished when a targeted temperature has been set by a G command. The instructions associated to this control are executed after the temperature lecture through the sensor. This measured temperature is compared with the desired temperature, and after the computation through the PID values, the final result is a PWM value that regulates the current through the heater, and therefore, the temperature which is dissipated. The PWM value remains until the next temperature lecture, where a new PWM is calculated and applied.

¹⁴ en.wikipedia.org/wiki/Ziegler%E2%80%93Nichols_method

2 Validation of the work station

In the precedent section we have explained the results of the technical developments implemented in order to enhance the process of bioprinting. This has been a multidisciplinary work, involving IT, electronics, mechanics, design and mechanisms science amongst others.

We have implemented a bioprinter with a precise 3-axis movement system, with a configurable printing process, being able to control the mesh structure and the pore size, with a user friendly GUI, security and error control both in the software and the ECU, a reliable communication and data transmission and new printing methods, IPF and IVF, that increase cell viability and the efficiency.

Now in this section we are going to show the results of the bioprinting process to validate our hypothesis and show the effective of the device in TE.

2.1 Volume-by-volume printing of 3D hybrid scaffolds

VbV bioprinting process allows us to configure the numbers of scaffold layers and material volume to be printed before the volume is filled with cells, ensuring that the high temperature of the thermoplastic will not affect cell viability. The first step for printing the cell laden construct will be to upload the desired external geometry and configure the printing process and the characteristics of the scaffolds. These characteristics include the configuration of several parameters related to scaffold porosity, infill trajectories, number of external perimeters, layer height, hot end configuration (as nozzle size, temperature, ...), speed of the printing head, number of

first layer “skirts”, and fan cooling of the scaffold. The configuration can be seen in the Figure 59.

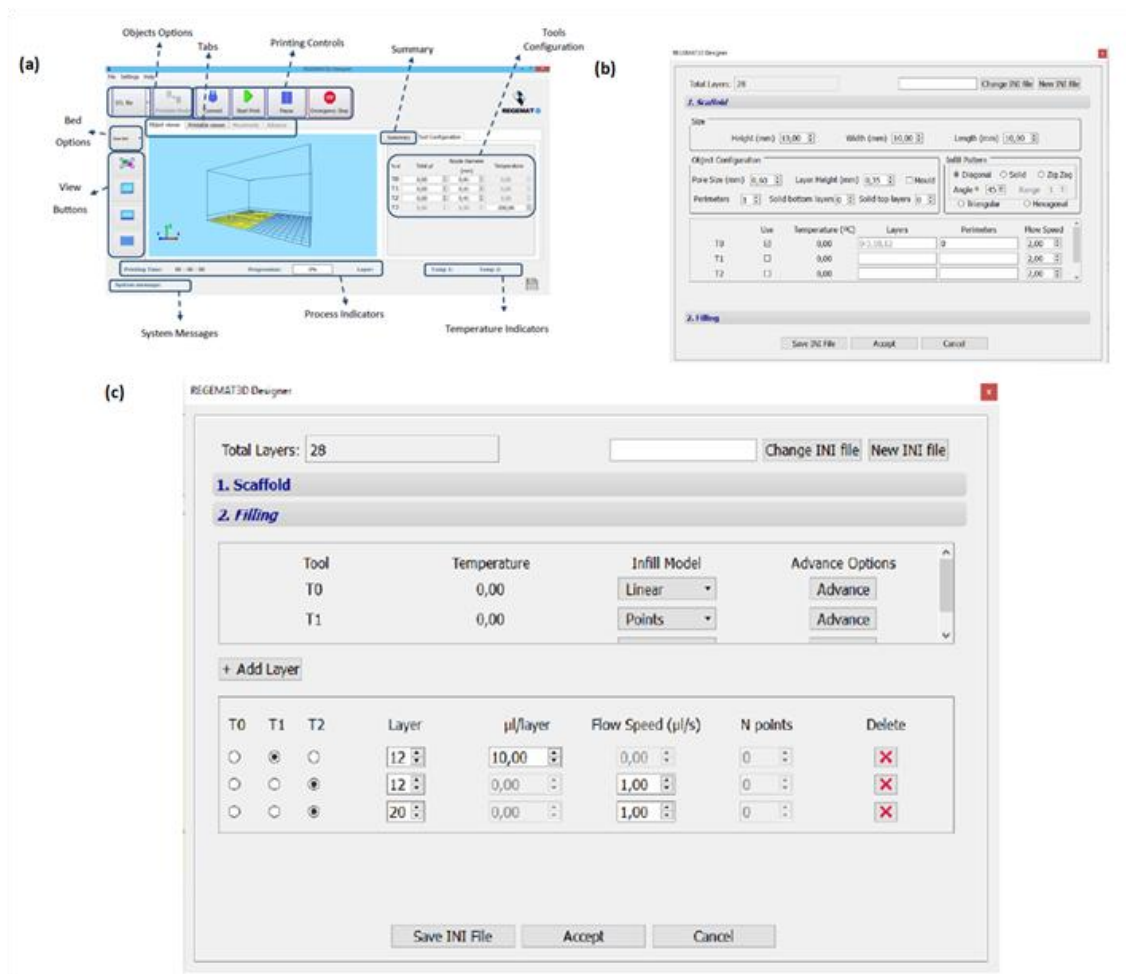


Figure 59 Bioprinter configuration. Layout of the Designer GUI (A) and scaffold parameters configuration (B). Example of VbV configuration process selecting the layer in which VbV will take place, the volume to be injected and the infill model (C) (Extracted from the publication of the author)

Cell-laden constructs were generated using the bioprinting system composed of a head and two different syringes, one containing cell-laden pre-gel (bioink) and the other one loaded with CaCl_2 solution (see figure below A and B). Using VbV the mesh structure and shape of the construct can be printed as desired to obtain the optimal stiffness and biodegradation time and the expected outcomes for the specific application (see Figure 60 C).

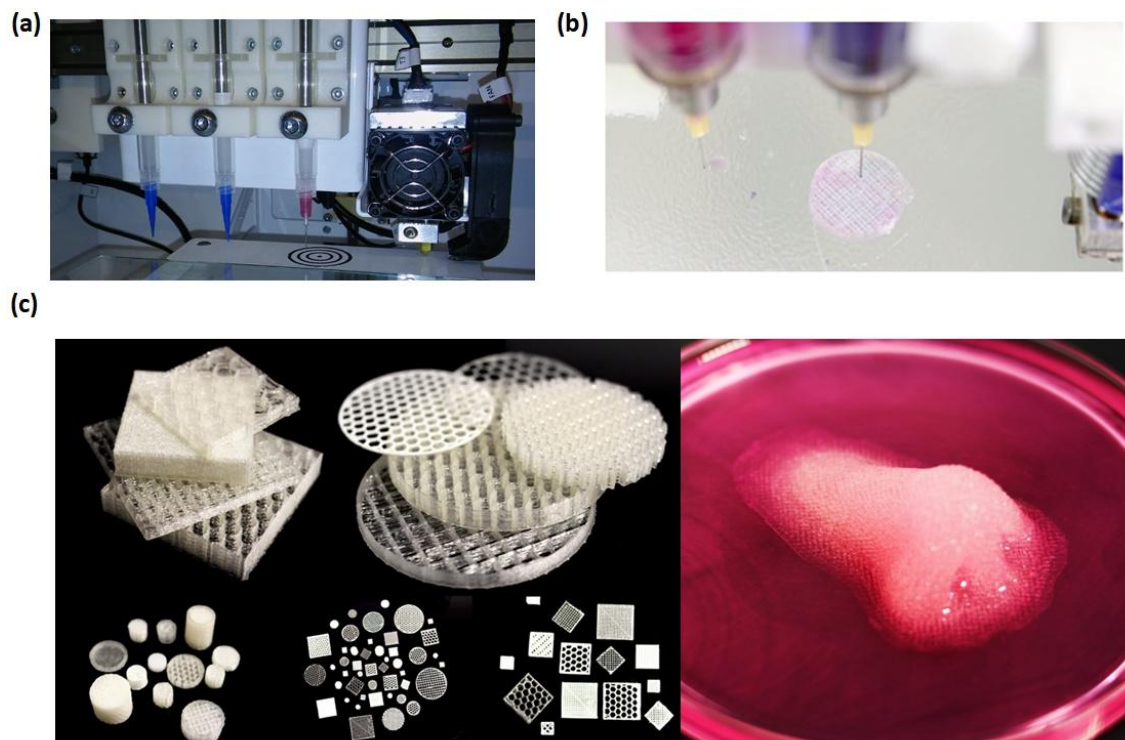


Figure 60 Biprinter system. Configuration of the printing head, with the FDM unit (right), a syringe with a pink needle (T0) and 2 syringes with a blue tip (T1,T2) (left) (A). Injection volume filling after a few layers in a cylindrical shape (B). Representative examples of shapes with different mesh structures that can be printed (C) (Extracted from the publication of the author)

The advantage of this method is that it has no shape or meshes structure restriction in comparison to typical FDM deposition shown in the bibliography with a zig-zag geometry to avoid cell contact with high temperature zones (see Figure 61 A).

We have configured the software to allow us to select in which layer we want to inject from a selected syringe, also the volume to be injected, and the number of points (see Figure 61 B and C). The printing head can be configured for every trial and in this case has three different syringes (T0, T1, T2) that allow the injection of different types of cells or multi component hydrogels (see Figure 61 B and C). After this, x layers volume were printed, the syringe fills it with the cell-loaded bioink injecting in the N points selected by the software (see Figure 61 C).

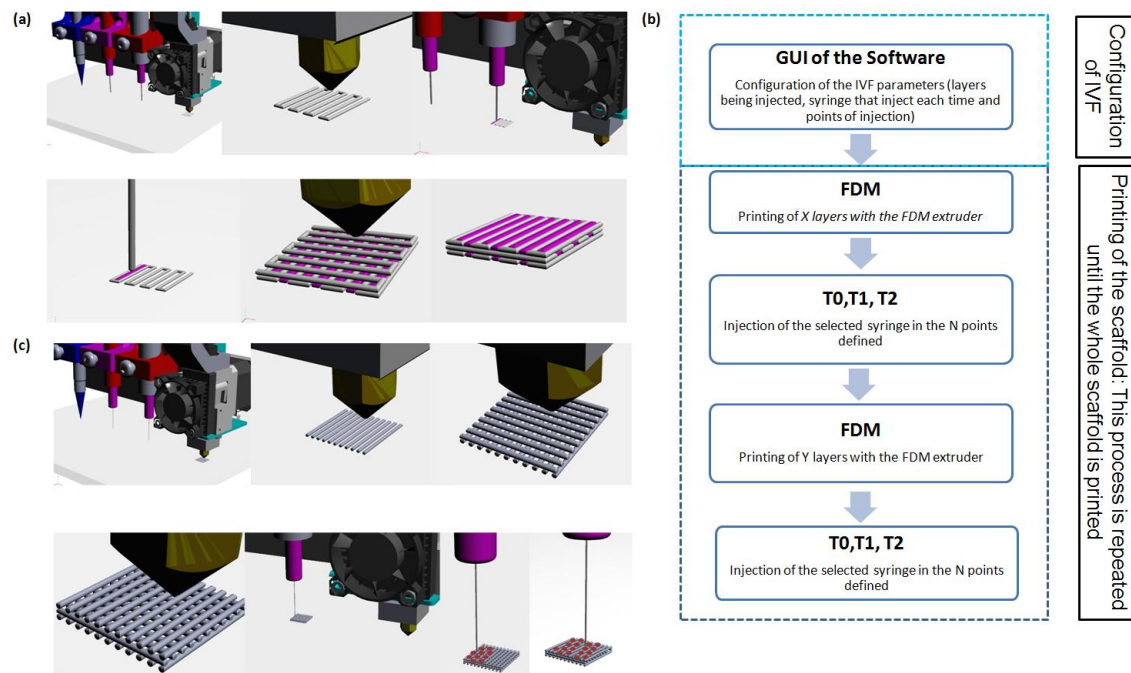


Figure 61 Comparison between conventional FDM deposition and VbV printing procedure. Schematic representation of the printing procedures found in the literature with restricted geometries to avoid the contact of the cell laden material (pink) with the high temperature parts of the printed thermoplastics (grey). FDM deposition of the first layer and filling the spaces with the cell laden materials. Zoom of the spaces filling, FDM of next layer, and restricted multimaterial scaffold (A). Working process diagram represented by schematic representation of the VbV printing procedure (B). FDM deposition of the x layers without restrictions in the mesh geometry. Zoom of the volume to be filled with the cell loaded bioink, and injection in the N points selected by the software (C) (Extracted from the publication of the author)

2.2 Evaluation of the VbV printing process on cell viability and distribution

To demonstrate that VbV is not aggressive, chondrocytes immersed in alginate were printed together with PLA (see Figure 62 A-C).

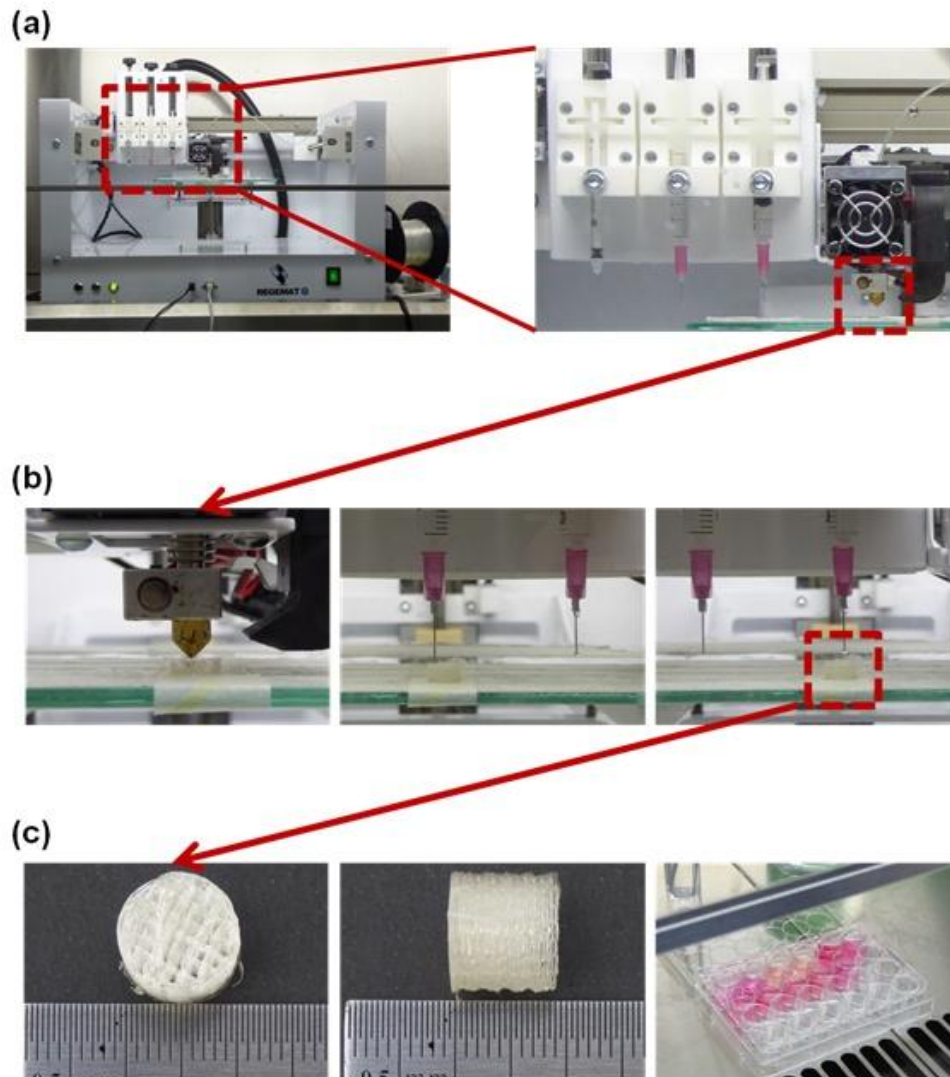


Figure 62 IVF printing process. Schematic images of the bioprinter with the FDM extruder (right) and the 3 syringes (T0,T1 and T2) (A) and the bioprinting process with the FDM deposition of 4 layers of PLA by the nozzle, and the injection of alginate with chondrocytes (T0) and calcium chloride (T1) in the selected points (B). Images of representative 3D printed scaffolds with cells embedded in alginate and cultured during 7 days (C) (Extracted from the publication of the author)

The cells used in this experiment were freshly isolated human chondrocytes cultured in a monolayer for 7-10 days were characterized before its use. Chondrocytes displayed a typical polygonal-shape with high expression of collagen 2 and proteoglycans, and a non-detectable expression of collagen 1 (see Figure 63 A).

Apoptosis analysis was performed to quantify live/dead cells after the printing process. First, chondrocytes immersed in alginate (ALG) were bioprinted with the aim of analyzing whether ALG, CaCl₂ solutions or stress induced by the nozzle affect cell viability. As shown in the figure below B, printed cells viability was always higher than 80%, and the values of apoptosis and necrosis were similar to control cells (CTL) not exposed to the printing process. Furthermore, PLA constructs (alginate+PLA) were analyzed to determine if PLA layers induce thermal damage. Results showed that only immediately after the printing process (0 min) live cells number decrease, and apoptotic and necrotic cells significantly increase ($p < 0.05$). After 30 min or 2 hours in culture, chondrocytes seem to recover from the stress of the printing procedure and no significant differences in apoptosis, necrosis or live cells when compared with CTL cells were found.

In addition, proliferation and metabolic activity of chondrocytes was quantified by alamar blue assay. Results showed an increment in the number of cells from day 0 until day 5, with a stabilization of growth between day 5 and day 7 (see Figure 63 C). Also, cell viability and cell distribution were checked at 24 hours and at 7 days using CTG (see Figure 63 D). After 24 hours in culture, individual cells with rounded shape appeared; however, 7 days later chondrocytes were able to migrate and proliferate throughout the scaffolds, completely colonizing the PLA fibers, and forming a homogeneous surface.

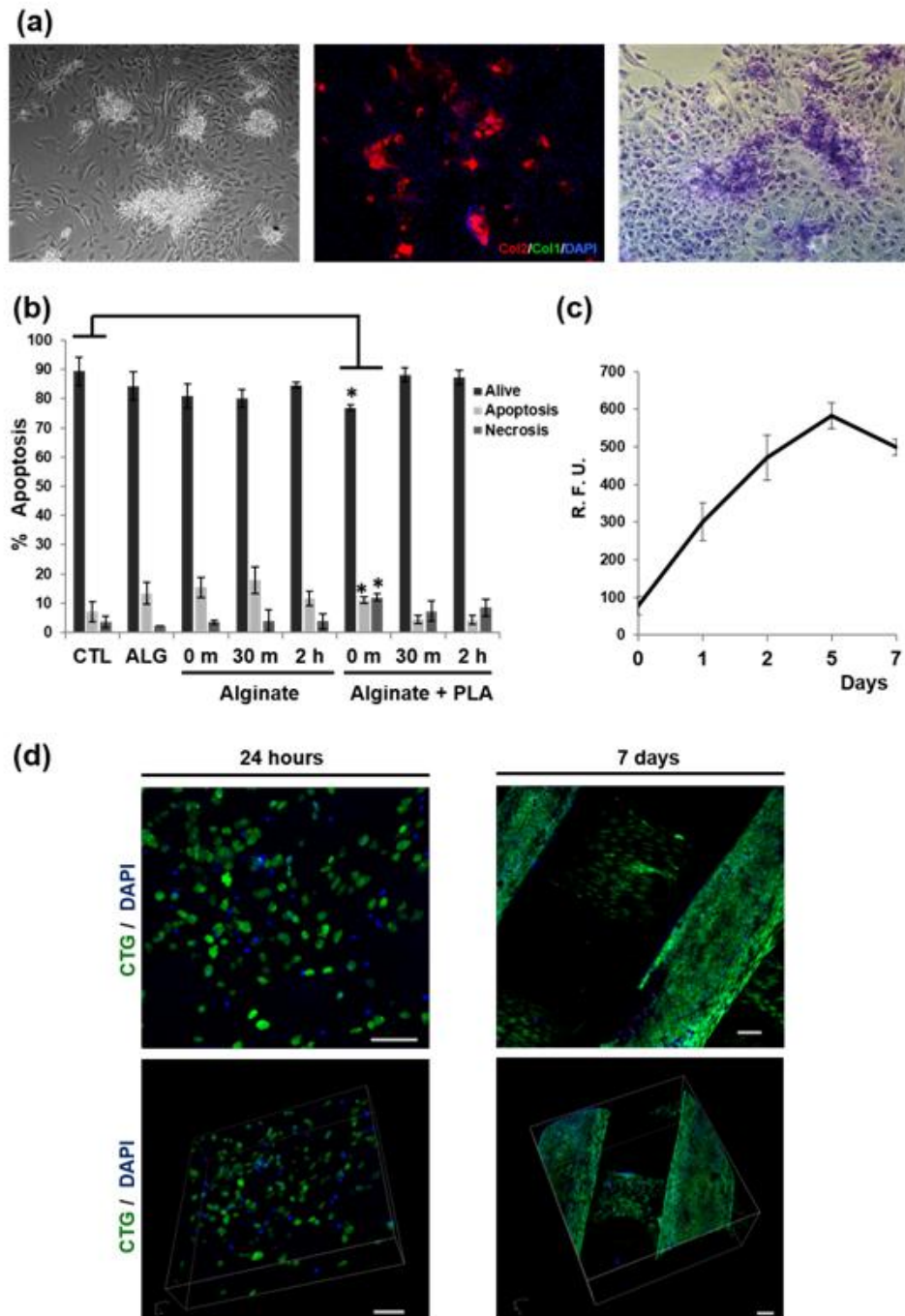


Figure 63 Effect of the VbV bioprinting process on cell viability. Characterization of freshly isolated chondrocytes that displayed a typical polygonal shape, high expression of collagen 2 (Col2) and proteoglycans. Original magnification: 10X (A). Cell viability values of chondrocytes manually printed with alginate (ALG) and bioprinted using the VbV method with alginate and alginate in combination with PLA. * $p < 0.05$ compared with control cells before printing process (B). Cell proliferation using Alamar blue assay at different time points (C). Confocal laser scanning microscopy images of bioprinted human chondrocytes stained with CTG (green) and DAPI (blue) after 24 hours and 7 days. Scale bars indicate 100 μm (D) (Extracted from the publication of the author)

3 New meshes structures, scaffolds and bioink formulations

In this section we present the results that validate the use of the system for printing different thermoplastic materials for the scaffolds with different characteristics (shown in Table 1) and different matrix geometries, as well as printing another no thermoplastic materials as scaffolds and different formulations of bioinks. The possibility of printing a wide range of biomaterials either as bioinks or scaffolds, with different mesh structures is a key factor in order to be able to develop a procedure for the creation of 3D constructs as a previous step to create a functional living tissue. Figure 64 shows the printing of the thermoplastics and different mesh structures:



Figure 64 Printing of different thermoplastic materials for the scaffolds

In the Figure 65 we can see the results of printing a meniscus structure and a implantation of it in a rabbit model:



3D Polycaprolactone meniscal substitute promotes mesenchymal stem cell adhesion and matrix synthesis

Landa-Solis C, Olivos Meza A, Cardenas Soria V, Olivos Díaz B, Silva Bermudez PS, Vanegas Contia D, Cesar Juarez AA, Estrada Villaseñor E, Perez Jimenez FJ, Ibarra C.
Instituto Nacional de Rehabilitación "Luis Guillermo Ibarra Ibarra"



Purpose: To evaluate the biocompatibility and growth potential of 3D-printing polycaprolactone meniscal scaffold to mesenchymal stem cells.

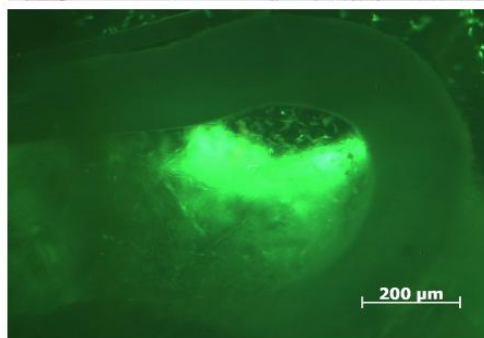
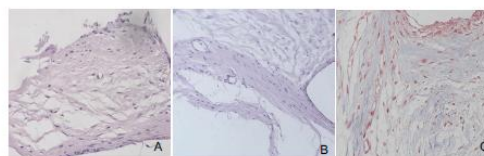
Methods: MRI of a patient was used for segmentation of medial meniscus. A polycaprolactone (PCL) meniscal scaffold was fabricated with a Regemat® 3D printer (Fig. 1) in a 50% scale. MSCs were isolated from bone marrow & characterized by flow cytometry (CD90+, CD73+, CD105+). Cells were cultured in monolayer during 21 days in DMEM + 20% adult human serum, + 1% antibiotic/antimycotics & then seeded in the 3D scaffold during 14-days. The construct was implanted in the subdermic region of the knee in New Zealand white rabbits for 6-weeks. Cell viability assessed with calcein. Histology & immunofluorescence were performed.



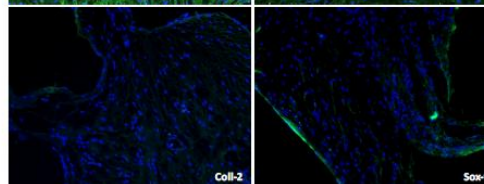
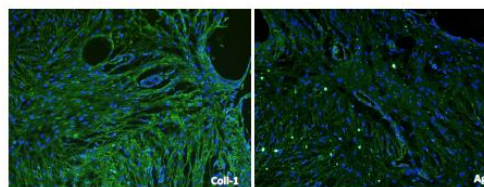
Results: At 14 days of seed and cultured cells with fibroblastic characteristic were observed on the surface and thickness of the meniscus scaffold. Cell viability was established in implant using calcein stain (green).



In gross appearance fibrous like-tissue was observed.



Cell viability was observed at 14-days of culture in the PCL meniscal scaffold.



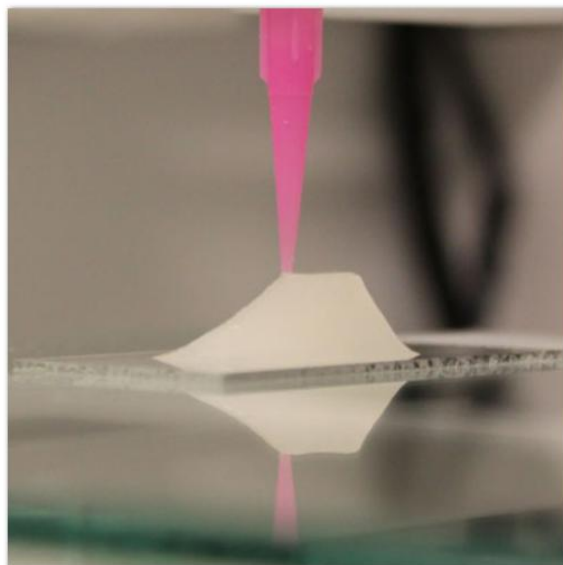
Type-1 collagen & aggrecan expression was positive by immunofluorescence.

Conclusions: 3D-printed polycaprolactone meniscal scaffold showed to be biocompatible to MSCs. MSCs were viable after cultured into 3D-printed scaffold. Fibrocartilage like tissue was formed at 6-weeks of implantation in a biorreactor with positive cartilage proteins expression.

References: 1. Auferheide, AC, Athanasiou, KA. Comparison of scaffolds and culture conditions for tissue engineering of the knee meniscus. *Tissue Eng.* 2005;11(7-8):1095-1104. 2. Kang, SW, Son, SM, Lee, JS. Regeneration of whole meniscus using meniscal cells and polymer scaffolds in a rabbit total meniscectomy model. *J Biomed Mater Res A.* 2006;77(4):659-671. 3. Kwon, H, Yoo, MK, Park, IK. A novel degradable polycaprolactone networks for tissue engineering. *Biomaterials.* 2003;24(5):801-808.

Figure 65 Poster presented by one of the user of REGEMAT3D. Printed meniscus from PCL

Figure 66 shows published results of printing non thermoplastic scaffolds using nanocellulose (Chinga-Carrasco 2018).



3D printing of a nanocellulose construct. (Image: Gary Chinga Carrasco, RISE PFI AS)

Figure 66 printing of nanocellulose using REGEMAT3D bioprinter

To conclude, Figure 67 shows published results of printing non thermoplastic scaffolds using and novel bioinks as methacrylate modified pectin bioink in the clinical application of skin (Pereira, Sousa et al. 2018). This publication has been done using REGEMAT 3D system by one of our users in Portugal.



Figure 67 Printing of methacrylate modified pectin bioink

Discussion

3D printing is revolutionizing many industries and is already being considered as a new industrial revolution. Also the healthcare area is taking advantage of these promising ranges of technologies being regenerative medicine one of the most benefited as these technologies have opened a wide range of possibilities to mimic the structure of living tissues. The main advantages of 3D printing for the manufacturing of medical devices and its application in TE are:

- As a layer by layer AM procedure we can add things and components during the procedure (this is very useful for TE as we can add biomolecules and cells during the procedure, creating a 3D structure seeded with living cells and biomolecules).
- We can create very complex shapes, mimicking the anatomical structure of living tissues and organs.
- We can manufacture mesh structures that can create complex internal structures that improve the attachment of surrounded tissues and tune the mechanical behaviour of the scaffold, that will affect the behaviour of the cells.

New advances in stem cell (SC) research during the last decades have opened a new promising research field with a lot of potential in finding solutions that can help patients around the world. However, there are still a lot of things to do. Research carried out nowadays with two-dimensional (2D) cell cultures do not mimic the 3D structure of a living tissue and do not provide the expected results.

Bioprinting technologies have emerged as a powerful tool for TE due to the ability to mimic the 3D structure of any tissue. The use of biomaterials, cells and biomolecules combined with this manufacturing technique is gaining an increasing interest within the scientific community (Boland et al., 2006; Tsang and Bhatia, 2007; Billiet et al., 2012).

SC therapies and 3D printing technologies can be used together to overcome the problems that researchers have found working with 2D cell cultures. 3D AM has shown a huge field of application in TE, but there are still many questions to answer and to be solved in order to develop a new manufacturing industrial procedure in SC based therapies for TR.

In order to offer a versatile tool to help researchers to obtain evidence on bioprinting technologies towards the clinical application we started many years ago developing a bioprinting system, easy adaptable and configurable to print different biomaterials and to create new procedures. We developed also a software package to help researchers to create their own algorithms to obtain the best results.

Nowadays there are a wide range of different bioprinting technologies, therefore, the election of an appropriate technology must be based on the characteristics of the tissue to regenerate (Cui et al., 2017). There are still many problems related to their use that have to be solved in order to offer a reliable and safe treatment for patients. It is still not understood the process of TR and tumour formation. Differentiation, dedifferentiation and transdifferentiation processes have to be deeply investigated and understood. The related problems of dedifferentiation and transdifferentiation and its mechanisms have to be investigated.

In the present work we have provided evidence on the potential of bioprinting for creating 3D constructs and its applications in TE. We have developed and validated using chondrocytes a bioprinting system with a very innovative manufacturing process. This system can print a scaffold structure using different biomaterials with cells, creating a 3D construct as a precursor of a living tissue. We have shown the effectiveness of the device in printing different mesh geometries that can improve the

results generating a more physiological stress distribution and validated it with chondrocytes for cartilage regeneration. We have also shown the development of a user-friendly software and a set of code and algorithms that allow to print thermoplastic materials with high temperature and without compromising the viability of the cells.

Bioprinting technologies show a very promising potential to find solutions to TR, but still requires research and development to achieve the clinical application; a lot of work must be done before we can successfully implant a complex tissue or organ. We believe that developing tools as the one shown in the present work we contribute to fostering the research and validation of TE for new applications in RM accelerating the uptake of the technology in clinical applications.

Using bioprinters we can create 3D scaffolds with cells and another biomolecules as GFs and cytokines, amongst others, however this is still far away from being a functional tissue. The maturation procedure and the stimuli applied to these constructs also play a very important role in the formation of a functional tissue. Further developments in the area of bioreactors are going to be a key factor in the development of functional tissues that can be implanted.

If we think about bioprinting as a technology to recreate all the structure in the same form as shown in a living tissue, we are going to fail. We have to think on bioprinting as a way of creating cell laden 3D constructs as a precursor of a functional tissue. The maturation and tissue formation process will be as important or even more than the bioprinting one.

The software and process shown in this work presents advantages when working with high temperature thermoplastics. Many available thermoplastic polymers with optimal mechanical properties for the application of cartilage regeneration amongst others that are currently approved for clinical use, have a high melting temperature that decreases

cell viability in a normal FDM bioprinting process. Low temperature biomaterials (Chinga-Carrasco 2018)(Zhang et al., 2015; Xing et al., 2015; Moghadam and Pioletti, 2016) and printing procedures (Visser et al., 2013) have been reported in the literature, but unfortunately these constructs present a lower mechanical and biodegradability behaviour. The optimal mechanical stiffness and biodegradation time of the construct depends on the rehabilitation procedure, higher joint loading after surgery will demand higher stiffness of the constructs and a higher biodegradation time. These main characteristics can be tuned using a specific scaffold architecture and printed thermoplastic's volume. Different compositions of PLA or the thermoplastic used will also have a big influence on the bioabsorption time and mechanical behaviour. The alginate used as a cell carrier has no relevant influence on the mechanical behaviour of the construct but is needed in order to keep the cells attached to the matrix and to promote cell growth and ECM formation. For example, PCL is one of the most representative mid temperature thermoplastic that is currently approved by the FDA; however, despite its very interesting properties such as its lower stiffness and tunable biomechanical properties and degradation time, its melting temperature of around 60°C still damages cells, is necessary a restriction in the printing procedure, in order to avoid the contact of the cell-laden material with the high temperature parts of the printed thermoplastics. (Kundu et al., 2015; Kim and Cho, 2009).

Using our developed bioprinter and software, we presented a novel printing process named VbV that helps to overcome the problems that arise when working with high temperature thermoplastics and combine the advantages of bioprinting and the fill up of decellularized ECM with desirable geometry. VbV allows the researcher to configure the numbers of scaffold layers, shape and mesh structure of each layer or volume to be filled up with the bioink. The geometric restrictions in thermoplastic polymers scaffolds

are based on the fact that in order to avoid cell damage due to high temperatures, zig-zag meshes are printed so the cells are placed in the spaces in between and the next layer is built on and rests on the thermoplastic of the previous layer, and in this way cells do not touch the printed thermoplastic (Kundu et al., 2015; Kim and Cho, 2009).

This is a clear geometric limitation of the mesh, and presents restrictions to the final properties of the scaffold (compromising the biodegradation time and mechanical behavior of the construct), and limits the internal contact area for cell adhesion. (Shim et al., 2016; Schuurman et al., 2011).

Our results show, that the developed procedure avoids cell damage without the geometrical restrictions that may compromise the performance of the tissue. This method has advantages when working on the regeneration of a weight-bearing tissue such as cartilage and can also be used as a strategy to print more complex and larger-sized tissues and organs.

Furthermore, scaffolds need to allow cell and biomolecules incorporation in order to promote the formation of new functional tissue (Murphy and Atala, 2014). Apart from the thermal damage described above, it has been shown that the long bioprinting time and the high shear stress at the nozzle decreases cell viability after extrusion being in the range of 40-86% (Chang et al., 2008). With the method presented here we can significantly reduce these drawbacks and have a higher cell viability and proliferation. Hybrid-polymer constructs have been made mixing high and low melting temperature thermoplastics with different compositions and with the aim of avoiding cell death and achieving optimum mechanical, biological and degradation properties. For example, PCL is used as a protective layer to prevent thermal damage caused by the high temperature of PLA or PLGA (Kim et al., 2016; Scaffaro et al., 2016). In our study, using our method we do not have these restrictions and we have freedom in designing

the desired strategy of biofabrication. The cell viability of chondrocytes after bioprinting were close to 90% of that of cells before printing, the VbV-based bioprinting process did not induce cell death with PLA, which is one of the thermoplastics with the highest and most restrictive melting temperature.

Furthermore, adequate cell proliferation and metabolic activity together with the need to maintain fully-differentiated chondrocytes after bioprinting are essential factors that determine the success of the tissue substitute (Brittberg et al., 1994). VbV procedure allows chondrocytes to maintain their proliferation capacity after bioprinting, being able to homogeneously colonize the scaffold in its totality. It is also well known that cell proliferation increases in constructs over time (Walser et al., 2016) and the proliferative capacity is correlated to an *in vitro* avoidance of senescence and phenotypic instability (Kim et al., 2005). This proliferation allows us to establish cell-to-cell connections that leads to the secretion of a specific ECM and the formation of a 3D structure that mimics the natural biological function of the cartilage (Skardal and Atala, 2015). Our results support the advantage of the VbV bioprinting process using higher temperature thermoplastic polymers such as PLA, since cells showed high viability and proliferative capacity and low apoptosis levels after bioprinting. Moreover, this technology represents an appropriate therapeutic advance for cartilage TE, because 3D constructs mimic the natural microenvironment of cartilage tissue allowing the maintenance of chondrocyte phenotype and ECM production (Takahashi et al., 2007). With these experiments using human chondrocytes we have shown the effectiveness of our developed system for the use in TE.

Further research and development in the area of new biomaterials will be crucial for the success of the technology in bringing new results to the clinical application. Also the maturation of the tissues is a key factor. In the next years we will see many new

developments in the area of bioreactors and new procedures to create functional tissues to be implanted after the bioprinting procedures. Anatomical bioreactors that also mimic the physiology of the tissue to be repaired are going to help researchers to create functional tissues *in vitro*. Manufacturing procedures with increased velocity and size are being developed to translate the manufacturing of small tissues to bigger organs. There are still many things to do but the future that awaits us is promising.

Conclusions

In conclusion, in this work we showed the effectiveness of bioprinting in creating cell-laden 3D constructs and its potential in TE. We have shown that the developed bioprinter, the software and the processes, as VbV and IVF, are effective for creating 3D constructs seeded with cell avoiding dedifferentiation and producing ECM. The developed process shown in the experiments enhances chondrocyte survival and distribution within the bioprinted scaffolds, using high temperature thermoplastic such as PLA without scaffold mesh geometry limitations. This new procedure works avoiding the contact of the thermoplastic and the cells at a higher temperature than the physiologically viable. The procedure shown solves the two main complications of common bioprinting techniques: i) it can be used with already clinically approved biomaterials and, ii) this process does not have restrictions in geometries that could limit the clinical application of 3D bioprinting in cartilage TE. To develop specific bioprinters, algorithms and procedures is a key factor to achieve the desired results.

The maturation procedure and the stimuli applied to these constructs also play a very important role in the formation of a functional tissue. More developments and research in the area of bioreactors and the maturation of the tissues are very important.

The use bioprinting and biofabrication strategies are going to play a very important role in the development of new TE based therapies.

The conclusions are:

- I. Using 3D AM and with the development of new algorithms, electronics and hardware shown, it is possible to layer by layer manufacture meshed functional multimaterial constructs with different external geometries and internal mesh structures and from different materials.

- II. The constructs can be seeded with cells during the printing procedure with high viability. An improved process has been developed to enhance cell survival and distribution in the construct as a precursor of a functional tissue to regenerate an injury.
- III. Chondrocytes can be bioprinted with high viability and they don't dedifferentiate in the scaffold and create the right ECM.

References

An, Y. H., S. K. Woolf, et al. (2000). "Pre-clinical in vivo evaluation of orthopaedic bioabsorbable devices." *Biomaterials* 21(24): 2635-2652.

Arai, K., S. Iwanaga, et al. (2011). "Three-dimensional inkjet biofabrication based on designed images." *Biofabrication* 3(3): 034113.

Awad, H. A., M. Q. Wickham, et al. (2004). "Chondrogenic differentiation of adipose-derived adult stem cells in agarose, alginate, and gelatin scaffolds." *Biomaterials* 25(16): 3211-3222.

Baroli, B. (2007). "Hydrogels for tissue engineering and delivery of tissue-inducing substances." *J Pharm Sci* 96(9): 2197-2223.

Billiet, T., E. Gevaert, et al. (2014). "The 3D printing of gelatin methacrylamide cell-laden tissue-engineered constructs with high cell viability." *Biomaterials* 35(1): 49-62.

Billiet, T., M. Vandenhaute, et al. (2012). "A review of trends and limitations in hydrogel-rapid prototyping for tissue engineering." *Biomaterials* 33(26): 6020-6041.

Boland, T., T. Xu, et al. (2006). "Application of inkjet printing to tissue engineering." *Biotechnol J* 1(9): 910-917.

Bolland, B. J., S. Tilley, et al. (2007). "Adult mesenchymal stem cells and impaction grafting: a new clinical paradigm shift." *Expert Rev Med Devices* 4(3): 393-404.

Bonaventure, J., N. Kadhom, et al. (1994). "Reexpression of cartilage-specific genes by dedifferentiated human articular chondrocytes cultured in alginate beads." *Exp Cell Res* 212(1): 97-104.

Bosworth, L. A., L. A. Turner, et al. (2013). "State of the art composites comprising electrospun fibres coupled with hydrogels: a review." *Nanomedicine* 9(3): 322-335.

Brittberg, M., L. Peterson, et al. (2003). "Articular cartilage engineering with autologous chondrocyte transplantation. A review of recent developments." *J Bone Joint Surg Am* 85-A Suppl 3: 109-115.

- Bueno, E. M., B. Bilgen, et al. (2004). "Increased rate of chondrocyte aggregation in a wavy-walled bioreactor." *Biotechnol Bioeng* 88(6): 767-777.
- Cannon, B. and J. Nedergaard (2004). "Brown adipose tissue: function and physiological significance." *Physiol Rev* 84(1): 277-359.
- Carver, S. E. and C. A. Heath (1999). "Influence of intermittent pressure, fluid flow, and mixing on the regenerative properties of articular chondrocytes." *Biotechnol Bioeng* 65(3): 274-281.
- Castro-Vinuelas, R., C. Sanjurjo-Rodriguez, et al. (2018). "Induced pluripotent stem cells for cartilage repair: current status and future perspectives." *Eur Cell Mater* 36: 96-109.
- Censi, R., P. Di Martino, et al. (2012). "Hydrogels for protein delivery in tissue engineering." *J Control Release* 161(2): 680-692.
- Chang, J. W., S. A. Park, et al. (2014). "Tissue-engineered tracheal reconstruction using three-dimensionally printed artificial tracheal graft: preliminary report." *Artif Organs* 38(6): E95-E105.
- Chang, R., J. Nam, et al. (2008). "Effects of dispensing pressure and nozzle diameter on cell survival from solid freeform fabrication-based direct cell writing." *Tissue Eng Part A* 14(1): 41-48.
- Chantarapanich, N., P. Puttawibul, et al. (2012). "Scaffold library for tissue engineering: a geometric evaluation." *Comput Math Methods Med* 2012: 407805.
- Chen, F. M., R. M. Shelton, et al. (2009). "Localized delivery of growth factors for periodontal tissue regeneration: role, strategies, and perspectives." *Med Res Rev* 29(3): 472-513.
- Chia, H. N. and B. M. Wu (2015). "Recent advances in 3D printing of biomaterials." *Journal of Biological Engineering* 9(1): 4.

Chinga-Carrasco, G. (2018). "Potential and Limitations of Nanocelluloses as Components in Biocomposite Inks for Three-Dimensional Bioprinting and for Biomedical Devices." *Biomacromolecules* 19(3): 701-711.

Chua, C. K., K. F. Leong, et al. (2014). 1 - Introduction to rapid prototyping of biomaterials. *Rapid Prototyping of Biomaterials*. R. Narayan, Woodhead Publishing: 1-15.

Chung, C. and J. A. Burdick (2008). "Engineering cartilage tissue." *Adv Drug Deliv Rev* 60(2): 243-262.

Comesaña, R., F. Lusquiños, et al. (2011). "Calcium phosphate grafts produced by rapid prototyping based on laser cladding." *Journal of the European Ceramic Society* 31(1–2): 29-41.

Csaki, C., P. R. Schneider, et al. (2008). "Mesenchymal stem cells as a potential pool for cartilage tissue engineering." *Ann Anat* 190(5): 395-412.

Cui, L., Y. Wu, et al. (2009). "Repair of articular cartilage defect in non-weight bearing areas using adipose derived stem cells loaded polyglycolic acid mesh." *Biomaterials* 30(14): 2683-2693.

Daly, W. T., A. M. Knight, et al. (2013). "Comparison and characterization of multiple biomaterial conduits for peripheral nerve repair." *Biomaterials* 34(34): 8630-8639.

Das, R. K. and O. F. Zouani (2014). "A review of the effects of the cell environment physicochemical nanoarchitecture on stem cell commitment." *Biomaterials* 35(20): 5278-5293.

de Peppo, G. M., A. Palmquist, et al. (2012). "Free-form-fabricated commercially pure Ti and Ti6Al4V porous scaffolds support the growth of human embryonic stem cell-derived mesodermal progenitors." *ScientificWorldJournal* 2012: 646417.

De Ugarte, D. A., K. Morizono, et al. (2003). "Comparison of multi-lineage cells from human adipose tissue and bone marrow." *Cells Tissues Organs* 174(3): 101-109.

Dhaliwal, K. and N. Lopez (2018). "Hydrogel dressings and their application in burn wound care." *Br J Community Nurs* 23(Sup9): S24-S27.

Digirolamo, C. M., D. Stokes, et al. (1999). "Propagation and senescence of human marrow stromal cells in culture: a simple colony-forming assay identifies samples with the greatest potential to propagate and differentiate." *Br J Haematol* 107(2): 275-281.

Ding, J., R. He, et al. (2012). "Multilayered mucoadhesive hydrogel films based on thiolated hyaluronic acid and polyvinylalcohol for insulin delivery." *Acta Biomater* 8(10): 3643-3651.

Esteve Ràfols, M. (2014). "Tejido adiposo: heterogeneidad celular y diversidad funcional." *Endocrinología y Nutrición* 61(2): 100-112.

Fang, Y. and R. M. Eglén (2017). "Three-Dimensional Cell Cultures in Drug Discovery and Development." *SLAS Discov* 22(5): 456-472.

FDA (2016). "Food and Drug Administration, Technical Considerations for Additive Manufactured Devices."

Fernandes, T. G., M. M. Diogo, et al. (2013). 4 - Stem cell separation. *Stem Cell Bioprocessing*. T. G. Fernandes, M. M. Diogo and J. M. S. Cabral, Woodhead Publishing: 115-141.

Ferrís-Oñate, J., I. Morales-Martín, et al. (2010). "FABIO project: Development of a new generation of customized medical devices. ." *Revista de Biomecánica* 53: 75-78.

Francis, L., K. V. Greco, et al. (2018). "Development of a novel hybrid bioactive hydrogel for future clinical applications." *J Biomater Appl* 33(3): 447-465.

Frazier, W. E. (2014). "Metal Additive Manufacturing: A Review." *Journal of Materials Engineering and Performance* 23(6): 1917-1928.

Freed, L. E., A. P. Hollander, et al. (1998). "Chondrogenesis in a cell-polymer-bioreactor system." *Exp Cell Res* 240(1): 58-65.

Freed, L. E., J. C. Marquis, et al. (1994). "Composition of cell-polymer cartilage implants." *Biotechnol Bioeng* 43(7): 605-614.

Freed, L. E. and G. Vunjak-Novakovic (1995). "Cultivation of cell-polymer tissue constructs in simulated microgravity." *Biotechnol Bioeng* 46(4): 306-313.

Freed, L. E., G. V. Vunjak-Novakovic, et al. (1993). "Kinetics of immobilized heparinase in human blood." *Ann Biomed Eng* 21(1): 67-76.

Fuller, J. A. and F. N. Ghadially (1972). "Ultrastructural observations on surgically produced partial-thickness defects in articular cartilage." *Clin Orthop Relat Res* 86: 193-205.

Garreta, E., D. Gasset, et al. (2007). "Fabrication of a three-dimensional nanostructured biomaterial for tissue engineering of bone." *Biomol Eng* 24(1): 75-80.

Gbureck, U., T. Hölzel, et al. (2007). "Direct Printing of Bioceramic Implants with Spatially Localized Angiogenic Factors." *Advanced Materials* 19(6): 795-800.

Gbureck, U., T. Hölzel, et al. (2007). "Resorbable Dicalcium Phosphate Bone Substitutes Prepared by 3D Powder Printing." *Advanced Functional Materials* 17(18): 3940-3945.

Gbureck, U., E. Vorndran, et al. (2007). "Low temperature direct 3D printed bioceramics and biocomposites as drug release matrices." *J Control Release* 122(2): 173-180.

Gemmiti, C. V. and R. E. Guldborg (2006). "Fluid flow increases type II collagen deposition and tensile mechanical properties in bioreactor-grown tissue-engineered cartilage." *Tissue Eng* 12(3): 469-479.

Ginebra, M. P., M. Espanol, et al. (2010). "New processing approaches in calcium phosphate cements and their applications in regenerative medicine." *Acta Biomater* 6(8): 2863-2873.

Glicklis, R., L. Shapiro, et al. (2000). "Hepatocyte behavior within three-dimensional porous alginate scaffolds." *Biotechnol Bioeng* 67(3): 344-353.

Gomes, M. E., M. T. Rodrigues, et al. (2017). "Tissue Engineering and Regenerative Medicine: New Trends and Directions-A Year in Review." *Tissue Eng Part B Rev* 23(3): 211-224.

Gomoll, A. H., H. Madry, et al. (2010). "The subchondral bone in articular cartilage repair: current problems in the surgical management." *Knee Surg Sports Traumatol Arthrosc* 18(4): 434-447.

Graf, T. and T. Enver (2009). "Forcing cells to change lineages." *Nature* 462(7273): 587-594.

Gray, H. (1918). "Anatomy of the Human Body." Philadelphia: Lea & Febiger, 1918; Bartleby.com, 2000.

Grimm, T. (2004). "User's Guide to Rapid Prototyping." Society of Manufacturing Engineers. Dearborn,MI,.

Hattori, H., K. Masuoka, et al. (2006). "Bone formation using human adipose tissue-derived stromal cells and a biodegradable scaffold." *J Biomed Mater Res B Appl Biomater* 76(1): 230-239.

He, W. and R. Benson (2014). 4 - Polymeric Biomaterials. *Handbook of Polymer Applications in Medicine and Medical Devices*. K. M. Ebnesajjad. Oxford, William Andrew Publishing: 55-76.

Hentze, H., P. L. Soong, et al. (2009). "Teratoma formation by human embryonic stem cells: evaluation of essential parameters for future safety studies." *Stem Cell Res* 2(3): 198-210.

- Hinton, T. J., Q. Jallerat, et al. (2015). "Three-dimensional printing of complex biological structures by freeform reversible embedding of suspended hydrogels." *Sci Adv* 1(9).
- Horwitz, E. M., P. L. Gordon, et al. (2002). "Isolated allogeneic bone marrow-derived mesenchymal cells engraft and stimulate growth in children with osteogenesis imperfecta: Implications for cell therapy of bone." *Proc Natl Acad Sci U S A* 99(13): 8932-8937.
- Hsu, S. H., C. C. Kuo, et al. (2006). "The effect of ultrasound stimulation versus bioreactors on neocartilage formation in tissue engineering scaffolds seeded with human chondrocytes in vitro." *Biomol Eng* 23(5): 259-264.
- Huang, T. Q., X. Qu, et al. (2014). "3D printing of biomimetic microstructures for cancer cell migration." *Biomed Microdevices* 16(1): 127-132.
- Hutmacher, D. W., M. Sittinger, et al. (2004). "Scaffold-based tissue engineering: rationale for computer-aided design and solid free-form fabrication systems." *Trends Biotechnol* 22(7): 354-362.
- Hwang, C. M., S. Sant, et al. (2010). "Fabrication of three-dimensional porous cell-laden hydrogel for tissue engineering." *Biofabrication* 2(3): 035003.
- Hwang, N. S., M. S. Kim, et al. (2006). "Effects of three-dimensional culture and growth factors on the chondrogenic differentiation of murine embryonic stem cells." *Stem Cells* 24(2): 284-291.
- Ivanova, E. P., K. Bazaka, et al. (2014). 1 - Introduction to biomaterials and implantable device design. *New Functional Biomaterials for Medicine and Healthcare*. E. P. Ivanova, K. Bazaka and R. J. Crawford, Woodhead Publishing: 1-31.
- Iwasaki, M., K. Nakata, et al. (1993). "Transforming growth factor-beta 1 stimulates chondrogenesis and inhibits osteogenesis in high density culture of periosteum-derived cells." *Endocrinology* 132(4): 1603-1608.

- Jakab, K., C. Norotte, et al. (2010). "Tissue engineering by self-assembly and bioprinting of living cells." *Biofabrication* 2(2): 022001.
- Janjanin, S., W. J. Li, et al. (2008). "Mold-shaped, nanofiber scaffold-based cartilage engineering using human mesenchymal stem cells and bioreactor." *J Surg Res* 149(1): 47-56.
- Jia, J., D. J. Richards, et al. (2014). "Engineering alginate as bioink for bioprinting." *Acta Biomaterialia* 10(10): 4323-4331.
- Johnson, L. L. (1986). "Arthroscopic abrasion arthroplasty historical and pathologic perspective: present status." *Arthroscopy* 2(1): 54-69.
- Jones, E. A., A. Crawford, et al. (2008). "Synovial fluid mesenchymal stem cells in health and early osteoarthritis: detection and functional evaluation at the single-cell level." *Arthritis Rheum* 58(6): 1731-1740.
- Juliandi, B., M. Abematsu, et al. (2011). Chapter 19 - Epigenetics, Stem Cells, and Cellular Differentiation. *Handbook of Epigenetics*. T. Tollefsbol. San Diego, Academic Press: 315-328.
- Jurgens, W. J., M. J. Oedayrajsingh-Varma, et al. (2008). "Effect of tissue-harvesting site on yield of stem cells derived from adipose tissue: implications for cell-based therapies." *Cell Tissue Res* 332(3): 415-426.
- Kamata, H., Y. Akagi, et al. (2014). "'Nonswellable' hydrogel without mechanical hysteresis." *Science* 343(6173): 873-875.
- Kanazawa, S., Y. Fujihara, et al. (2013). "Tissue responses against tissue-engineered cartilage consisting of chondrocytes encapsulated within non-absorbable hydrogel." *J Tissue Eng Regen Med* 7(1): 1-9.
- Kermanizadeh, A., M. Lohr, et al. (2014). "Hepatic toxicology following single and multiple exposure of engineered nanomaterials utilising a novel primary human 3D liver microtissue model." *Part Fibre Toxicol* 11(1): 56.

- Khalil, S. and W. Sun (2007). "Biopolymer deposition for freeform fabrication of hydrogel tissue constructs." *Materials Science and Engineering: C* 27(3): 469-478.
- Kim, B. S., J. Jang, et al. (2016). "Three-dimensional bioprinting of cell-laden constructs with polycaprolactone protective layers for using various thermoplastic polymers." *Biofabrication* 8(3): 035013.
- Kim, J. Y. and D.-W. Cho (2009). "Blended PCL/PLGA scaffold fabrication using multi-head deposition system." *Microelectron. Eng.* 86(4-6): 1447-1450.
- Kim, S. E., J. H. Park, et al. (2003). "Porous chitosan scaffold containing microspheres loaded with transforming growth factor-beta1: implications for cartilage tissue engineering." *J Control Release* 91(3): 365-374.
- Kimelman, N., G. Pelled, et al. (2007). "Review: gene- and stem cell-based therapeutics for bone regeneration and repair." *Tissue Eng* 13(6): 1135-1150.
- Klammert, U., U. Gbureck, et al. (2010). "3D powder printed calcium phosphate implants for reconstruction of cranial and maxillofacial defects." *J Craniomaxillofac Surg* 38(8): 565-570.
- Klammert, U., T. Reuther, et al. (2009). "Cytocompatibility of brushite and monetite cell culture scaffolds made by three-dimensional powder printing." *Acta Biomater* 5(2): 727-734.
- Koga, H., L. Engebretsen, et al. (2009). "Mesenchymal stem cell-based therapy for cartilage repair: a review." *Knee Surg Sports Traumatol Arthrosc* 17(11): 1289-1297.
- Kolesky, D. B., R. L. Truby, et al. (2014). "3D bioprinting of vascularized, heterogeneous cell-laden tissue constructs." *Adv Mater* 26(19): 3124-3130.
- Kontakis, G. M., J. E. Pagkalos, et al. (2007). "Bioabsorbable materials in orthopaedics." *Acta Orthop Belg* 73(2): 159-169.

- Kulkarni, R. K., K. C. Pani, et al. (1966). "Polylactic acid for surgical implants." *Arch Surg* 93(5): 839-843.
- Kundu, J., J. H. Shim, et al. (2015). "An additive manufacturing-based PCL-alginate-chondrocyte bioprinted scaffold for cartilage tissue engineering." *J Tissue Eng Regen Med* 9(11): 1286-1297.
- Kuo, C. K., W. J. Li, et al. (2006). "Cartilage tissue engineering: its potential and uses." *Curr Opin Rheumatol* 18(1): 64-73.
- Lam, C. X. F., X. M. Mo, et al. (2002). "Scaffold development using 3D printing with a starch-based polymer." *Materials Science and Engineering: C* 20(1–2): 49-56.
- Landers, R. and R. Mülhaupt (2000). "Desktop manufacturing of complex objects, prototypes and biomedical scaffolds by means of computer-assisted design combined with computer-guided 3D plotting of polymers and reactive oligomers." *Macromolecular Materials and Engineering* 282(1): 17-21.
- Leong, K. F., C. M. Cheah, et al. (2003). "Solid freeform fabrication of three-dimensional scaffolds for engineering replacement tissues and organs." *Biomaterials* 24(13): 2363-2378.
- Lin, C. H., S. H. Hsu, et al. (2009). "A scaffold-bioreactor system for a tissue-engineered trachea." *Biomaterials* 30(25): 4117-4126.
- Lin, C. S., Z. C. Xin, et al. (2008). "Recent advances in andrology-related stem cell research." *Asian J Androl* 10(2): 171-175.
- Liu, V. and S. Bhatia (2002). "Three-Dimensional Photopatterning of Hydrogels Containing Living Cells." *Biomedical Microdevices* 4(4): 257-266.
- Lopes, D., C. Martins-Cruz, et al. (2018). "Bone physiology as inspiration for tissue regenerative therapies." *Biomaterials* 185: 240-275.

Lopez-Ruiz, E., G. Jimenez, et al. (2016). "Polymers, scaffolds and bioactive molecules with therapeutic properties in osteochondral pathologies: what's new?" *Expert Opin Ther Pat* 26(8): 877-890.

Lopez-Ruiz, E., G. Jimenez, et al. (2018). "Impact of TGF-beta family-related growth factors on chondrogenic differentiation of adipose-derived stem cells isolated from lipoaspirates and infrapatellar fat pads of osteoarthritic patients." *Eur Cell Mater* 35: 209-224.

Lopez-Ruiz, E., M. Peran, et al. (2013). "Chondrocytes extract from patients with osteoarthritis induces chondrogenesis in infrapatellar fat pad-derived stem cells." *Osteoarthritis Cartilage* 21(1): 246-258.

Ma, L., J. Barker, et al. (2012). "Towards personalized medicine with a three-dimensional micro-scale perfusion-based two-chamber tissue model system." *Biomaterials* 33(17): 4353-4361.

Maeda, Y., H. Hojo, et al. (2013). "Bone healing by sterilizable calcium phosphate tetrapods eluting osteogenic molecules." *Biomaterials* 34(22): 5530-5537.

Maffulli, N., U. G. Longo, et al. (2010). "Meniscal tears." *Open Access J Sports Med* 1: 45-54.

Martin, I., D. Wendt, et al. (2004). "The role of bioreactors in tissue engineering." *Trends Biotechnol* 22(2): 80-86.

Matsusue, Y., T. Yamamuro, et al. (1993). "Arthroscopic multiple osteochondral transplantation to the chondral defect in the knee associated with anterior cruciate ligament disruption." *Arthroscopy* 9(3): 318-321.

Melchels, F. P. W., M. A. N. Domingos, et al. (2012). "Additive manufacturing of tissues and organs." *Progress in Polymer Science* 37(8): 1079-1104.

Melchels, F. P. W., J. Feijen, et al. (2010). "A review on stereolithography and its applications in biomedical engineering." *Biomaterials* 31(24): 6121-6130.

- Melchor, J., E. López-Ruiz, et al. (2018). "In-bioreactor ultrasonic monitoring of 3D culture human engineered cartilage." *Sensors and Actuators B: Chemical* 266: 841-852.
- Merceron, C., C. Vinatier, et al. (2008). "Adipose-derived mesenchymal stem cells and biomaterials for cartilage tissue engineering." *Joint Bone Spine* 75(6): 672-674.
- Mironov, V., T. Boland, et al. (2003). "Organ printing: computer-aided jet-based 3D tissue engineering." *Trends Biotechnol* 21(4): 157-161.
- Mironov, V., G. Prestwich, et al. (2007). "Bioprinting living structures." *Journal of Materials Chemistry* 17(20): 2054–2060.
- Mitalipov, S. and D. Wolf (2009). "Totipotency, pluripotency and nuclear reprogramming." *Adv Biochem Eng Biotechnol* 114: 185-199.
- Mobasheri, A., G. Kalamegam, et al. (2014). "Chondrocyte and mesenchymal stem cell-based therapies for cartilage repair in osteoarthritis and related orthopaedic conditions." *Maturitas* 78(3): 188-198.
- Murphy, S. V. and A. Atala (2014). "3D bioprinting of tissues and organs." *Nat Biotechnol* 32(8): 773-785.
- Nakamura, M., A. Kobayashi, et al. (2005). "Biocompatible inkjet printing technique for designed seeding of individual living cells." *Tissue Eng* 11(11-12): 1658-1666.
- Nerem, R. M. and D. Seliktar (2001). "Vascular tissue engineering." *Annu Rev Biomed Eng* 3: 225-243.
- Ng, C. P., A. R. Sharif, et al. (2014). "Enhanced ex vivo expansion of adult mesenchymal stem cells by fetal mesenchymal stem cell ECM." *Biomaterials* 35(13): 4046-4057.
- Ng, R., R. Zang, et al. (2012). "Three-dimensional fibrous scaffolds with microstructures and nanotextures for tissue engineering." *RSC Advances* 2(27): 10110-10124.

- Nichol, J. W., S. T. Koshy, et al. (2010). "Cell-laden microengineered gelatin methacrylate hydrogels." *Biomaterials* 31(21): 5536-5544.
- Norotte, C., F. S. Marga, et al. (2009). "Scaffold-free vascular tissue engineering using bioprinting." *Biomaterials* 30(30): 5910-5917.
- Obokata, H. and C. A. Vacanti (2014). Chapter 31 - Stem Cells in Tissue Engineering. *Principles of Tissue Engineering (Fourth Edition)*. R. L. L. Vacanti. Boston, Academic Press: 595-608.
- O'Brien, C. M., B. Holmes, et al. (2015). "Three-Dimensional Printing of Nanomaterial Scaffolds for Complex Tissue Regeneration." *Tissue Engineering Part B: Reviews* 21(1): 103-114.
- Ovsianikov, A. and B. N. Chichkov (2012). "Three-dimensional microfabrication by two-photon polymerization technique." *Methods Mol Biol* 868: 311-325.
- Ovsianikov, A., M. Gruene, et al. (2010). "Laser printing of cells into 3D scaffolds." *Biofabrication* 2(1): 014104.
- Ozbolat, I., K. Moncal, et al. (2017). "Evaluation of bioprinter technologies. ." *Addit Manuf.* 13: 179–200.
- Ozbolat, I. T., H. Chen, et al. (2014). "Development of 'Multi-arm Bioprinter' for hybrid biofabrication of tissue engineering constructs." *Robotics and Computer-Integrated Manufacturing* 30(3): 295-304.
- Pastides, P., M. Chimutengwende-Gordon, et al. (2013). "Stem cell therapy for human cartilage defects: a systematic review." *Osteoarthritis Cartilage* 21(5): 646-654.
- Paterson, M. and J. F. Kennedy (1991). "Polymers: Biomaterials and medical applications Edited by J. I. Kroschwitz, John Wiley & Sons, Inc., New York, 1989. pp. xxvi + 555, price £47.00. ISBN 0-471-5 1207-9." *Polymer International* 25(3): 200-200.

- Peltola, S. M., F. P. Melchels, et al. (2008). "A review of rapid prototyping techniques for tissue engineering purposes." *Ann Med* 40(4): 268-280.
- Peppas, N. A. (1992). "Principles of polymerization: G. Odian, 3rd edition, Wiley, New York, 1991,768 pages, \$59.95." *Journal of Controlled Release* 22(3): 294.
- Peran, M., M. A. Garcia, et al. (2012). "Functionalized nanostructures with application in regenerative medicine." *Int J Mol Sci* 13(3): 3847-3886.
- Pereira, R. F., A. Sousa, et al. (2018). "A single-component hydrogel bioink for bioprinting of bioengineered 3D constructs for dermal tissue engineering." *Materials Horizons*.
- Petersen, T. and L. Niklason (2007). "Cellular lifespan and regenerative medicine." *Biomaterials* 28(26): 3751-3756.
- Pham, D. and R. Gault (1998). "A comparison of rapid prototyping technologies." *Int J Mach Tools Manuf.* 38(10–11): 1257–1287.
- Phillips, M. I. (2012). "Gene, stem cell, and future therapies for orphan diseases." *Clin Pharmacol Ther* 92(2): 182-192.
- Pina, S., R. F. Canadas, et al. (2017). "Biofunctional Ionic-Doped Calcium Phosphates: Silk Fibroin Composites for Bone Tissue Engineering Scaffolding." *Cells Tissues Organs* 204(3-4): 150-163.
- Pittenger, M. F., A. M. Mackay, et al. (1999). "Multilineage potential of adult human mesenchymal stem cells." *Science* 284(5411): 143-147.
- Placzek, M. R., I. M. Chung, et al. (2009). "Stem cell bioprocessing: fundamentals and principles." *J R Soc Interface* 6(32): 209-232.
- Rastegar, F., D. Shenaq, et al. (2010). "Mesenchymal stem cells: Molecular characteristics and clinical applications." *World J Stem Cells* 2(4): 67-80.

- Rezza, A., R. Sennett, et al. (2014). "Adult stem cell niches: cellular and molecular components." *Curr Top Dev Biol* 107: 333-372.
- Rice, M. A., K. R. Waters, et al. (2009). "Ultrasound monitoring of cartilaginous matrix evolution in degradable PEG hydrogels." *Acta Biomater* 5(1): 152-161.
- Rimann, M., S. Laternser, et al. (2014). "An in vitro osteosarcoma 3D microtissue model for drug development." *J Biotechnol* 189: 129-135.
- Roseti, L., V. Parisi, et al. (2017). "Scaffolds for Bone Tissue Engineering: State of the art and new perspectives." *Mater Sci Eng C Mater Biol Appl* 78: 1246-1262.
- Roy, S. and S. Gatién (2008). "Regeneration in axolotls: a model to aim for!" *Exp Gerontol* 43(11): 968-973.
- Saini, S. and T. M. Wick (2003). "Concentric cylinder bioreactor for production of tissue engineered cartilage: effect of seeding density and hydrodynamic loading on construct development." *Biotechnol Prog* 19(2): 510-521.
- Santos, C. F. L., A. P. Silva, et al. (2012). "Design and production of sintered β -tricalcium phosphate 3D scaffolds for bone tissue regeneration." *Materials Science and Engineering: C* 32(5): 1293-1298.
- Sanz-Herrera, J. A., J. M. Garcia-Aznar, et al. (2009). "A mathematical approach to bone tissue engineering." *Philos Trans A Math Phys Eng Sci* 367(1895): 2055-2078.
- Sanz-Herrera, J. A., J. M. Garcia-Aznar, et al. (2009). "On scaffold designing for bone regeneration: A computational multiscale approach." *Acta Biomater* 5(1): 219-229.
- Saravanan, S., S. Vimalraj, et al. (2018). "A review on injectable chitosan/beta glycerophosphate hydrogels for bone tissue regeneration." *Int J Biol Macromol* 121: 38-54.
- Sastry, S. V., J. R. Nyshadham, et al. (2000). "Recent technological advances in oral drug delivery - a review." *Pharm Sci Technolo Today* 3(4): 138-145.

Scaffaro, R., F. Lopresti, et al. (2016). "Integration of PCL and PLA in a monolithic porous scaffold for interface tissue engineering." *J Mech Behav Biomed Mater* 63: 303-313.

Scheven, B. A., R. M. Shelton, et al. (2009). "Therapeutic ultrasound for dental tissue repair." *Med Hypotheses* 73(4): 591-593.

Schmeichel, K. L. and M. J. Bissell (2003). "Modeling tissue-specific signaling and organ function in three dimensions." *J Cell Sci* 116(Pt 12): 2377-2388.

Schmidt-Nielsen, B. (1994). "August Krogh and capillary physiology." *Int J Microcirc Clin Exp* 14(1-2): 104-110.

Schnabel, M., S. Marlovits, et al. (2002). "Dedifferentiation-associated changes in morphology and gene expression in primary human articular chondrocytes in cell culture." *Osteoarthritis Cartilage* 10(1): 62-70.

Schulz, R. M. and A. Bader (2007). "Cartilage tissue engineering and bioreactor systems for the cultivation and stimulation of chondrocytes." *Eur Biophys J* 36(4-5): 539-568.

Schuurman, W., V. Khristov, et al. (2011). "Bioprinting of hybrid tissue constructs with tailorable mechanical properties." *Biofabrication* 3(2): 021001.

Schuurman, W., P. A. Levett, et al. (2013). "Gelatin-methacrylamide hydrogels as potential biomaterials for fabrication of tissue-engineered cartilage constructs." *Macromol Biosci* 13(5): 551-561.

Selvaggi, T. A., R. E. Walker, et al. (1997). "Development of antibodies to fetal calf serum with arthus-like reactions in human immunodeficiency virus-infected patients given syngeneic lymphocyte infusions." *Blood* 89(3): 776-779.

Shachar, M. and S. Cohen (2003). "Cardiac tissue engineering, ex-vivo: design principles in biomaterials and bioreactors." *Heart Fail Rev* 8(3): 271-276.

- Shelbourne, K. D., S. Jari, et al. (2003). "Outcome of untreated traumatic articular cartilage defects of the knee: a natural history study." *J Bone Joint Surg Am* 85-A Suppl 2: 8-16.
- Sheyn, D., O. Mizrahi, et al. (2010). "Genetically modified cells in regenerative medicine and tissue engineering." *Adv Drug Deliv Rev* 62(7-8): 683-698.
- Shiota, M., T. Heike, et al. (2007). "Isolation and characterization of bone marrow-derived mesenchymal progenitor cells with myogenic and neuronal properties." *Exp Cell Res* 313(5): 1008-1023.
- Singh, S. and J. Singh (2003). "Effect of polyols on the conformational stability and biological activity of a model protein lysozyme." *AAPS PharmSciTech* 4(3): E42.
- Smith, S., W. Neaves, et al. (2007). "Adult versus embryonic stem cells: treatments." *Science* 316(5830): 1422-1423; author reply 1422-1423.
- Smoljanovic, T., I. Bojanic, et al. (2009). "Adverse effects of posterior lumbar interbody fusion using rhBMP-2." *Eur Spine J* 18(6): 920-923; author reply 924.
- Steinert, A. F., G. D. Palmer, et al. (2009). "Enhanced in vitro chondrogenesis of primary mesenchymal stem cells by combined gene transfer." *Tissue Eng Part A* 15(5): 1127-1139.
- Stiller, M., E. Kluk, et al. (2014). "Performance of beta-tricalcium phosphate granules and putty, bone grafting materials after bilateral sinus floor augmentation in humans." *Biomaterials* 35(10): 3154-3163.
- Takahashi, K. and S. Yamanaka (2006). "Induction of pluripotent stem cells from mouse embryonic and adult fibroblast cultures by defined factors." *Cell* 126(4): 663-676.
- Tirella, A., A. Orsini, et al. (2009). "A phase diagram for microfabrication of geometrically controlled hydrogel scaffolds." *Biofabrication* 1(4): 045002.

Toh, W. S., E. H. Lee, et al. (2010). "Cartilage repair using hyaluronan hydrogel-encapsulated human embryonic stem cell-derived chondrogenic cells." *Biomaterials* 31(27): 6968-6980.

Troyer, D. L. and M. L. Weiss (2008). "Wharton's jelly-derived cells are a primitive stromal cell population." *Stem Cells* 26(3): 591-599.

Tsang, V. L. and S. N. Bhatia (2004). "Three-dimensional tissue fabrication." *Adv Drug Deliv Rev* 56(11): 1635-1647.

Ulloa-Montoya, F., C. M. Verfaillie, et al. (2005). "Culture systems for pluripotent stem cells." *J Biosci Bioeng* 100(1): 12-27.

Unger, C., N. Kramer, et al. (2014). "Modeling human carcinomas: Physiologically relevant 3D models to improve anti-cancer drug development." *Adv Drug Deliv Rev* 79-80C: 50-67.

Vachon, A., L. R. Bramlage, et al. (1986). "Evaluation of the repair process of cartilage defects of the equine third carpal bone with and without subchondral bone perforation." *Am J Vet Res* 47(12): 2637-2645.

Vazquez-Vela, M. E., N. Torres, et al. (2008). "White adipose tissue as endocrine organ and its role in obesity." *Arch Med Res* 39(8): 715-728.

Vinatier, C., D. Magne, et al. (2007). "Engineering cartilage with human nasal chondrocytes and a silanized hydroxypropyl methylcellulose hydrogel." *J Biomed Mater Res A* 80(1): 66-74.

Vivien, D., P. Galera, et al. (1990). "Differential effects of transforming growth factor-beta and epidermal growth factor on the cell cycle of cultured rabbit articular chondrocytes." *J Cell Physiol* 143(3): 534-545.

Vozzi, G., C. J. Flaim, et al. (2002). "Microfabricated PLGA scaffolds: a comparative study for application to tissue engineering." *Materials Science and Engineering: C* 20(1-2): 43-47.

Vunjak-Novakovic, G., L. E. Freed, et al. (1996). "Effects of mixing on the composition and morphology of tissue-engineered cartilage." *AICHE Journal* 42(3): 850-860.

Wagner, E. R., D. Bravo, et al. (2013). "Novel Porous Polycaprolactone Fumarate (PCLF) Scaffold for Adipocyte-Derived Mesenchymal Stem Cell Engineering and Platelet Lysate-Enhanced Ligament Differentiation: Not a clinical study." *The Journal of Hand Surgery* 38(10, Supplement): e42.

Wang, X., Y. Yan, et al. (2007). "Rapid prototyping as a tool for manufacturing bioartificial livers." *Trends Biotechnol* 25(11): 505-513.

Wei, Y., X. Sun, et al. (2007). "Adipose-derived stem cells and chondrogenesis." *Cytotherapy* 9(8): 712-716.

Weinzierl, K., A. Hemprich, et al. (2006). "Bone engineering with adipose tissue derived stromal cells." *J Craniomaxillofac Surg* 34(8): 466-471.

Weissman, I. L., D. J. Anderson, et al. (2001). "Stem and progenitor cells: origins, phenotypes, lineage commitments, and transdifferentiations." *Annu Rev Cell Dev Biol* 17: 387-403.

Wiria, F. E., K. F. Leong, et al. (2007). "Poly-epsilon-caprolactone/hydroxyapatite for tissue engineering scaffold fabrication via selective laser sintering." *Acta Biomater* 3(1): 1-12.

Wong, K. V. and A. Hernandez (2012). "A Review of Additive Manufacturing." *ISRN Mechanical Engineering* 2012: 10.

Xia, W., Y. Q. Jin, et al. (2009). "Adenoviral transduction of hTGF-beta1 enhances the chondrogenesis of bone marrow derived stromal cells." *Biotechnol Lett* 31(5): 639-646.

Xu, M., X. Wang, et al. (2010). "An cell-assembly derived physiological 3D model of the metabolic syndrome, based on adipose-derived stromal cells and a gelatin/alginate/fibrinogen matrix." *Biomaterials* 31(14): 3868-3877.

- Xu, X., J. P. Urban, et al. (2006). "Influence of perfusion on metabolism and matrix production by bovine articular chondrocytes in hydrogel scaffolds." *Biotechnol Bioeng* 93(6): 1103-1111.
- Xu, Y., P. Malladi, et al. (2005). "Adipose-derived mesenchymal cells as a potential cell source for skeletal regeneration." *Curr Opin Mol Ther* 7(4): 300-305.
- Yeong, W. Y., C. K. Chua, et al. (2004). "Rapid prototyping in tissue engineering: challenges and potential." *Trends Biotechnol* 22(12): 643-652.
- Yoshimura, K., K. Sato, et al. (2008). "Cell-assisted lipotransfer for facial lipoatrophy: efficacy of clinical use of adipose-derived stem cells." *Dermatol Surg* 34(9): 1178-1185.
- Zein, I., D. W. Hutmacher, et al. (2002). "Fused deposition modeling of novel scaffold architectures for tissue engineering applications." *Biomaterials* 23(4): 1169-1185.
- Zhang, S. and H. Wang (2018). "Current Progress in 3D Bioprinting of Tissue Analogs." *SLAS Technol* 26(2472630318799971): 2472630318799971.
- Zhao, X. Y., W. Li, et al. (2009). "iPS cells produce viable mice through tetraploid complementation." *Nature* 461(7260): 86-90.
- Zhao, Y., R. Yao, et al. (2014). "Three-dimensional printing of Hela cells for cervical tumor model in vitro." *Biofabrication* 6(3): 035001.
- Zhou, H., S. Wu, et al. (2009). "Generation of induced pluripotent stem cells using recombinant proteins." *Cell Stem Cell* 4(5): 381-384.
- Zhu, X. H., D. Y. Arifin, et al. (2010). "Study of cell seeding on porous poly(d,l-lactic-co-glycolic acid) sponge and growth in a Couette–Taylor bioreactor." *Chemical Engineering Science* 65(6): 2108-2117.
- Zuk, P. A., M. Zhu, et al. (2002). "Human adipose tissue is a source of multipotent stem cells." *Mol Biol Cell* 13(12): 4279-4295.

Zuk, P. A., M. Zhu, et al. (2001). "Multilineage cells from human adipose tissue: implications for cell-based therapies." *Tissue Eng* 7(2): 211-228.

Zvaifler, N. J., L. Marinova-Mutafchieva, et al. (2000). "Mesenchymal precursor cells in the blood of normal individuals." *Arthritis Res* 2(6): 477-488.